PNNL-16625

Pacific Northwest
National Laboratory
Operated by Battelle for the
U.S. Department of Energy

Probabilistic Fracture Mechanics Evaluation of Selected Passive Components – Technical Letter Report

F. A. Simonen, S. R. Doctor, S. R. Gosselin,
D. L. Rudland,(a) H. Xu,(a) G.M. Wilkowski,(a)
B.O.Y. Lydell(b)

May 2007

Prepared for the U.S. Nuclear Regulatory Commission
under a Related Services Agreement with the U.S.
Department of Energy Contract DE-AC05-76RL01830

(a) Engineering Mechanics Corporation of Columbus
Columbus, Ohio 43221 (b) Sigma-Phase Inc. Vail, Arizona
85641

DISCLAIMER

PACIFIC NORTHWEST NATIONAL LABORATORY
operated by
BATTELLE
for the
UNITED STATES DEPARTMENT OF ENERGY
under Contract DE-AC05-76RL01830

Printed in the United States of America

Available to DOE and DOE contractors from the
Office of Scientific and Technical Information,
P.O. Box 62, Oak Ridge, TN 37831-0062;
ph: (865) 576-8401
fax: (865) 576-5728
email: reports@adonis.osti.gov

Available to the public from the National Technical Information Service,
U.S. Department of Commerce, 5285 Port Royal Rd., Springfield, VA 22161
ph: (800) 553-6847
fax: (703) 605-6900
email: orders@ntis.fedworld.gov
online ordering: http://www.ntis.gov/ordering.htm

This document was printed on recycled paper.
(8/00)

PNNL-16625

Probabilistic Fracture Mechanics Evaluation of Selected Passive Components – Technical Letter Report

F. A. Simonen, S. R. Doctor, S. R. Gosselin,

D. L. Rudland,[(a)] H. Xu,[(a)] G.M. Wilkowski,[(a)]

B.O.Y. Lydell[(b)]

May 2007

Prepared for the
U.S. Nuclear Regulatory Commission
under a Related Services Agreement
with the U.S. Department of Energy
Contract DE-AC05-76RL01830

Pacific Northwest National Laboratory
Richland, Washington 99352

(a) Engineering Mechanics Corporation of Columbus
Columbus, Ohio 43221
(b) Sigma-Phase Inc.
Vail, Arizona 85641

Abstract

This report addresses the potential application of probabilistic fracture mechanics computer codes to support the Proactive Materials Degradation Assessment (PMDA) program as a method to predict component failure probabilities. The present report describes probabilistic fracture mechanics calculations that were performed for selected components using the PRO-LOCA and PRAISE computer codes. The calculations address the failure mechanisms of stress corrosion cracking, intergranular stress corrosion cracking, and fatigue for components and operating conditions that are known to make particular components susceptible to cracking. It was demonstrated that the two codes can predict essentially the same failure probabilities if both codes start with the same fracture mechanics model and the same inputs to the model. Comparisons with field experience showed that both codes predict relatively high failure probabilities for components under operating conditions that have resulted in field failures. It was found that modeling assumptions and inputs tended to give higher calculated failure probabilities than those derived from data on field failures. Sensitivity calculations were performed to show that uncertainties in the probabilistic calculations were sufficiently large to explain the differences between predicted failure probabilities and field experience.

Executive Summary

The U.S. Nuclear Regulatory Commission (NRC) has supported the research program Proactive Materials Degradation Assessment (PMDA). The objective of this program has been to predict future occurrences of materials degradation that may or may not have been observed in the field or in the laboratory. Evaluations have focused on materials degradation modes associated with operating environments for specific components, including stress corrosion cracking, fatigue, flow-accelerated corrosion, boric acid corrosion, thermal embrittlement, and radiation effects. A detailed review addressed over 2000 components in the primary, secondary, and tertiary systems of specific reactor designs. A group of experts provided their judgments to score individual components in terms of "degradation susceptibility" and the "extent of knowledge" available for developing mitigation actions.

This report addresses the possible application of probabilistic fracture mechanics computer codes to support the PMDA program as a method to predict component failure probabilities. Probabilistic fracture mechanics calculations are described that were performed for selected components using the PRO-LOCA and PRAISE computer codes. The calculations address the failure mechanisms of stress corrosion cracking, intergranular stress corrosion cracking, and fatigue for components and operating conditions that are known to have failed components in the field. The calculations allowed the two computer codes to be benchmarked against each other and, more importantly, benchmarked against field experience.

A review of the calculations showed how uncertainties and modeling assumptions can impact calculated failure probabilities. Comparisons with field experience showed that both codes are capable of predicting high failure probabilities for the components for which operating conditions have resulted in field failures. It was found that assumptions made to deal both with uncertainties in the treatment of degradation mechanisms and with estimates of input parameters can give significantly higher failure probabilities than those derived from data on field failures. Sensitivity calculations were performed to address uncertainties associated with residual stresses, operating stresses, and temperatures. Results of these calculations showed that the identified uncertainties in the probabilistic calculations were sufficiently large to explain the differences between the predicted and observed failure probabilities.

Acknowledgments

The authors wish to thank the U.S. Nuclear Regulatory Commission Office of Nuclear Regulatory Research for supporting this work and, in particular, the NRC Program Managers, Drs. J. Muscara and S. N. Malik.

Abbreviations and Acronyms

ANL	Argonne National Laboratory
ASME	American Society of Mechanical Engineers
BWR	boiling water reactor
CRDM	control rod drive mechanism
DB	database
EBD	equivalent pipe break diameter
EMC^2	Engineering Mechanics Corporation of Columbus
FAC	flow-accelerated corrosion
FR	flow rate
HELB	high-energy line break
IAEA	International Atomic Energy Agency
ID	inner diameter
IGSCC	intergranular stress corrosion cracking
ISI	inservice inspection
LER	licensing event report
LOCA	loss-of-coolant accident
LWR	light water reactor
NDE	nondestructive examination
NRC	Nuclear Regulatory Commission
OPDE	operating piping failure data exchange
PFM	probabilistic fracture mechanics
PIRT	Phenomena Identification and Ranking Technique
PMDA	Proactive Materials Degradation Assessment
PNNL	Pacific Northwest National Laboratory
POD	probability of detection
PRA	probabilistic risk assessment
PSA	probabilistic safety assessment
PWR	pressurized water reactor
PWSCC	primary water stress corrosion cracking
RI-ISI	risk-informed in-service inspection

SRM	structural reliability modeling
TTF	time to failure
USNRC	United States Nuclear Regulatory Commission

Contents

Figures

Tables

1.0 Introduction

The U.S. Nuclear Regulatory Commission (NRC) has supported the research program Proactive Materials Degradation Assessment (PMDA).[(a)] The objective of this program has been to assess the possible future occurrence of materials degradation in components of light water reactors. A central intent of the PMDA program has been to predict degradation that may or may not have been observed in the field or in the laboratory. Another objective is to consider the possibility of unexpected increases in degradation with time.

The PMDA program has included an assessment, conducted under contract with Brookhaven National Laboratory, of past and possible future materials degradation in light water reactors. The study used a Phenomena Identification and Ranking Technique (PIRT)-type of process involving eight experts from five countries who met to discuss the technical issues and perform individual assessments. The analyses focused on materials degradation modes associated with operating environments for specific components, such as stress corrosion cracking, fatigue, flow-accelerated corrosion, boric acid corrosion, thermal aging embrittlement, and radiation effects for existing plants. The work encompassed passive components whose failure would lead to release of radioactivity, or would affect safety systems. The study did not address design issues such as mechanics and thermal hydraulics, the consequences of degradation, or the failure of active components such as valves and pumps.

A detailed review by the panel of experts addressed over 2000 components in the primary, secondary, and tertiary systems of pressurized water reactors (PWRs) and boiling water reactors (BWRs). Each expert individually provided judgments to score individual components in terms of "degradation susceptibility" and the "extent of knowledge" available for development of mitigation actions. These inputs were compiled and were used to generate a summary to reflect the collective judgments of the experts.

This report describes a study performed for NRC by Pacific Northwest National Laboratory (PNNL) with subcontractor support from the Engineering Mechanic Corporation of Columbus (EMC^2) and Sigma Phase Inc. The study addressed the application of probabilistic fracture mechanics computer codes to support the PMDA program as a method to predict component failure probabilities. The probability of failure information would be used in probabilistic risk assessments to evaluate the risk importance of various components found to be susceptible to future degradation.

This report describes probabilistic fracture mechanics (PFM) calculations that were performed for selected components using the PRO-LOCA (Rudland et al. 2006, Unpublished[(b)]) and PRAISE (Harris and Dedhia 1992; Harris et al. 1981, 1986) computer codes. One code (PRAISE) was originally developed for the NRC during the 1980s and has been applied by PNNL and other organizations to a range of risk-informed applications, most notably for risk-informed inservice inspection. The other code (PRO-LOCA) is currently being developed for NRC by Battelle Memorial Institute and EMC^2, and is

---

(a) USNRC. 2005. *Proactive Materials Degradation Mechanism Assessment*. Draft NUREG/CR Report. U.S. Nuclear Regulatory Commission, Washington, D.C.

(b**)** Rudland DL, H Xu, G Wilkowski, N Ghadiali, F Brust and P Scott. Unpublished. *Evaluation of Loss-of-Coolant Accident (LOCA) Frequencies Using the PRO-LOCA Code*, Technical Letter Report, December 2005.

intended to incorporate the best elements of other PFM codes, advances in the fracture mechanics, and data on fracture behavior of materials of interest to nuclear pressure boundary components. The scope of both codes is the prediction of piping failure probabilities for various degradation mechanisms including failures from preexisting welding flaws, fatigue crack initiation, intergranular stress corrosion cracking (IGSCC), and primary water stress corrosion cracking (PWSCC). Both codes simulate the progress of degradation from the initiation of small cracks, to the growth of these cracks to become small through-wall leaking flaws, and finally the occurrence of large leaks and piping ruptures.

Calculations were performed by PNNL and EMC^2 to allow the two computer codes to be benchmarked against each other and, more importantly, benchmarked against field experience. The objective was to determine the extent to which uncertainties and modeling assumptions may impact calculated failure probabilities. The comparisons with field experience were intended to establish whether the codes were capable of predicting relatively high failure probabilities for those components and operating conditions that have resulted in field failures. Sensitivity calculations were also performed to address uncertainties associated with residual stresses, applied stresses, and temperatures. Results of these calculations were intended to identify those uncertainties in the probabilistic calculations that are sufficiently large to explain the differences between predicted failure probabilities and failure probabilities based on field experience.

Section 2 provides background on past and present efforts to develop probabilistic fracture mechanics codes both in the U.S. and overseas. The capabilities and limitations of the two codes (PRAISE and PRO-LOCA as applied in this report) are summarized along with prior NRC-related applications to piping integrity issues. Also discussed in Section 2 and in Appendix A are methods that use data from field experience to estimate failure probabilities as a function of time and plant operating conditions.

Section 3 presents calculations performed with both PRAISE and PRO-LOCA. Results of calculations for PWSCC, IGSCC, and thermal fatigue are used to benchmark the failure probabilities as predicted by the two codes. Each set of calculations is also benchmarked against failure probabilities derived in Appendix A from a field experience database.

Section 4 is a discussion of the model assumptions, the uncertain nature of inputs, and their impacts on calculated failure probabilities. Another issue is the unexplained differences in crack-growth rates between laboratory tests and the apparently lower crack-growth rates observed in components under field conditions as indicated by the lower-than-predicted occurrence rates for relatively large and leaking cracks. The objective is to reconcile the consistently high failure probabilities predicted by the probabilistic fracture mechanics calculations relative to the lower failure probabilities indicated by field experience.

Chapter 5 describes some calculations with the PRAISE code that use a crack initiation model developed for fatigue cracking. This model is used with inputs based on laboratory data for crack initiation by PWSCC in Alloy 182. The calculations allowed crack initiation to be predicted with a model that (with sufficient laboratory data) can account for material, environment, stress, and temperature effects. Sensitivity calculations address the effects of uncertainties in stresses that could occur, such as when the combination of operating stress and residual stresses gives calculated stresses that exceed the material yield strength. Other calculations address variations of stress around the circumference of a pipe and uncertainties in plant operating conditions.

Section 6 summarizes the results and conclusions from the probabilistic fracture mechanics calculations and suggests future calculations that could give predictions of component failure probabilities that better agree with field experience.

2.0 Methodology

This section describes the computer codes used for the benchmarking effort along with the methods and results from an application of a database on reported failure events at operating nuclear power plants.

2.1 Probabilistic Fracture Mechanics Codes

The two PFM codes applied for the calculations in this report are PRO-LOCA (Rudland et al. 2006, Unpublished[(a)]) and PRAISE (Harris et al. 1981, 1986; Harris and Dedhia 1992). These two codes were developed for the NRC to address piping failures, with PRAISE being developed and enhanced over a time period starting in the 1980s and PRO-LOCA being a more recent code developed starting in 2003 and seen as a successor to PRAISE. In this section, we briefly describe the features and historical development of the two codes along with reference to other codes that have also been applied to predict failure probabilities of nuclear pressure boundary components. The other probabilistic fracture mechanics codes for piping were not developed for NRC, but by other organizations, and as such are not generally available in the public domain (Bell and Chapman 2003; Bishop 1997). Excluded from the discussion are other significant probabilistic fracture mechanics codes, such as FAVOR (Dickson 1994; Dickson et al. 2004; Williams et al. 2004) and VISA-II (Simonen et al. 1986), which were specifically developed to predict failure probabilities for reactor pressure vessels that are subject to radiation embrittlement.

The first version of PRAISE (Harris et al. 1981) was developed in the 1980s by Lawrence Livermore National Laboratory under contract to NRC, with the initial application to address seismic-induced failures of large-diameter reactor coolant piping. This version of the code addressed failures (small leaks and ruptures) associated with fabrication flaws in welds that were allowed to grow as fatigue cracks until they either caused the pipe to leak or exceed a critical size needed to result in unstable crack growth and pipe rupture. The next major enhancement to the code (Harris et al. 1986) addressed IGSCC and simulated both crack initiation and crack growth. The enhanced code allowed for crack initiation at multiple sites around the circumference of a girth weld and simulated linking adjacent cracks to form longer cracks more likely to cause larger leaks and pipe ruptures.

In the early 1990s a version of PRAISE (pc-PRAISE) was developed to run on personal computers (Harris and Dedhia 1992). The mid-1990s saw the development of methods for risk-informed inservice inspection, for which there were many new applications of PRAISE. A new commercial version of PRAISE (winPRAISE) was made available by Dr. David Harris of Engineering Mechanics Technology that simplified the input to the code with an interactive front end (Harris and Dedhia 1998). During this same time period, PNNL made numerous applications of PRAISE to apply probabilistic fracture mechanics to support the development of improved approaches to inservice inspection (Khaleel and Simonen 1994a, 1994b, 2000; Khaleel et al. 1995; Simonen et al. 1998, Simonen and Khaleel 1998a, 1998b). The objective of this work was to ensure that changes to inspection requirements could be justified in terms of reduced failure probabilities for inspected components. Other work at PNNL for NRC (Khaleel et al. 2000) involved evaluations of fatigue critical components that could potentially attain calculated fatigue usage factors in excess of design limits (usage factors greater than unity).

(a) Rudland DL, H Xu, G Wilkowski, N Ghadiali, F Brust and P Scott. Unpublished. *Evaluation of Loss-of-Coolant Accident (LOCA) Frequencies Using the PRO-LOCA Code*, Draft Technical Letter Report, December 2005.

The most recent upgrades to PRAISE (Khaleel et al. 2000) were developed to support these fatigue evaluations, with the upgrade consisting of a model similar to that for IGSCC but directed at predicting the probabilities of initiating fatigue cracks. This new model was used to develop the technical basis for changes to Appendix L of American Society of Mechanical Engineers (ASME) Section XI that addresses fatigue critical locations in pressure boundary components (Gosselin et al. 2005). The PRAISE code has been extensively documented, successfully applied to a range of structural integrity issues, and has been available since the 1980s as a public domain computer code. However, the code has not been maintained and upgraded in an ongoing manner. Upgrades have been performed to meet the needs of immediate applications of the code and as such have served to fill very specific gaps in capabilities of PRAISE.

The development of the PRO-LOCA code was motivated by an NRC need to address issues related to loss-of-coolant accident (LOCA) events. The need for an improved probabilistic fracture mechanics code became evident during an expert elicitation process that was funded by NRC (Tregoning et al. 2005) to establish estimates of LOCA frequencies and to quantify the uncertainties in the estimates. A version of the PRO-LOCA code was developed and applied in calculations described in this report. Development of the code is expected to continue in future years including documentation of the code and preparation of detailed user instructions needed to support the release of the code to outside organizations.

A report on the status of PRO-LOCA has been prepared by Battelle Memorial Institute and EMC^2 and the reader is directed to this report (Rudland et al. Unpublished[(a)]) for features and technical basis for PRO-LOCA. Like PRAISE, the PRO-LOCA code addresses the failure mechanisms of preexisting cracks, fatigue associated with initiated cracks, and IGSCC. While both codes include calculations for crack-tip stress intensity factors, the differing computational approaches can give small differences in numerical results. The two codes have different treatments for stresses due to dead-weight loadings and due to piping system thermal expansion bending moments. PRO-LOCA accounts for the through-wall variation of these stresses whereas PRAISE neglects the variation in stress. The PRO-LOCA model for the initiation and growth of fatigue cracks is essentially the same as that in PRAISE whereas the IGSCC model differs significantly from the predictive model in PRAISE.

PRO-LOCA has an additional capability to predict failure probabilities for PWSCC. Other improved capabilities not incorporated in other codes such as PRAISE are in the areas of leak rate predictions and the prediction of critical crack sizes. These enhancements are largely based on the results of some 20 years of NRC-supported research on the integrity of degraded piping. PRO-LOCA has also incorporated an improved basis for simulating weld residual stresses.

Other probabilistic fracture mechanics codes for piping have been developed to calculate failure probabilities for piping. The SRRA code (Bishop 1997; Westinghouse Owners Group 1997) developed by Westinghouse follows much the same approach as the PRAISE code, but is limited to failures associated with cyclic fatigue stresses considers only preexisting fabrication flaws. Fatigue crack initiation has been approximated by assuming a very small initial crack, but with only one initiation site per weld. Stress corrosion cracking is similarly treated by postulating a very small initial crack, and

---

(a) Rudland DL, H Xu, G Wilkowski, N Ghadiali, F Brust and P Scott. Unpublished. *Evaluation of Loss-of-Coolant Accident (LOCA) Frequencies Using the PRO-LOCA Code*, Draft Technical Letter Report, December 2005.

growing the crack according to user-specified parameters for a crack growth equation. The SRRA code includes an importance sampling procedure that gives reduced computation times compared to the Monte Carlo approaches used by PRO-LOCA and PRAISE. Also the model can simulate uncertainties in a wide range of parameters such as the applied stresses.

The European NURBIM (Brickstad et al. 2004) has looked at a number of codes including PRAISE as part of an international benchmarking study. Included were a Swedish code NURBIT (Brickstad and Zang 2001), the PRODIGAL code from the United Kingdom (Bell and Chapman 2003), a code developed in Germany by GRS (Schimpfke 2003), a Swedish code ProSACC (Dillstrom 2003) and another code (STRUEL) from the United Kingdom (Mohammed 2003). The results of the NURBIM study (Brickstad et al. 2004; Dillstrom 2003) will not be documented here. The present review concluded that none of the other benchmarked codes provided capabilities significantly different than or superior to the capabilities of PRAISE. In any case, the predictions of all such codes are limited in large measure by the quality of the values that can be established for the input parameters, as well as the validation (or lack of validation) with service experience.

2.2 Application of Database on Field Experience

This section summarizes methods based on evaluations of data from field experience that are used to estimate component failure probabilities. A more complete discussion of these methods can be found in Appendix A. Failure probabilities estimated by detailed evaluations in Appendix A are summarized here for the components that are addressed by probabilistic fracture mechanics calculations described in Section 3.0 of the present report.

Application of Data to Estimate Failure Probabilities – Risk-informed evaluations require realistic estimates of pipe failure rates and rupture frequencies that relate to specific combinations of materials, degradation mechanisms, and plant operating conditions. As described in Appendix A, there are basically five approaches for estimating piping reliability:

(1) Structural reliability modeling (SRM) based on probabilistic fracture mechanics,
(2) Analytical modeling using Markov theory and statistical analysis of service data,
(3) Direct statistical estimation using service data,
(4) Expert judgment/expert elicitation, and
(5) Any combination of (1) through (4).

The discussion below addresses statistical estimation using service data (Method 3). The term "failure" can in general imply any degraded state requiring remedial action. Remedial actions include repairs and replacements with or without more resistant material. Precise definitions of failure are important to make distinctions between different through-wall flaw sizes that have different effects on plant operation and safety. In recent risk-informed applications (Tregoning et al. 2005), the definitions of structural failure modes listed in Table 2.1 were used.

Table 2.1. Example Definitions of Structural Failure for PWR LOCA

Mode of Structural Failure	Equivalent Pipe Break Diameter (EBD) [mm]	Peak Through-wall Flow Rate (FR) [kg/s]
Perceptible Leak	> 0	FR > 0
Large Leak	15 < EBD ≤ 50	0.5 < FR ≤ 5
Small Breach	50 < EBD ≤ 100	5 < FR ≤ 20
Breach	100 < EBD ≤ 250	20 < FR ≤ 100
Large Breach	250 < EBD ≤ 500	100 < FR ≤ 400
Major Breach	EBD > 500	FR > 400 (6,300 gpm)

In reporting results of the benchmarking calculations, an additional "failure" mode of crack initiation was defined that included cracks of less than through-wall depth.

The database PIPExp-2006 (Lydell and Olsson 2006; OECD 2005, 2006) was applied to estimate failure frequencies. With emphasis on light water reactors (LWRs) and covering the period 1970 to the present, PIPExp-2006 is a frequently updated and maintained database on pipe failures in commercial nuclear power plants worldwide. Currently the database includes 6600 pipe failure reports plus an additional 465 records on water hammer events that challenged or degraded the structural integrity of an affected piping pressure boundary.

Table 2.2 summarizes input data and results from the Appendix A evaluations of service experience for the selected components. The number of welds found to have through-wall cracks is seen to be very small – ranging from zero to seven reported events per component category. Because the number of events has been small, there are large statistical uncertainties in estimates of frequencies of through-wall cracks. Uncertainties are particularly large for the pressurizer surge nozzle and pressurizer spray nozzle, because there have been only two cases of repairs (cracks with less than through-wall depths) and no cases of through-wall cracks.

In cases with no reported failures for a particular component of interest, there are however methods that can be applied to estimate (or bound) failure frequencies. Two approaches can be characterized as follows:

(1) A bounding frequency is calculated based on the assumption that one failure occurs. The key input is then the number of relevant weld-years of operation for which no failures have been reported for the component of interest. The results can be viewed as an upper bound to the failure frequency. As an example, the present evaluations in effect assumed a single weld with a through-wall crack in the pressurizer spray line nozzle weld. In this case, there have been reported cracks (less than through-wall) that have required repairs, which makes it credible that a through-wall crack could occur.

Table 2.2. Summary of Input Data and Results from Estimation of Failure Frequencies from Database on Operating Experience

Component/Inspection Location		Number of Weld-Years	Number of Cracked/Repaired Welds	Number of Welds with Through-Wall Cracks	Mean Frequency of Through-Wall Flaw [1/Weld-Year]
PWR Hot Leg Bi-metallic Weld (RPV Nozzle-to-Safe-end)		All: 10,784 2-Loop: 2,510 3-Loop: 3,570 4-Loop: 4,704	2[(a)]	1[(a)]	9.1×10^{-5} [(b)]
PWR Pressurizer Spray Line Nozzle Bi-Metallic Weld	Case 1[(c)]	$1 \times 3621 = 3{,}621$	1	0	1.5×10^{-6}
	Case 2[(d)]	$5 \times 3621 = 18{,}105$	5	1	2.1×10^{-5}
	Case 3[(e)]	$1 \times 3621 = 3{,}621$	1	Assume 1	7.3×10^{-5}
PWR Pressurizer Surge Line Nozzle Bi-Metallic Weld	Case 1[(f)]	$2 \times 3621 = 7{,}242$	2	0	1.2×10^{-6}
	Case 2[(g)]	$7 \times 3621 = 25{,}347$	7	1	1.6×10^{-5}
	Case 3[(h)]	$2 \times 3621 = 7{,}242$	2	Assume 1	4.3×10^{-5}
BWR Reactor Recirculation 12-inch Weld (pre-1988) U.S. BWR/3 & BWR/4		25,137	120	7	2.8×10^{-4} [(i)]
BWR Reactor Recirculation 28-inch Weld (pre-1988) U.S. BWR/3 & BWR/4		19,551	72	5	2.6×10^{-4} [(i)]

(a) Service experience through December 2005.
(b) This is a composite failure rate under assumption of equal susceptibility to PWSCC in 2-loop, 3-loop, and 4-loop PWR plants with bi-metallic welds.
(c) Case 1 accounts for existing service experience with bi-metallic pressurizer spray line bi-metallic welds.
(d) Case 2 assumes equal PWSCC susceptibility for bi-metallic pressurizer spray line weld and relief line welds – 5 welds per plant.
(e) Same as Case 1 except that the flaw found at Millstone-3 is assumed to be near or at through-wall.
(f) Case 1 accounts for existing service experience with bi-metallic surge line welds (hot-leg side and pressurizer side).
(g) Case 2 assumes equal PWSCC susceptibility for bi-metallic surge line welds, pressurizer spray line weld, and pressurizer relief line welds (7 welds per plant).
(h) Same as Case 1 except that 1 of 2 flaws in the service experience is near or at through-wall.
(i) Average failure rate across all welds in a typical Reactor Recirculation System.

(2) The population of components is expanded to include a larger base of components that have similar materials, designs, and operating conditions as the particular component of interest. The success of this approach requires appropriate judgments regarding components that should be included in the larger population. By considering more components, the relevant data is more likely to show some actual failure events and will cover a much larger number of weld-years of operation. By expanding the population, estimated failure frequencies can either increase (the number of events increases significantly) or can decrease (a much larger number of weld-years of operation with no significant increase in failure events).

PWR Hot-Leg Bi-Metallic Weld – This example considered the bi-metallic hot-leg weld at the joint between the reactor coolant piping and the reactor pressure vessel nozzle. The database showed one event with a through-wall crack (V.C. Summer event of 2000). Consideration of cracked welds with less than though-wall crack depths added another event (Ringhals-4). The calculated failure frequency is listed in Table 2.2 as 9.1×10^{-5} per weld-year based on the number of relevant welds per plant and the number of reactor years of operation up to the year 2000. With the additional Ringhals-4 event, the frequency increases to 1.5×10^{-4}. In this evaluation, the relevant population was limited to the hot leg. Other bi-metallic welds in PWR plants (PWR cold-leg weld and other PWR bi-metallic welds of piping of various diameters) were excluded from consideration. There was some failure experience for the hot leg (although limited to one event) and the higher temperature of the hot leg and other unique attributes of the hot leg can justify a special evaluation for this component.

PWR Pressurizer Surge Nozzle Bi-Metallic Weld – This example considered the bi-metallic weld at the joint between the surge line and the pressurizer. The database showed no events with a through-wall crack. Consideration of cracked welds with less than though-wall crack depths showed two events. Two calculated failure frequencies are listed in Table 2.2 as 1.2×10^{-6} and 1.6×10^{-5} per weld-year based on the number of relevant welds per plant (one) and the number of reactor years of operation up to the year 2005. In this evaluation, two assumptions were made regarding the relevant population. In one case, the population was limited only to surge line nozzle welds. In the other case, bi-metallic welds in PWR plants (other PWR bi-metallic welds in piping of various diameters but not the hot-leg weld) were included. The order of magnitude difference in the two estimated failure frequencies comes from the different number of weld-years of operations between the two assumptions regarding the population of relevant welds and failure history (the difference is due to one through-wall flaw).

PWR Pressurizer Spray Line Nozzle Bi-Metallic Weld – This example considered the bi-metallic weld at the joint between the spray line and the pressurizer. The database showed no events with a through-wall crack. Consideration of cracked welds with less than though-wall crack depths showed two events. Two calculated failure frequencies are listed in Table 2.2 as 1.5×10^{-6} and 2.1×10^{-5} per weld-year based on the number of relevant welds per plant (one) and the number of reactor years of operation up to the year 2005. In this evaluation, two assumptions were made regarding the relevant population. In one case the population was limited only to spray line nozzle welds. In the other case bi-metallic welds in PWR plants (other PWR bi-metallic welds in piping of various diameters but not the hot-leg weld) were included. The order of magnitude difference in the two estimated failure frequencies comes from the different number of weld-years of operation between the two assumptions regarding the population of relevant welds and the failure history (one through-wall flaw).

BWR Reactor Recirculation 12-Inch Weld – This example considered the circumferential welds in stainless steel piping in the BWR recirculation systems for time periods pre-1988 before mitigation measures (augmented inspections, water chemistry improvements, etc.) were implemented at BWR plants. The database showed seven events with through-wall cracks. Consideration of cracked welds with less than though-wall crack depths added 120 events. The calculated failure frequency (through-wall cracks) is listed in Table 2.2 as 2.8×10^{-4} per weld-year based on the number of relevant welds per plant and the number of reactor years of operation up to the year 1988. In this case, because of the reasonable number of reported failure events and the already broad scope of the selected population, there was no reason to consider a wider population of welds to provide a more robust basis for estimating a failure frequency.

BWR Reactor Recirculation 28-Inch Weld – This example considered the circumferential welds in stainless steel piping in the BWR recirculation systems for time periods pre-1988 before mitigation measures (augmented inspections, water chemistry improvements, etc.) were implemented at BWR plants. The data based showed five events with through-wall cracks. Consideration of cracked welds with less than though-wall crack depths added 72 events. The calculated failure frequency (through-wall cracks) is listed in Table 2.2 as 2.6×10^{-4} per weld-year based on the number of relevant welds per plant and the number of reactor years of operation up to the year 1988. In this case, because of the reasonable number of reported failure events and the already broad scope of the selected population, there was no reason to consider a wider population of welds to provide a more robust basis for estimating a failure frequency.

3.0 Benchmarking of PRO-LOCA and PRAISE

The benchmarking effort had the dual objectives of (1) comparing calculated failure probabilities with failure probabilities derived from data from failure events at operating plants, and (2) comparing the calculated failure probabilities from the PRO-LOCA (Rudland et al. 2006) and PRAISE codes (Harris et al. 1981, 1986; Harris and Dedhia 1992; Khaleel et al. 2000). The cases for the benchmarking were selected to cover a range of degradation mechanisms (fatigue, IGSCC, and PWSCC) and for components that have experienced service-related degradation. Therefore, the calculated probabilities could be compared to probabilities estimated from a database on reported service failures.

The specific components selected were

- dissimilar metal Alloy 182 welds in PWR primary coolant systems subject to PWSCC,
- stainless steel welds in BWR recirculation systems subject to IGSCC, and
- thermal fatigue nozzles connected to a PWR primary coolant pipe.

Details of the component designs, materials, temperature/environmental conditions, and the sources and levels of stress imposed during plant operation are described. Results of the probabilistic fracture mechanics calculations are presented along with failure probabilities obtained from the evaluations of data on service failures that are described in Appendix A.

A detailed description of the two PFM codes is beyond the scope of this report. Details of the codes will be discussed only in the context of particular calculations covered by the benchmarking effort. Particular attention is given to those details of the fracture mechanics models that may explain differences in calculated probabilities and failure probabilities as indicated by field failures.

Crack-tip stress intensity factors for the PRAISE code required that complex through-wall variations in stresses be evaluated. For this purpose, calculations were performed external to PRAISE with the TIFFANY code (Dedhia et al. 1982) to generate input values for the "g-functions" used by PRAISE.

3.1 PWR Hot Leg Bi-metallic Weld – PWSCC

This set of calculations addressed the Alloy 182 weld connecting the hot-leg piping to the reactor pressure vessel nozzle. This case corresponded to the leakage location reported for the V.C. Summer plant that occurred in 2000. Specific parameters for this calculation were:

- Temperature = 216°C (600°F)
- Inner Diameter = 737 mm (29.0 in.)
- Wall Thickness = 63.5 mm (2.5 in.)
- Number of Circumferential Subunits = 44 (subunit length ~ 50 mm (2 in.)
- Residual and Operational Stresses – see Figure 3.1 and Figure 3.2
- Depth of Initiated Cracks = 3 mm (0.12 in.)
- Length of Initiated Cracks = 10 mm (0.39 in.)

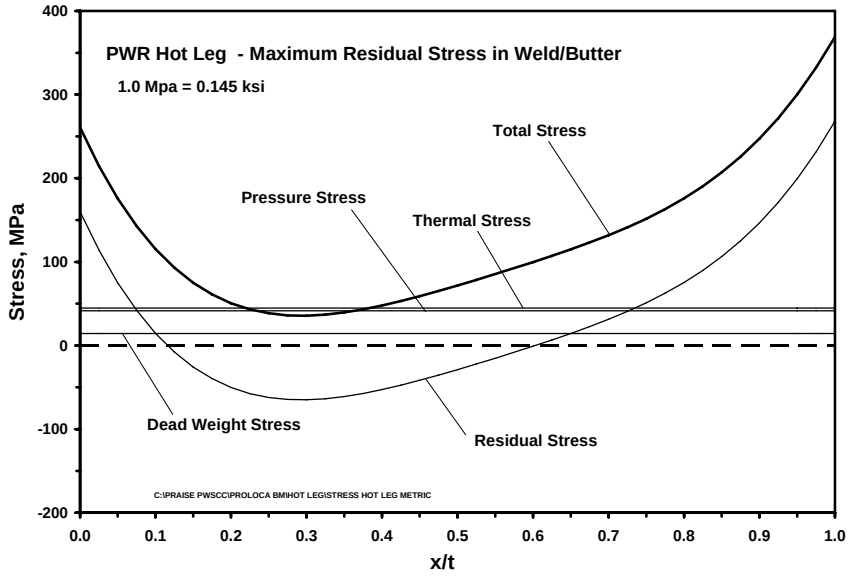

Figure 3.1. Stress Input for Hot-Leg Weld without 15% Grid Out and Repair

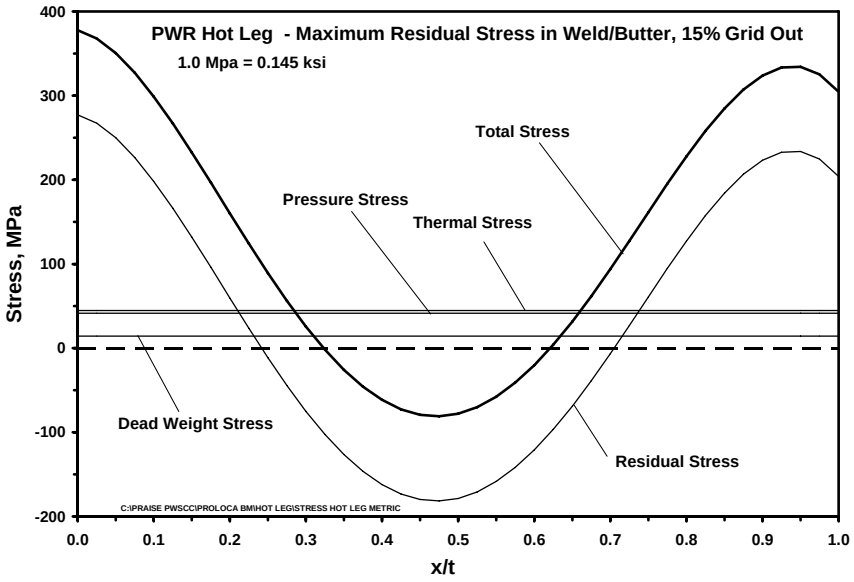

Figure 3.2. Stress Input for Hot-Leg Weld with 15% Grid Out and Repair

Modeling Considerations – Although the PRAISE code does not have an explicit option to simulate PWSCC, it does have an option to simulate piping failures due to fatigue loading, both from the growth of preexisting fabrication flaws and from flaws that initiate by fatigue during the service life of the component. It was possible to address PWSCC with the existing fatigue model in PRAISE. The equations in PRAISE for predicting crack initiation and crack growth by fatigue (Khaleel et al. 2000) and PWSCC were established to be mathematically equivalent to those in PRO-LOCA (Rudland et al. 2006).

The time scale for PWSCC was interpreted in terms of the cycles per year for the application of the fatigue model. The sustained operating stresses and temperatures were provided to PRAISE as inputs for a cyclic stress transient. The constant for the Paris types of fatigue crack growth law was appropriately adjusted in accordance with a specific number of cycles of stress per year of plant operation. The structure of the PRAISE code is also designed to simulate probabilities of crack initiation. The user must provide a subroutine with appropriate equations for crack initiation such as the equations described in the documentation for the PRO-LOCA.

For the hot-leg calculations, the PRO-LOCA and PRAISE codes used common inputs for the multiple cracking models. These inputs specified the number of potential crack initiation sites (44) and the dimensions of the initiated cracks. At this point the code then began the simulation of the crack growth process using a fracture mechanics model.

Crack initiation was predicted using equations described in documentation for the PRO-LOCA code. These equations had been developed by W. Shack of Argonne National Laboratory (ANL) for Alloy 600 and Alloy 182 based on service-related cracking data of Alloy 600 control rod drive mechanism (CRDM) nozzles (Shack 2003). These equations use a Weibull distribution function to simulate the scatter in crack initiation times with a triangular distribution to characterize the uncertainty in the scale parameter of the Weibull function. In each case, the calculated initiation times were adjusted for the effects of temperature using an Arrhenius relationship with activation energy of 210 kJ/mole (50 kcal/mole). In addition, the CRDM data were adjusted for a higher stress in a dissimilar metal butt weld compared to the CRDM component (stress ratio = 1.0/0.75). This ratio was assumed to be a common value applicable to butt welds in general, independent of such factors as pipe-wall thickness. The CRDM initiation equations, appropriate to the entire component, were transformed to give values appropriate to a smaller subunit of the CRDM. In this regard, the predicted times to initiate one or more cracks in a particular component become a function of the number of subunits. Larger components will be predicted to have initiated cracks sooner than smaller components.

Stress Inputs – Two residual stress distributions were addressed using the equation and parameters of Table 3.1 (Cases 1 and 2). In this table the coefficients (σ_{0RS}, σ_{1RS}, σ_{2RS}, σ_{3RS} and σ_{4RS}) define polynomial correlations of residual stress distributions that were established by finite-element calculations. The parameter σ_y is the yield stress of the weld material. The more bounding distribution of Case 2 described a weld that had experienced a grind out at the inside surface of the pipe to a depth of a/t = 15%. The other stresses, as indicated in Figure 3.3 and Figure 3.4, were associated with the internal pressure, dead-weight loading, and a thermal expansion bending moment acting on the pipe cross section.

Results of Calculations – Figure 3.3 and Figure 3.4 show calculated probabilities as a function of time for (1) crack initiation (initiation of one or more cracks) and (2) through-wall cracking. The numerical agreement between PRO-LOCA and PRAISE is seen to be excellent. Both codes predict a 50% probability of crack initiation at about 10 years and a 50% probability of a through-wall crack by about 20 years for Cases 1 and 2. The model developed for PRO-LOCA and also used for these PRAISE calculations to simulate crack initiation times gives results that are independent (for a given temperature) of the estimated stress at the inner surface of the pipe. Therefore, the crack initiation curves for the two residual stress distributions (Figure 3.1 and Figure 3.2) for Cases 1 and 2 are identical. However, crack

Table 3.1. Residual Stress Distributions for Dissimilar Metal Welds
(x = distance from inner surface; t = wall thickness)

$$\sigma_{WRS} = \sigma_{0RS} + \sigma_{1RS}\left(\frac{x}{t}\right) + \sigma_{2RS}\left(\frac{x}{t}\right)^2 + \sigma_{3RS}\left(\frac{x}{t}\right)^3 + \sigma_{4RS}\left(\frac{x}{t}\right)^4$$

Case	σ_{0RS}/σ_y	σ_{1RS}/σ_y	σ_{2RS}/σ_y	σ_{3RS}/σ_y	σ_{4RS}/σ_y	σ_y Used, MPa	σ_y Used, ksi	Comment
1	0.750	-9.271	27.711	-32.912	14.979	213.3	30.9	Hot leg – Alloy 182 weld at 324°C (615°F), using maximum stress in weld/butter
2	1.300	-1.084	-33.189	73.310	-39.381	213.3	30.9	Hot leg – Alloy 182 weld at 324°C (615°F), using maximum stress in weld/butter, 15% ID grind out
3	1.728	-5.494	-10.655	32.048	-16.535	213.3	30.9	Surge line – Alloy 182 weld at 324°C (615°F), 15% ID grind out
4	-0.500	-6.427	33.158	-41.320	15.734	213.3	30.9	Spray line – Alloy 182 weld at 324°C (615°F)

growth rates are a function of the residual and operating stresses. There are different curves for through-wall crack probabilities (Figure 3.3 and Figure 3.4) for Cases 1 and 2, with Figure 3.4 indicating less time to grow cracks to through-wall depths because there are higher stresses associated with the 15% grind out and repair case.

Comparison with Service Experience – Service failure data were evaluated to estimate a probability of through-wall cracking for the hot-leg weld based on operating experience. From Appendix A it is noted that cracking has been observed in the PWR hot-leg weld with through-wall cracks observed at the V.C. Summer plant and part through-wall cracking at the Ringhals plant in Sweden. A failure frequency was calculated based on the number of reported failures, the number hot-leg–to–vessel welds, and the number of plant years of operation. The resulting frequency of through-wall cracks as given in Appendix A was 9.1×10^{-5} failures per weld per year after about 20 years of operation. Using a plant availability of 80 percent, 20 years of plant operation would correspond to 16 years in the PFM calculations. At 16 years (from Figure 3.3 and Figure 3.4), the PFM calculations give cumulative probabilities of through-wall cracking ranging from 0.1 (Figure 3.3) to 0.4 (Figure 3.4). In contrast, the operating data gives a cumulative probability of $20 \times (9.1 \times 10^{-5}) = 1.82 \times 10^{-3}$ per weld or one cracked weld out of a total population of 550 welds. Assuming 100 PWR plants covered by the database and four welds per plant, the operating experience shows that one or two plants would have experienced leaks at this hot-leg weld of interest.

Conclusions – The PFM models over-predict the probability of through-wall PWSCC cracks in the hot-leg weld by a factor of about 100. These results, along with other results reported below, suggest that the fracture mechanics models and/or the inputs to the models do not adequately represent the hot-leg welds in the population of PWR plants of interest. It is noted that the one hot-leg failure (V.C. Summer)

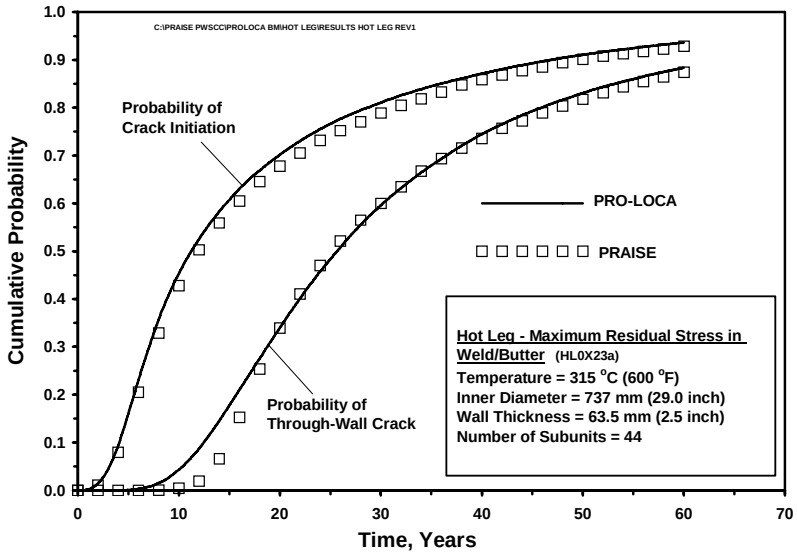

Figure 3.3. Calculated Failure Probabilities for Hot- Leg Weld without 15% Grid Out and Repair

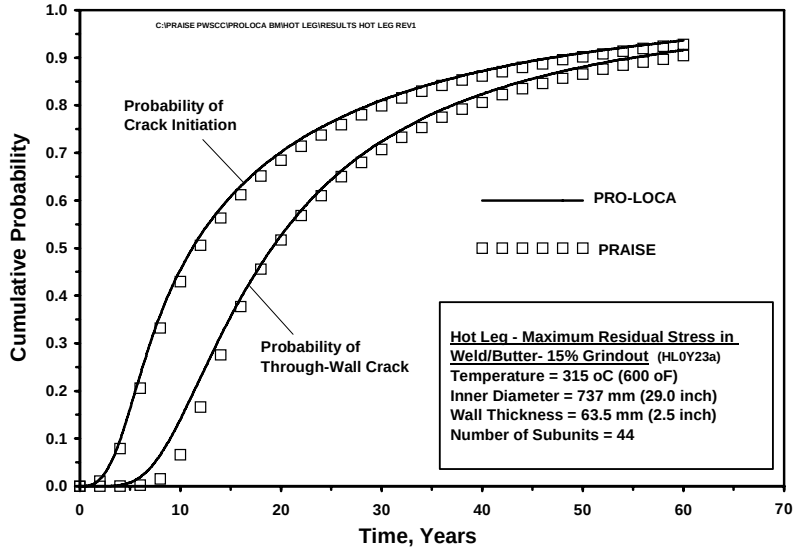

Figure 3.4. Calculated Failure Probabilities for Hot-Leg Weld with 15% Grid Out and Repair

had an inner-diameter (ID) weld repair and associated weld residual stresses, which may not be representative of other welds. The calculations (Figure 3.3) for a more representative weld (without repairs) showed a somewhat lower calculated failure probability, but even this probability was significantly greater than expected from operating experience. Additional reasons for the predictions of relatively high-failure probabilities are discussed in Section 4. Sensitivity calculations are performed in Section 5 for the hot-leg case that show that an alternative PFM model for crack initiation along with refined estimates of operating stresses predicts probabilities more consistent with field experience.

3.2 PWR Surge Nozzle Weld – PWSCC

This set of calculations addressed the Alloy 182 weld connecting the surge line to the pressurizer. Specific parameters for this calculation were

- Temperature = 345°C (653°F)
- Inner Diameter = 282 mm (11.12 in.)
- Wall Thickness = 35.7 mm (1.41 in.)
- Number of Circumferential Subunits = 44
- Residual Stress = See Figure 3.5
- Depth of Initiated Cracks = 3 mm (0.12 in.)
- Length of Initiated Cracks = 10 mm (0.39 in.)

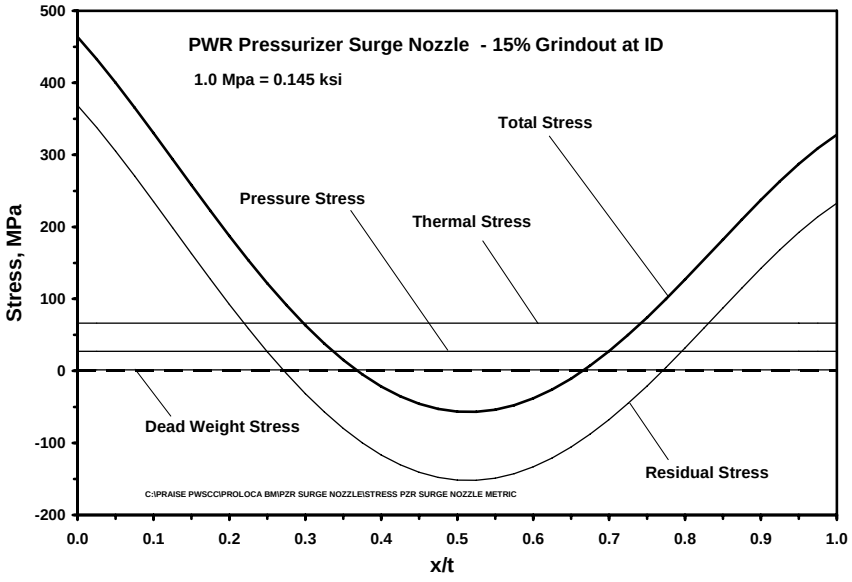

Figure 3.5. Stress Input for Pressurizer Surge Nozzle Weld with 15% Grind Out and Repair

Modeling Considerations – The PRO-LOCA and PRAISE codes used common inputs for the multiple-cracking simulation. These inputs specified the number of potential crack sites (44) and the dimensions of the initiated cracks. Starting with the initiated crack size, the model then began the simulation of the crack-growth process using a fracture mechanics model.

Crack initiation times were predicted using equations described in documentation for the PRO-LOCA code. These equations had been developed by W. Shack of Argonne National Laboratory for Alloy 600 and Alloy 182 based on service-related cracking data for Alloy 600 CRDM nozzles. The equations use a Weibull distribution function to simulate the scatter in crack-initiation times with a triangular distribution to characterize the uncertainty in the scale parameter of the Weibull function. In each case, the calculated initiation times were adjusted for temperature effects using an Arraheius relationship with activation

energy of 210 kJ/mole (50 kcal/mole). Except for an adjustment to account for the higher temperature of the surge nozzle, the calculated initiation times were the same as for the previous hot-leg example. As for the hot-leg example, the CRDM data correlation was adjusted for a higher stress in a dissimilar metal butt weld compared to the CRDM component (ratio = 1.0/0.75). Again, this stress ratio was assigned a common value applicable to all butt welds independent of factors such as pipe-wall thickness.

Stress Inputs – The residual stress distribution and operating stresses were as shown in Figure 3.5. The operating stresses were associated with the internal pressure, dead-weight loading, and a thermal expansion bending moment acting on the pipe cross section.

Results of Calculations – Figure 3.6 shows the calculated failure probabilities as a function of time for (1) crack initiation (initiation of one or more cracks) and (2) through-wall cracking. The numerical agreement between PRO-LOCA and PRAISE is seen to be excellent. Both codes predict a 50% probability of crack initiation by about 3 years and a 50% probability of a through-wall crack by about 6 years.

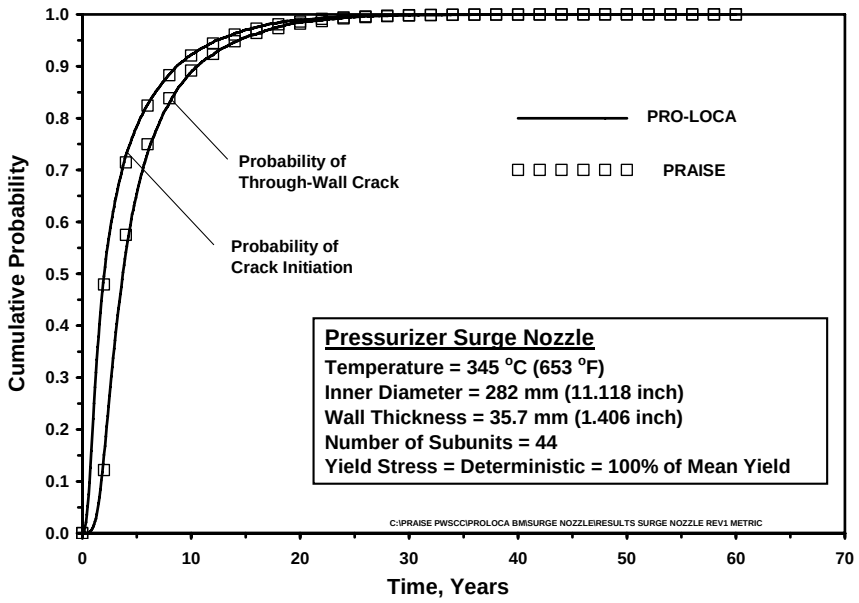

Figure 3.6. Calculated Failure Probabilities for Pressurizer Surge Nozzle Weld with 15% Grind Out and Repair

Comparison with Service Experience – Service failure data were evaluated to estimate a probability of through-wall cracking based on operating experience. A failure frequency was calculated in Appendix A based on the number of reported failures. There were two reported events for the surge nozzle location in the mode of cracked or repaired welds, but no failures that involved through-wall cracks. A failure frequency was calculated with consideration of the welds in the relevant population of plants and the corresponding number of plant years of operation. The resulting frequency of through-wall cracks as listed in Table 2.2 was estimated to be 1.2×10^{-6} failures per weld per year. Using a plant

availability of 80 percent, plant operation for 6 years would correspond to 4.8 years for the PFM calculations. At 4.8 years (from Figure 3.6), the probabilistic fracture mechanics calculations predict a cumulative probability of through-wall cracking about 0.50. In contrast, the operating data gives a cumulative probability of $6 \times (1.2 \times 10^{-6}) = 7.2 \times 10^{-6}$ per weld.

Conclusions – The PFM calculations are seen to over predict the probability of through-wall PWSCC cracks in the surge nozzle by about four orders of magnitude. Possible reasons for the large difference are discussed below. Based on sensitivity calculations performed for the hot leg in Section 5, an alternative PFM model for crack initiation along with refined estimates of operating stresses and temperatures would be expected to predict probabilities more consistent with field experience.

3.3 PWR Spray Nozzle Weld – PWSCC

This set of calculations addressed the Alloy 182 weld connecting the small-diameter spray line to the pressurizer. Specific parameters for this calculation were

- Temperature = 345°C (653°F)
- Inner Diameter = 87.4 mm (3.44 in.)
- Wall Thickness = 13.5 mm (0.531 in.)
- Number of Circumferential Subunits = 44
- Residual Stress = See Figure 3.7
- Depth of Initiated Cracks = 3 mm (0.12 in.)
- Length of Initiated Cracks = 10 mm (0.39 in.)

Modeling Considerations – The PRO-LOCA and PRAISE codes used common inputs for the multiple-cracking model. These inputs specified the number of potential crack sites (11) and the dimensions of the initiated cracks. PWSCC crack initiation was predicted using the equations described in the documentation for the PRO-LOCA code. These equations were proposed by W. Shack of ANL for Alloy 600 and Alloy 182 based on service-related cracking data for Alloy 600 CRDM nozzles. These equations use a Weibull distribution function to simulate the scatter in crack-initiation times with a triangular distribution to characterize the uncertainty in the scale parameter of the Weibull function. In each case, the calculated times to crack initiation were adjusted for the effects of temperature using an Arrhenius relationship with activation energy of 210 kJ/mole (50 kcal/mole). Again, the CRDM cracking data were adjusted for a higher stress in a dissimilar metal butt weld compared to the CRDM component (ratio = 1.0/0.75).

Stress Inputs – Two residual stress distributions of Figure 3.7 and Figure 3.8 were used. The spray-line example presented unusual difficulties because the best-estimate residual stresses of Figure 3.7 gave compressive residual stress at the inner surface. The result was a very low level of tensile total stress (48 MPa or 7 ksi) at the inner surface location where the PWSCC cracks were assumed to initiate. In the model, the crack initiation times were predicted by the ANL equations as adopted by the PRO-LOCA code. Therefore, the initiation times were not related to the tensile stress of 48 MPa (7 ksi). Rather, initiation times were calculated by equations that considered the estimated stress level for the individual weld. The operating stresses, as indicated in Figure 3.7 and Figure 3.8, were associated with internal pressure, dead-weight loading, and a thermal expansion bending moment acting on the pipe cross section.

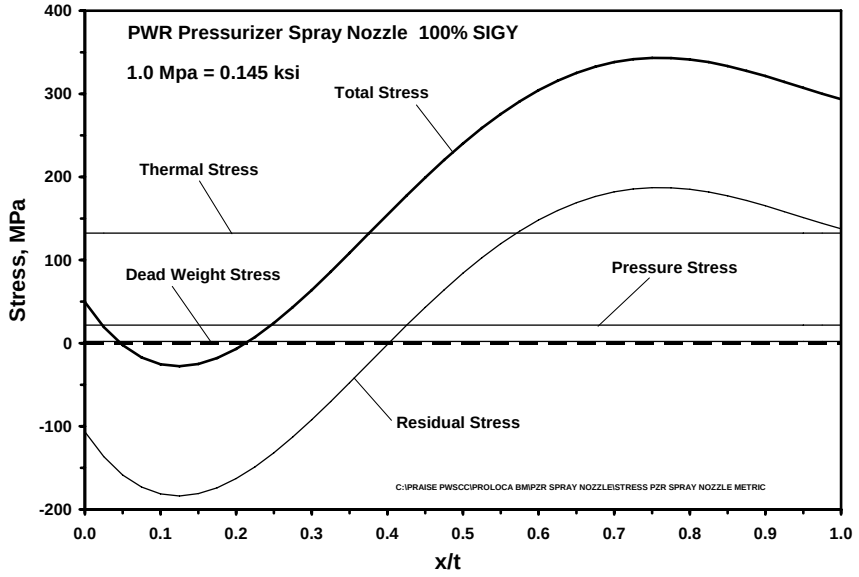

Figure 3.7. Stress Input for Pressurizer Spray Nozzle Weld

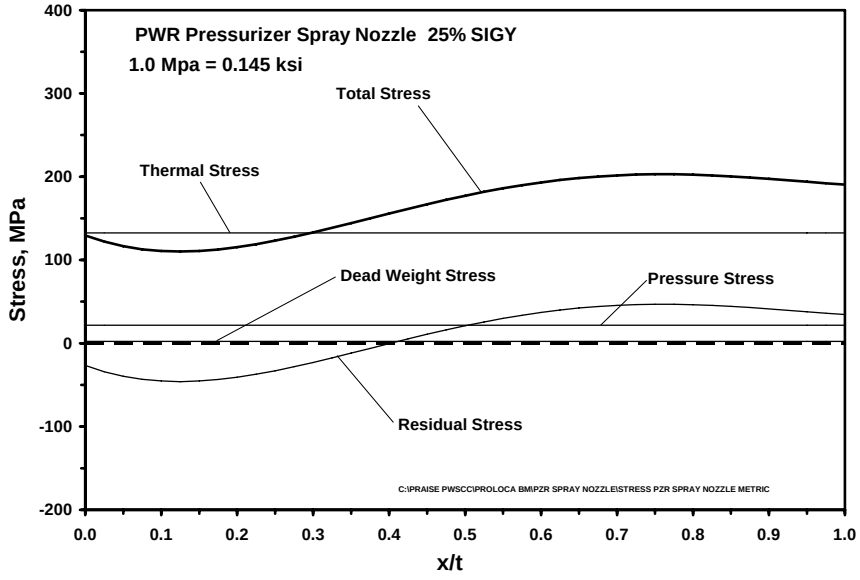

Figure 3.8. Stress Input for Pressurizer Spray Nozzle Weld with Residual Stress Reduced by Factor of 0.25

For the best-estimate residual stress (Figure 3.7), calculations with PRAISE were found to give zero probabilities for through-wall cracks, because the initiated PWSCC cracks were predicted not to grow. The low stress levels at the inner surface of the pipe gave crack-tip stress intensity factors too small to exceed the threshold value (9.0 MPa√meter or 8.19 ksi√in.) needed for the growth of cracks by PWSCC.

It was then proposed that the residual stress distribution of Figure 3.7 may have been an unrealistic representation of the actual stresses. Therefore, the scale factor (material yield strength) used to estimate residual stresses were arbitrarily adjusted downward (to 25% of the nominal yield strength). The modified residual stress (Figure 3.8), when added to the operating stresses, then gave an inner-surface stress of about 139 MPa (20 ksi), which gave a crack-tip stress intensity factor for the initiated crack (depth of 3 mm or 0.12 in.), which was slightly greater than the threshold value for crack growth. The adjusted distribution of residual stress was used for purposes of the benchmarking calculations.

Results of Calculations – Figure 3.9 shows calculated failure probabilities as a function of time for (1) crack initiation (initiation of one or more cracks) and (2) through-wall cracking. The numerical agreement between PRO-LOCA and PRAISE is again seen to be excellent. Both codes predict a 50% probability of crack initiation by about 4 years and a 50% probability of a through-wall crack by about 6 years.

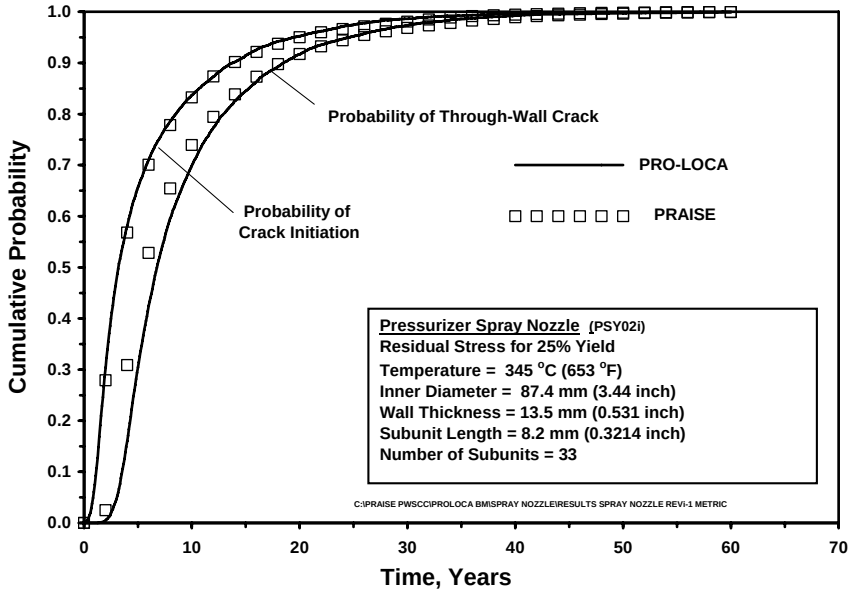

Figure 3.9. Calculated Failure Probabilities for Pressurizer Spray Nozzle Weld

Comparison with Service Experience – Failure data were evaluated to estimate a probability of though-wall cracking based on operating experience. A failure frequency was calculated (see Appendix A) based on the number of reported failures, the number of dissimilar metal spray line welds, and the number of plant years of operation. The resulting frequency (from Table 2.2) of through-wall cracks came to 1.6×10^{-5} failures per weld per year. Using a plant availability of 80 percent, 8 years of plant operation would correspond to about 6 years for the PFM calculations. At 6 years (from Figure 3.9), the calculations give a cumulative probability of through-wall cracking of about 0.5. In contrast, the operating data gives a cumulative probability of $8 \times (1.6 \times 10^{-5}) = 1.28 \times 10^{-4}$.

Conclusions – The PFM calculations are seen to over predict the probability of through-wall PWSCC cracks in the spray nozzle by about four orders of magnitude. Possible reasons for the large difference are

discussed in Section 4, but are at least partly attributable to the arbitrary assignment of residual stress inputs. Based on sensitivity calculations performed for the hot leg in Section 5, an alternative PFM model for crack initiation along with refined estimates of operating stresses and temperatures would be expected to predict probabilities more consistent with field experience.

3.4 BWR Stress Corrosion Cracking

This calculation addressed IGSCC of a stainless steel weld in the recirculation system of a BWR plant. The material was taken to be 304 grade stainless steel and the environment corresponded to normal water chemistry with no credit taken for any of the mitigation measures to prevent IGSCC implemented after about 1987. The intent was to model the circumstances before actions such as described in NUREG-0313 (Hazelton and Koo 1988) were implemented. Specific parameters for this calculation were

- Temperature = 288°C (550°F)
- Inner Diameter = 324 mm (12.75 in.)
- Wall Thickness = 17.2 mm (0.678 in.)
- Number of Circumferential Subunits = 44
- Residual Stress = See Figure 3.5
- Depth of Initiated Cracks = 3 mm (0.12 in.)
- Length of Initiated Cracks = 10 mm (0.39 in.)

Modeling Considerations – Calculations were performed only with the PRO-LOCA code because revision of PRAISE to use updated equations for IGSCC crack initiation and growth was beyond the scope of the study. The PRO-LOCA model simulated the effects of multiple cracking on weld integrity. Inputs prescribed the number of potential crack sites (44) and the dimensions of the initiated cracks.

Stress Inputs – Operating stresses were associated with the internal pressure, dead-weight loading, and thermal expansion bending moments, which together give an operating stress of 141 MPa (20.41 ksi). Details of calculations are described in an ASME paper (Rudland et al. 2006). The oxygen level during steady operation was 0.20 ppm, the coolant conductivity was 0.20 μs/cm, and the degree of sensitization was 7.04 C/cm^2.

Results of Calculations – Figure 3.10 and Figure 3.11 show calculated failure probabilities as a function of time for both crack initiation and for through-wall cracks. PRO-LOCA predicted a probability for crack initiation at 20 years of about 50 percent. The probability of a through-wall crack does not attain 50 percent until about 40 years. Figure 3.10 uses a logarithmic scale to present the same failure probabilities as shown in Figure 3.11. The logarithmic scale allows the plot to show relatively small calculated probabilities from PRO-LOCA for the larger sizes of pipe breaks. The Category 1 LOCA (>378 liter/min [100 gal/min]) is seen to reach a probability of about 1.0×10^{-2} after 40 years of plant operation, whereas the larger LOCA categories are limited to much lower probabilities on the order of 1.0×10^{-4}.

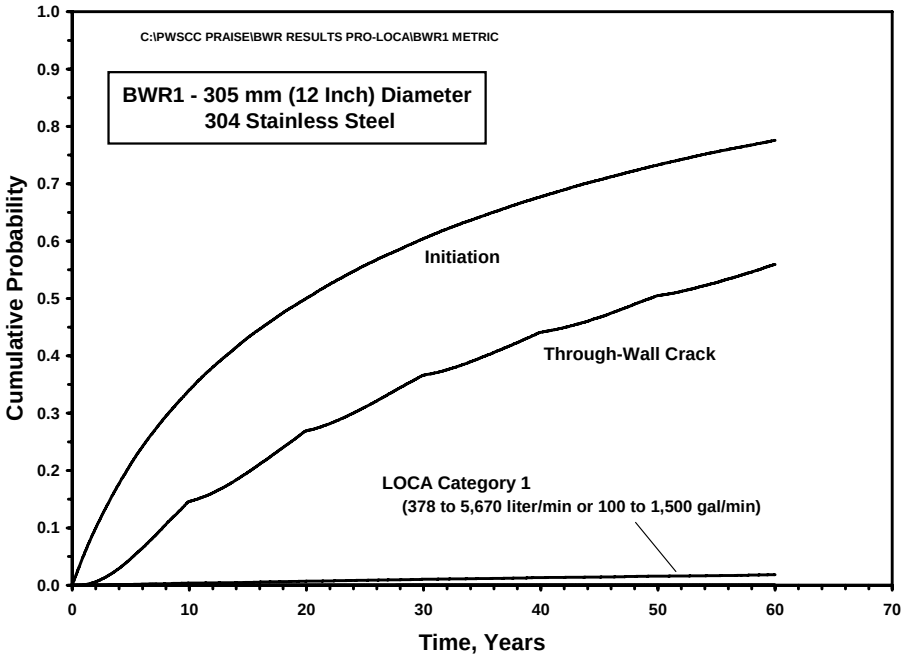

Figure 3.10. Calculated Failure Probabilities from PRO-LOCA for 305-mm (12-in.) Diameter BWR Stainless Steel Pipe Weld (Linear Scale)

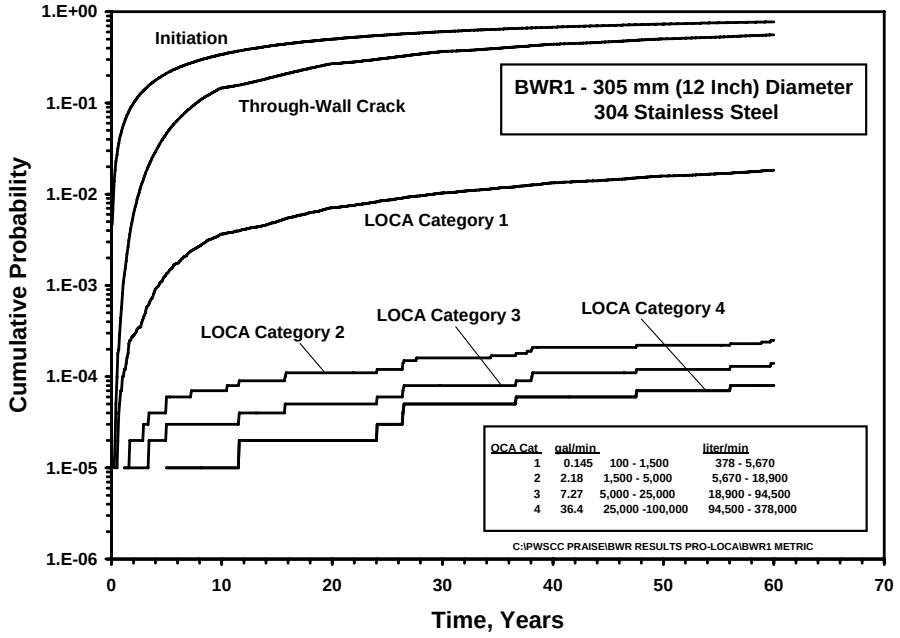

Figure 3.11. Calculated Failure Probabilities from PRO-LOCA for 305-mm (12-in.) Diameter BWR Stainless Steel Pipe Weld (Logarithmic Scale)

Comparison with Service Experience – Failure data from field experience were used to estimate a probability of through-wall cracking. The relevant data were for BWR recirculation piping with nominal pipe sizes in the range of 305 mm (12 in.) and for operating data covering the time period prior to about 1988. Corrective actions (e.g., improved water chemistries and residual stress reductions) were implemented for the post-1988 time periods, and field data show reductions in frequencies of cracking events. For the through-wall cracking, the data gives a failure frequency of 2.80×10^{-4} per weld per calendar year (Table 2.2). The corresponding failure rate from the PFM calculations assumed that the plants operated over 80 percent of each calendar year. Figure 3.10 shows a 20 percent cumulative probability of failure after about 15 years of full-power operation. This gives a failure frequency of $0.20/(0.8 \times 15) = 1.67 \times 10^{-2}$ or about 60 greater than the observed rate from field experience. Sensitivity calculations for IGSCC of BWR piping have been performed by D.O. Harris using the PRAISE code (Tregoning et al. 2005). These results show that uncertainties in modeling IGSCC (e.g., levels of welding residual stresses) can explain the differences between calculated and observed failure probabilities.

Conclusions – In summary, the PRO-LOCA model over predicted the probability of through-wall IGSCC cracks in the BWR piping welds by a factor of about 60. These results, along with other results reported below, suggest that some revisions to the fracture mechanics model and the inputs to the model are needed to achieve a better correlation between predicted and observed failure probabilities.

3.5 PWR Thermal Fatigue

Probabilistic calculations with the PRAISE code simulated fatigue crack initiation and growth for conditions of thermal fatigue applicable to the nozzle cracking that occurred at the Oconee-2 plant. This event resulted in a through-wall leaking crack as described in the licensing event report Licensing Event Report (LER) No. 270/97-001 (USNRC 1997). Fracture mechanics calculations were performed with the PRAISE code for the charging inlet nozzle shown by Figure 3.12.

The cracking was attributed to the loss of a thermal sleeve, which protected the inner surface of the nozzle from fluctuating fluid temperatures. Upon loss of the thermal sleeve, it is believed that thermal fatigue stresses caused fatigue cracks to initiate in a relatively short time period (one year or less). A through-wall crack was found after the plant operating staff detected leakage. The leakage was observed to increase significantly over a period of a few hours and the plant shut down. The leaking crack was subsequently found to extend over a large fraction of the pipe circumference as indicated in Figure 3.13.

Modeling Considerations – The object of the benchmark calculation was to determine if the PRAISE code would (1) predict a very high probability for a through-wall crack within a time period of one year or less and (2) predict linking cracks from multiple initiation sites to give a long through-wall crack extending over half the pipe circumference.

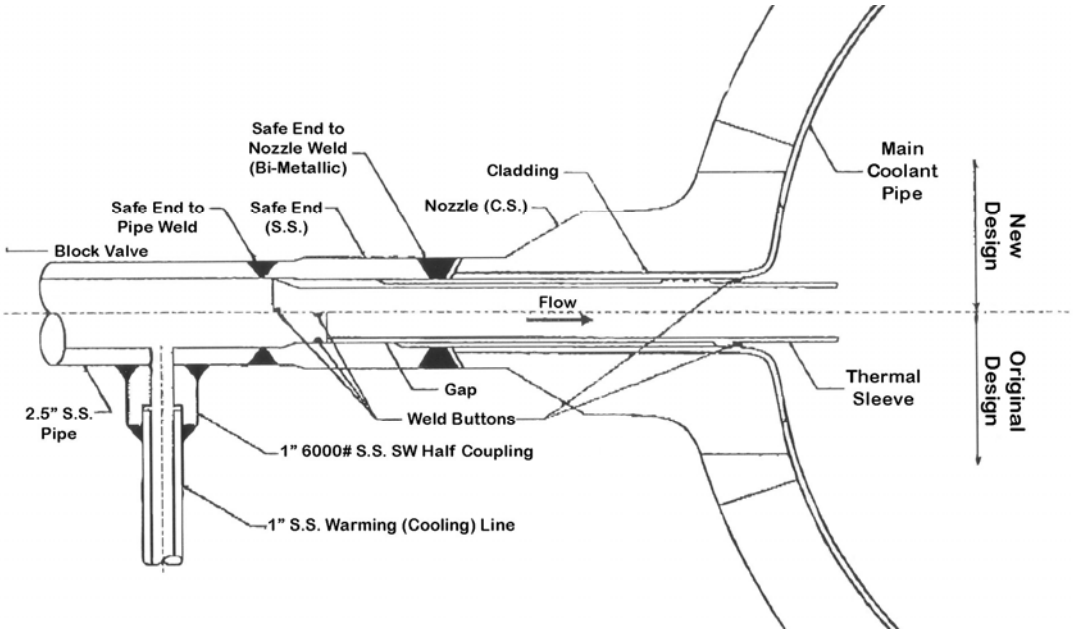

Figure 3.12. Drawing of Oconee-2 Nozzle

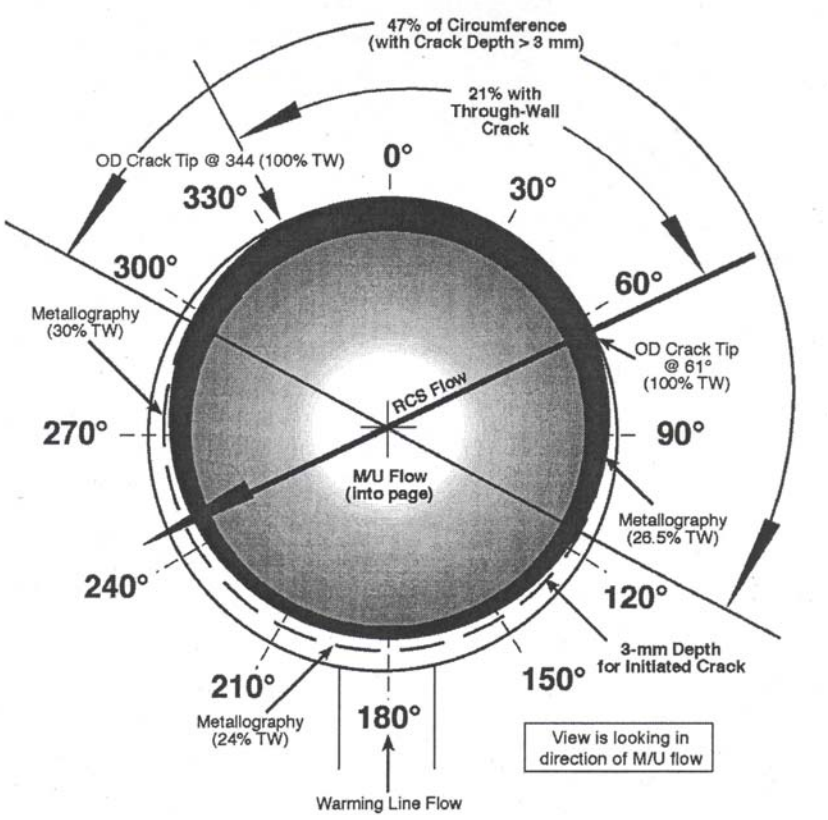

Figure 3.13. Final Configuration of Thermal Fatigue Crack in Failed Oconee-2 Nozzle

Stress Inputs – The dimensions of the 76-mm (3-in.) Schedule 160 nozzle are shown in Figure 3.12. Although possible thermal fatigue loadings have been evaluated (Boman et al. 2000), there remain uncertainties regarding the thermal hydraulic conditions that imposed cyclic thermal stresses to the cracked weld. For purposes of the present calculations, it was assumed that cyclic fluid temperatures were imposed in a uniform manner about the circumference of the nozzle. The differences in system fluid temperatures near the nozzle were known to exceed 149°C (300°F) and this presented a potential for high thermal stress at the nozzle. Because results of finite element stress calculations were not available, the PFM calculations considered a range of cyclic stresses. A large number of stress cycles were assumed to have occurred over a short period of one year (at a rate of one cycle per minute).

Results of Calculations – Probabilistic calculations were performed for several values of cyclic stress ranging from 207 MPa to 517 MPa (30 ksi to 75 ksi). Results of failure probability calculations are shown in Figure 3.14 through Figure 3.18. The highest level of stress (517 MPa or 75 ksi) is seen (Figure 3.14) to give a calculated probability of failure exceeding 50 percent in about 150 days. On the other extreme, the lowest value of stress (207 MPa or 30 ksi) gave only a small probability (about 0.03) for the initiation of a fatigue crack and an even lower probability for a through-wall crack. The results for the lowest stress indicted that a crack would grow to a through-wall depth over a time period as long as two years. At the lowest stress levels, crack initiation is predicted to occur in a fraction of the nozzles, even when cyclic stresses were applied for several years. This is a result of scatter in the fatigue-endurance limit that is part of the crack initiation model used by the PRAISE code.

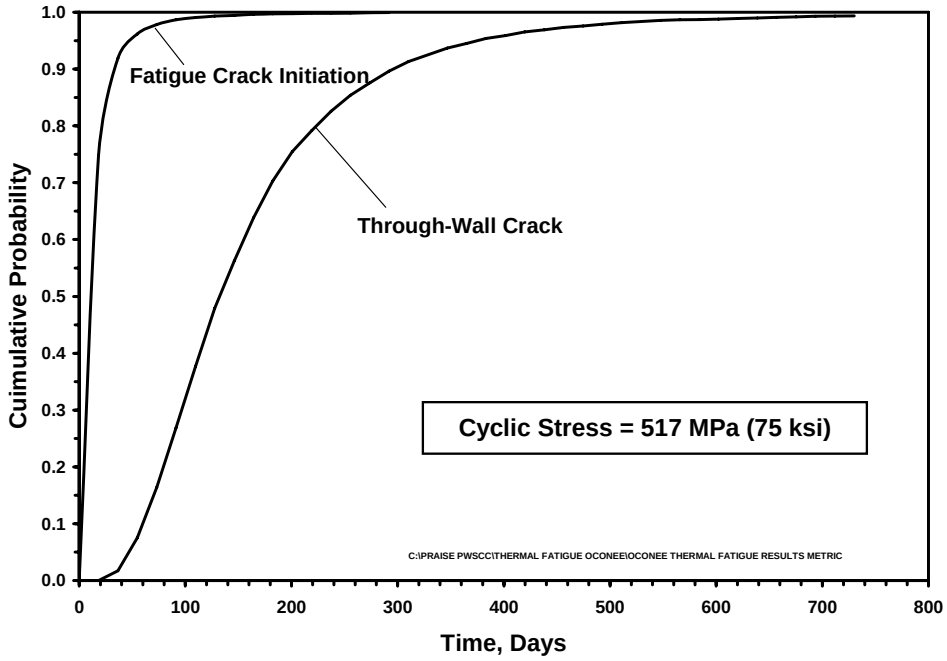

Figure 3.14. Calculated Failure Probabilities for Thermal Fatigue of Weld in 63.5-mm (2.5-in.) Diameter Nozzle for Cyclic Stress of 517 MPa (75 ksi)

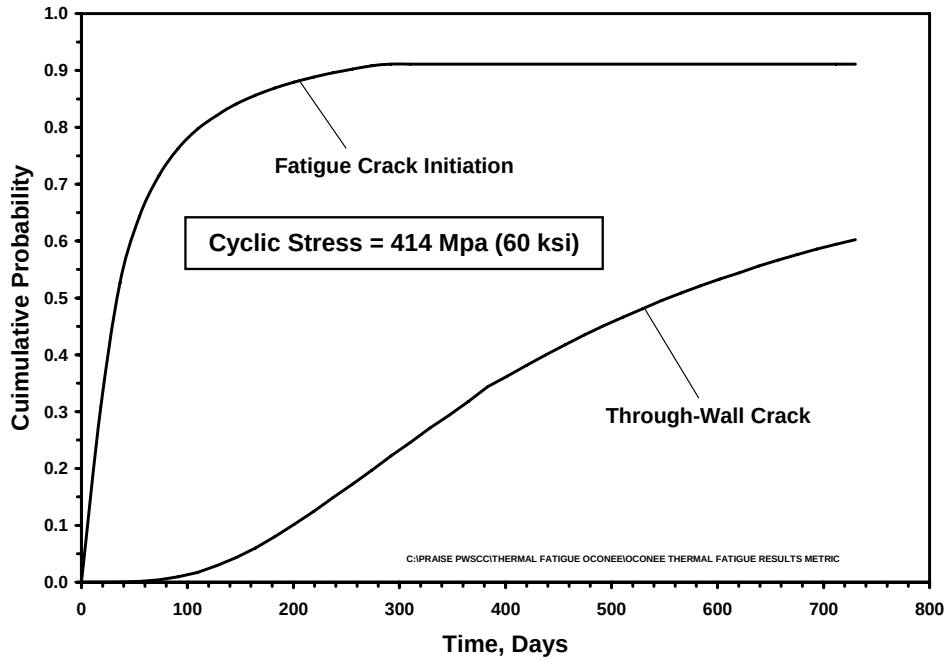

Figure 3.15. Calculated Failure Probabilities for Thermal Fatigue of Weld in 63.5-mm (2.5-in.) Diameter Nozzle for Cyclic Stress of 414 MPa (60 ksi)

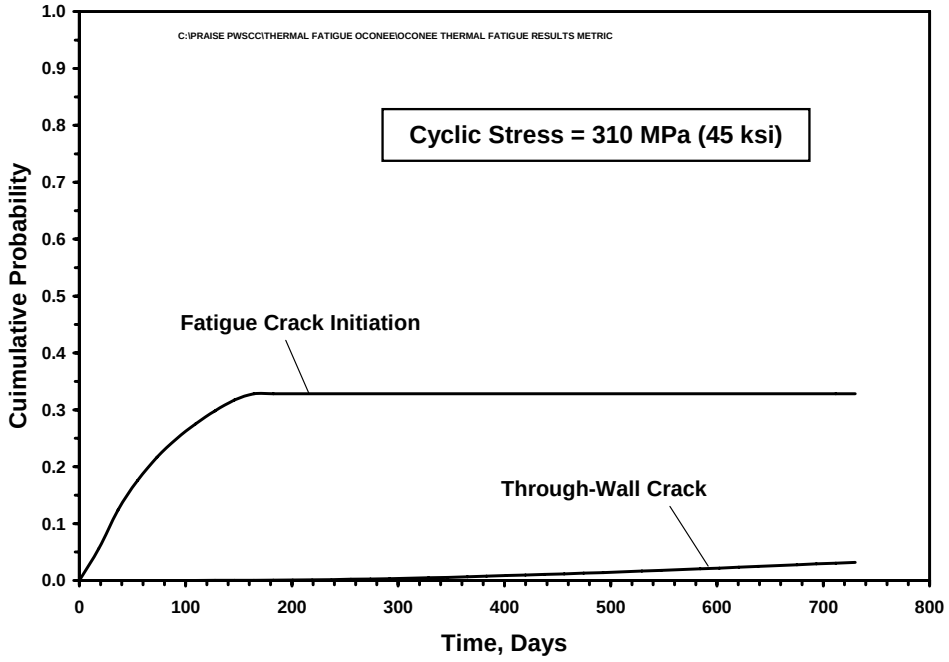

Figure 3.16. Calculated Failure Probabilities for Thermal Fatigue of Weld in 63.5-mm (2.5-in.) Diameter Nozzle for Cyclic Stress of 310 MPa (45 ksi)

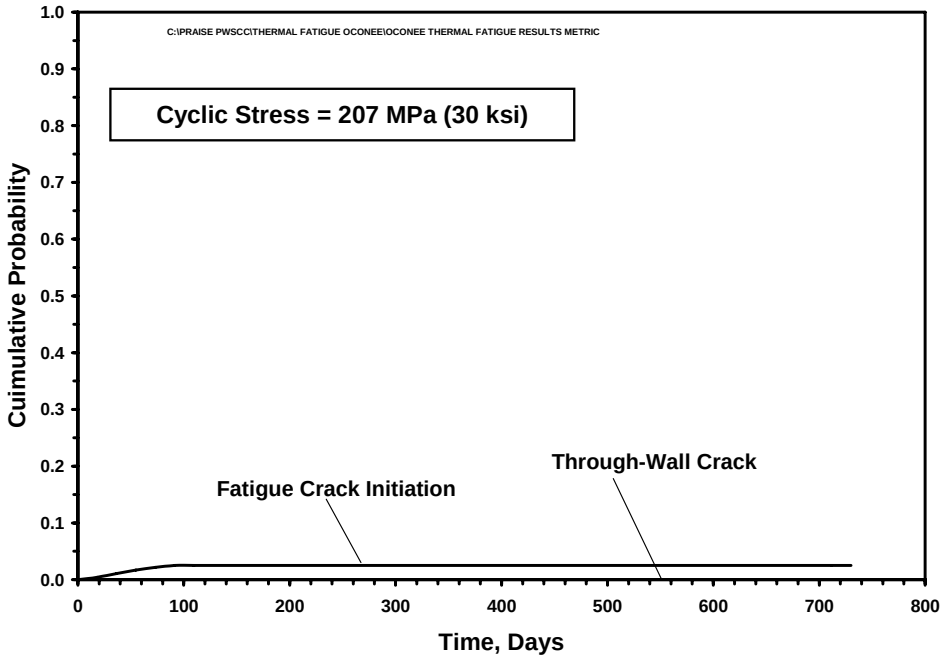

Figure 3.17. Calculated Failure Probabilities for Thermal Fatigue of Weld in 63.5-mm (2.5-in.) Diameter Nozzle for Cyclic Stress of 207 MPa (30 ksi)

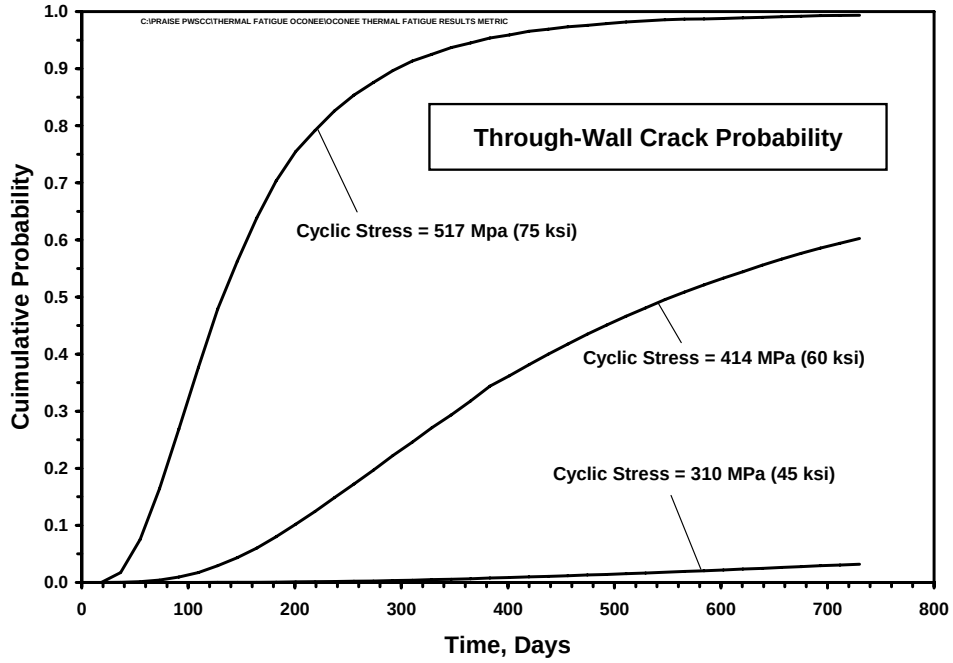

Figure 3.18. Calculated Probabilities of Through-Wall Cracks for Thermal Fatigue of Weld in 63.5-mm (2.5-in.) Diameter Nozzle as a Function of Cyclic Stress

Table 3.2 is an output table generated by PRAISE that shows the degree to which cracks have initiated and grown to various depths and lengths. Cracks were simulated to start at potential initiation sites extending around the circumference of the nozzle. Table 3.2 shows that small cracks are predicted to initiate at the various sites around the circumference. It is also seen that a large fraction of the these cracks are later predicted to link with cracks at adjacent sites such that over time a large fraction of the pipe circumference becomes cracked, consistent with the crack configuration (Figure 3.13) observed on the Oconee-2 nozzle.

Comparison with Field Experience – In summary, an application of the PRAISE code demonstrates the ability of probabilistic fracture mechanics to predict failure probabilities consistent with field failures. The predictions also demonstrate that the multiple-cracking feature of the fracture mechanics model can predict long circumferential flaws also consistent with field failures. Although the calculations were performed only with the PRAISE code, similar results would be expected from the PRO-LOCA code given the similarity of the fracture mechanics models used by the two codes.

Table 3.2. Output Table from PRAISE with Characteristics of Simulated Cracks and Extent of Linking of Multiple Cracks

```
At time (yrs)   2.00

    .00< a/h <=   .30

% circumf.  [ ALL ]|[  1  ][  2  ][  3  ][  4  ][  5  ][6-10 ][11-15][16-20][21-30][31-40][ >41 ]

    .0- 20.0      0|      0      0      0      0      0      0      0      0      0      0      0
  20.0- 40.0      0|      0      0      0      0      0      0      0      0      0      0      0
  40.0- 60.0      0|      0      0      0      0      0      0      0      0      0      0      0
  60.0- 80.0      0|      0      0      0      0      0      0      0      0      0      0      0
  80.0-100.0      0|      0      0      0      0      0      0      0      0      0      0      0

    .30< a/h <=   .60

% circumf.  [ ALL ]|[  1  ][  2  ][  3  ][  4  ][  5  ][6-10 ][11-15][16-20][21-30][31-40][ >41 ]

    .0- 20.0     74|     74      0      0      0      0      0      0      0      0      0      0
  20.0- 40.0      0|      0      0      0      0      0      0      0      0      0      0      0
  40.0- 60.0      0|      0      0      0      0      0      0      0      0      0      0      0
  60.0- 80.0      0|      0      0      0      0      0      0      0      0      0      0      0
  80.0-100.0      0|      0      0      0      0      0      0      0      0      0      0      0

    .60< a/h <=   .80

% circumf.  [ ALL ]|[  1  ][  2  ][  3  ][  4  ][  5  ][6-10 ][11-15][16-20][21-30][31-40][ >41 ]

    .0- 20.0     21|     21      0      0      0      0      0      0      0      0      0      0
  20.0- 40.0     17|      4     13      0      0      0      0      0      0      0      0      0
  40.0- 60.0      0|      0      0      0      0      0      0      0      0      0      0      0
  60.0- 80.0      0|      0      0      0      0      0      0      0      0      0      0      0
  80.0-100.0      0|      0      0      0      0      0      0      0      0      0      0      0

    .80< a/h <=   .95

% circumf.  [ ALL ]|[  1  ][  2  ][  3  ][  4  ][  5  ][6-10 ][11-15][16-20][21-30][31-40][ >41 ]
    .0- 20.0      1|      1      0      0      0      0      0      0      0      0      0      0
  20.0- 40.0     14|     10      4      0      0      0      0      0      0      0      0      0
  40.0- 60.0      2|      2      0      0      0      0      0      0      0      0      0      0
  60.0- 80.0      0|      0      0      0      0      0      0      0      0      0      0      0
  80.0-100.0      0|      0      0      0      0      0      0      0      0      0      0      0

    .95< a/h <= 99.00

% circumf.  [ ALL ]|[  1  ][  2  ][  3  ][  4  ][  5  ][6-10 ][11-15][16-20][21-30][31-40][ >41 ]

    .0- 20.0     13|     13      0      0      0      0      0      0      0      0      0      0
  20.0- 40.0     66|      2     64      0      0      0      0      0      0      0      0      0
  40.0- 60.0    161|     10     85     66      0      0      0      0      0      0      0      0
  60.0- 80.0    267|      6     55    142     64      0      0      0      0      0      0      0
  80.0-100.0    496|      0     40    155    221     80      0      0      0      0      0      0

              >0   >0.3h  >0.6h  >0.8h  >.95h

 Uncracked      0      0      0      0      0
  0 - 20%       0      0      0      7     10
  20-40%       25     25     40     53     65
  40-60%      161    161    167    165    161
  60-80%      318    318    297    279    268
   >80%       496    496    496    496    496
```

4.0 Reconciliation of Calculated and Observed Failure Probabilities

The objective of this section is to reconcile the higher failure probabilities predicted by probabilistic calculations compared to the probabilities derived from field experience. The previous section of this report described calculations with the PRO-LOCA and PRAISE codes for selected LWR components. These calculations addressed failure mechanisms for particular components that have been susceptible to service-induced cracking. While the two codes can predict essentially the same failure probabilities, both codes predicted significantly higher failure probabilities than probabilities derived from data on field failures. In this section, we discuss uncertainties in the fracture mechanics calculations that can explain the differences between calculated and observed failure probabilities.

4.1 Model and Input Uncertainties

Probabilistic fracture mechanics codes have been developed by various organizations to address specific damage mechanisms such as fatigue and stress corrosion cracking. Such codes have, nevertheless, failed to predict field failures, most often because the codes did not address a relevant failure mechanism experienced in the field. For example, certain fatigue models only consider failures from the growth of fabrication flaws and do not consider the initiation of fatigue cracks. When the relevant mechanisms have been addressed, the probabilistic models have then been able to predict the occurrence of failure mechanisms that are consistent with field experience. However, these calculations (as illustrated by the results of Section 3 and the piping fatigue calculations of NUREG/CR-6674 [Khaleel et al. 2000]) have tended was to over predict failure probabilities. The following suggests some reasons for this trend:

Welding Residual Stresses – Inputs for residual stresses in the calculations of Section 3 were based on finite-element calculations that simulated the welding processes. Experimental stress measurements have also been made on some piping welds, but such measurements are expensive and seldom performed. There are no available residual stress measurements for bi-metallic welds to compare with the stresses from the finite-element calculations.

The finite-element calculations of residual stresses assumed a sequence of weld passes and heat inputs and used estimated material properties both at the high temperatures during welding and over the range of temperatures as the weld cools. For any particular weld, the actual welding parameters could differ in detail from those assumed in calculations, and the finite-element modeling also has uncertainties. Some welds can be subject to repairs involving local grind outs of weld passes and welding. Some of the calculations described in Section 3 explicitly accounted for such repairs, and the resulting stress inputs and the calculated failure probabilities show significant effects of such repairs.

The stress inputs used in Section 3 also did not account for changes in residual stresses that can occur during construction and after welds go into plant operation. For example, a safe-end bi-metallic weld may experience additional residual stress changes from welding of the other side of the safe end to the pipe loop. Hydro testing of the piping system can cause yielding and redistribution of the original residual stresses. Service stresses are also superimposed on residual stresses. If residual stresses are already at or near yield, the additional operational stress of a cyclic nature and over long time periods

could cause decreases in peak stresses and associated stress redistributions. Section 5 presents sensitivity calculations that predict significant effects of such yielding and stress redistribution.

Crack Initiation Predictions – The PRO-LOCA and PRAISE calculations of Section 3 have predicted the initiation of PWSCC cracking in piping welds by application of cracking experience for CRDM nozzles. Factors have been applied to crack initiation times to account for effects of temperature and stress levels in welds versus the CRDM component. Another approach for predicting crack initiation is presented in Section 5, which makes use of laboratory data. Both approaches are subject to uncertainties. While both methods account for effects of temperature and stress, there are no explicit treatments of other parameters related to material characteristics and environmental conditions that also impact crack initiation. The randomness in crack-initiation times that is related to variability in these other parameters is not modeled other than indirectly through the statistical distributions used with predictive equations for crack initiation.

Crack-Growth Rates – Section 4.2 provides a detailed discussion of uncertainties in crack-growth rates for PWSCC. As noted above, calculated failure probabilities have been higher than those derived from field experience. This is an indication that cracks may not grow as fast as predicted from laboratory data. The same trend has been noted in the literature by others. Various explanations have been offered including retardation from ligaments in the wake of growing stress corrosion cracks. Other explanations involve effects of corrosion products within the crack on the local chemistry at a crack tip. Observations of changes in the aspect ratios of growing cracks have indicated faster growth rates where a crack intersects the surface compared to slower growth rates for the crack front within the wall thickness. Another issue is the appropriate value (or even if such a value exists) for a threshold stress intensity factor for crack growth.

Circumferential Stress Variations – The PFM calculations have assumed a uniform distribution of stress around the pipe circumference, where some stress categories (dead weight and thermal expansion bending moments) will contribute to circumferential stress variations. The calculations have conservatively assumed that all stresses extend at peak values around the full circumference. An account of circumferential stress variations will reduce predicted probabilities of crack initiation at locations of lower stresses and also reduce crack-growth rates at the lower stress locations. Section 5 presents sensitivity calculations that predict effects of circumferential-stress variations.

Temperatures – Predicted crack initiation times and growth rates for stress corrosion cracking (IGSCC and PWSCC) are sensitive to temperature. The probabilistic calculations were based on nominal temperatures for the welds of interest. Actual temperatures could differ from these nominal temperatures. Design temperatures are conservative or bounding values, such that the use of design temperatures as inputs to probabilistic calculations will result in the over-prediction of failure probabilities. The probabilistic codes do not allow for the explicit treatment of uncertainties in temperatures. Section 5 presents sensitivity calculations that predict the possible effects of temperature uncertainties.

Temperature Factor – The results of Section 3 show a strong effect of temperature on calculated failure probabilities for PWSCC. Temperature effects are based on an Arrhenius equation that requires an input for activation energy. This activation energy was taken to be 50 kcal/mole for crack initiation and 31 kcal/mole for crack growth. Uncertainties in these two values could have a significant impact on the calculated failure probabilities.

Reporting of Field Data – There are uncertainties in the failure probabilities estimated from failures as reported from the field. The reporting for the PIPExp-2006 database on the number of through-wall crack failures is believed to be relatively complete. However, the numbers of failure events for through-wall cracks have been small (in many cases, no failures for the component of interest), which increases the statistical uncertainty for the estimated frequencies because the number of events is very small. Upper and lower bounds for failure frequencies can nevertheless be estimated based on the number of reported events, the number of components, and reactor operating years covered by the database. The numbers are larger for cracks that have less than through-wall depths. However, the reported numbers for such cracked welds are likely to be less than the actual numbers of such cracked welds because of cracks that go undetected due to nondestructive examination (NDE) limitations.

Multiple-Cracking Model – The multiple-cracking models used in PRO-LOCA and PRAISE represent a best effort to account for the initiation, growth, and linking of cracks around the circumference of a weld. The circumference dimensions of the subunits has been assigned to be generally consistent with observed cracks in failed components and/or from consideration of the size of laboratory specimens used to generate crack initiation data. The dimensions (depths and lengths) of the initiated cracks are based in part on judgments regarding the size of an initiated crack that can be detected for the test procedure. Another consideration is that the initiated crack depth should be sufficiently large that fracture mechanics methods can be applied to predict crack growth. Another important modeling consideration is the criteria used to predict the linking of growing cracks in adjacent circumferential subunits. Both PRO-LOCA and PRAISE apply the ASME Section XI flaw proximity rule to determine when two adjacent flaws should be linked. Alternatives to this rule have been considered but have not been implemented into either code. Alternative rules could delay the occurrences of crack linking and thereby give somewhat lower probabilities for through-wall cracks. The effects on predicted probabilities of the larger categories of leaks would be greater than for the probabilities of through-wall cracks.

Independence/Correlation of Crack Initiation and Growth Rates – The probabilistic treatments of crack initiation and crack growth are based on assumptions regarding statistical correlations between sampled parameters. Initiation times for the circumferential subunits of a given weld have been assumed to be independent, such that the crack initiation in one subunit does not imply an increased probability of initiation for other subunits of the same weld. The development of the PRO-LOCA code has included evaluations of various strategies to simulate correlations between crack initiations for the subunits, but these were not included in the version of the code used for calculations described in this report. Introduction of such correlations would increase the probability of linking cracks in adjacent subunits, with a resulting increase in the probabilities of through-wall cracks. Both codes use a common sample parameter to predict the growth of all cracks in a given weld. This approach (correlation between subunits) differs from that used to simulate crack initiation (independence between subunits). There is no correlation between the random sampling for crack initiation and the sampling for crack-growth rates. For example, a crack that initiates relatively early in life does not have a higher-than-average crack-growth rate. Introduction of such a correlation between crack initiation and growth would serve to increase the probability of through-wall cracks.

Insights from NUREG/CR-6674 Calculations – PRAISE calculations of NUREG/CR-6674 (Khaleel et al. 2000) predicted that many leaks should have occurred in PWR and BWR piping systems, while no such leaks have been reported. A review of the possible reasons for this inconsistency noted that the

cyclic stress inputs used in the calculations were based on conservative inputs originally developed for design-fatigue calculations. Some of the conservatism was removed by reducing the number of cycles to a number that was more consistent with operating experience. Cyclic-stress magnitudes were still believed to be unrealistically high because (1) actual thermal transients during operation are often less severe than assumed in the design-stress calculations and (2) load pairs were estimated from conservative design methods which assume worst-case sequences of transients. This approach can give some very high cyclic stresses not experienced during service. The calculations of NUREG/CR-6674 also accounted for reactor-water environmental effects on fatigue crack initiation that required assumptions regarding strain rates for each stress cycle along with environmental parameters such as oxygen content. Lacking exact details of plant-operating conditions, the calculations used somewhat conservative inputs. Although individual inputs were each consistent with possible operating conditions, it is unlikely that all of the conservative inputs would be present at the same time for any given component. The PRAISE model did not allow for explicit modeling of such uncertainties.

4.2 Crack-Growth Rate Considerations

The probabilistic fracture mechanics calculations with PRO-LOCA and PRAISE illustrate that predictions of crack-growth rates (and crack initiation) are subject to large uncertainties and variability. Calculations have, therefore, characterized growth parameters with statistical-distribution functions. The assumption is that the scatter in crack-growth rates growth in the field can be estimated from the observed scatter in laboratory measurements. The following discussion describes some recent information from laboratory studies of PWSCC crack-growth rates. The concern is that a systematic bias may exist for growth rates for field conditions relative to growth rates from laboratory measurements, both in terms of average growth rates and the level of scatter in growth rates. A better understanding of such biases could help to develop improved fracture mechanics models that could give better agreement between predicted failure probabilities with plant-operating experience.

The growth of stress corrosion cracks in structural alloys used for nuclear applications is intrinsically a variable process because of variations in local metallurgical characteristics and crack-driving stresses. Stress corrosion cracking is not dominated by a single variable and, therefore, determination of thresholds for cracking and crack-growth rates requires an understanding of the controlling variables such as stress intensity (Amzallag et al. 2002), corrosion potential, pH, temperature (Andresen 1998), alloy composition and purity, alloy strength, grain boundary condition, etc. (Andresen 2005).

Laboratory tests are intended to provide insights into the processes that influence cracking and to provide evidence for susceptibility to cracking. However, quantification of susceptibility requires crack-growth rate measurements under well-controlled conditions and, if possible, for conditions relevant to cracking of components in the field. Without controlled conditions, data on measured crack rates present a very wide scatter that makes interpretation and application of the data difficult because trends in the data are not reproducible. To obtain reproducible data, testing should follow well-prescribed procedures (Andresen 1998). Testing procedures should include control of the mechanical driving force (crack-tip stress intensity), temperature, water chemistry, and characterization of the alloy metallurgy. In this regard, compact-tension specimens are specifically designed and fabricated to specifications that promote crack growth. Test specimens are notched, side-grooved, and fatigue pre-cracked to introduce a well-defined straight crack front with a sharp tip, conditions that may not exist for cracks growing in components under field conditions.

Crack growth is often observed to become retarded after a period of laboratory testing (Andresen 1998). Inhomogeneity in metallurgy along the crack path (White et al. 2005) can cause changes in the direction of the crack growth, crack branching, changes in cracking mode (intergranular versus transgranular), creation of remaining ligaments in the crack wake, and other ill-defined resistance for crack growth. After observing a retardation of crack growth, testing procedures often impose light fatigue cycling to restore the crack growth back to the original rate. The procedure of light fatigue cycling can give more reproducible crack-growth rates that are useful for quantifying alloy susceptibility for cracking, but may not be representative of the conditions that control crack growth under field conditions.

Stress corrosion cracking in service can differ from cracking in the laboratory. Although laboratory conditions are meant to replicate the service conditions as closely as possible, the characterization of uncertain field conditions presents a challenge. Service cracks must first initiate before they can grow, unlike laboratory pre-cracked specimens. This makes estimates of crack-growth rates difficult (Amzallag et al. 2002), because the time and crack size that defines the initiated crack is difficult to estimate. Also, a major challenge for evaluating service cracks is defining the actual stress intensity driving crack growth in structures having complex variations in metallurgical characteristics and local stresses caused by such factors as welding or surface cold-working (Amzallag et al. 2002). Apart from the calculation of stress intensity factors, service cracks are non-ideal cracks in terms of crack fronts, remaining ligaments, and mode of cracking. Specimens fabricated for testing will also have different metallurgical characteristics compared to materials (including weld deposits) fabricated for service. These differences may complicate measurements of crack-growth rates. The service chemical and thermal histories are not as constant as in laboratory tests. Chemistry control (Morin et al. 1993) at operating plants may have improved in recent years. Temperature variations during periodic shut downs may induce a low-temperature cracking (Mills et al. 2002) effect that deviates from that seen in laboratory tests.

5.0 Calculations Using Laboratory Data for Initiation of PWSCC

It has been noted that the PRO-LOCA model for the initiation of PWSCC cracks applies a probabilistic correlation for the time-to-crack initiation that was derived from data on service cracking observed in CRDM nozzles. This model allows for adjustments to account for stress levels and operating temperatures relative to the stresses and temperatures relevant to the CRDM data. In this section, we describe an alternative probabilistic method for predicting the imitation of PWSCC cracks that is based on laboratory test data. This model explicitly accounts for surface-stress levels that would be provided as inputs to PRO-LOCA. The crack-growth rates are predicted using the same specified stress inputs. The discussion below describes the alternative crack-initiation model and then applies this model in a set of sensitivity calculations that address the effects of stress and temperature.

5.1 Calculational Method

In reviewing the PRO-LOCA calculations and making comparisons with the PRAISE code, it was noted that PRAISE uses a probabilistic model to predict the number of cycles to initiate fatigue cracks given the cyclic stress level and the material and environmental parameters. In this section we describe a probabilistic crack initiation model that was developed for PWSCC crack initiation, which was implemented as an adaptation of the existing fatigue cracking initiation model in PRAISE. The section concludes with a set of demonstration calculations for an Alloy 182 weld in the hot leg of a PWR.

In the PRAISE calculations, PWSCC crack imitation times are treated as an equivalent number of fatigue cycles for crack initiation. This allowed the PRAISE code to treat PWSCC by using an existing code capability that was developed to simulate the initiation of fatigue cracks. The model is presented in this report as an exploratory effort. The predicted failure probabilities from the model appear to be reasonable and consistent with field experience. However, further work is needed to seek additional PWSCC data and to refine the statistical treatment of the data. Refinements of the predictive equations could be used in the future with the PRO-LOCA code.

The proposed PWSCC models closely follow the approach developed in past work for fatigue and stress corrosion applications of PRAISE. A family of curves relates the crack initiation times to the applied stress, temperature, and environmental parameters. Each curve from the family of curves corresponds to a different probability of crack initiation. The parameters for the probabilistic curves are related in part to the scatter in the laboratory test data compared to the best fit curve.

Figure 5.1 was reproduced from documentation for the PRO-LOCA code. The data on this plot came from work by Amzallag et al. (2002), and the curve shown in Figure 5.1 was originally developed for possible use in PRO-LOCA calculations (Scott 1991, 1996), although no calculations based on the Amzallag data were performed because another formulation was adopted. This adopted formulation did not use laboratory data, but rather was based on adjustments to data on reported field failures for Alloy 600 control rod drive nozzles. As indicated in Figure 5.1, the best-fit curve to the Amzallag data (Scott 1991, 1996) would predict very long times to crack initiation for relatively low stresses in the range of 320 MPa (46 ksi). For application to the crack initiation model of the PRAISE code, PNNL developed statistical fits to the data presented in Figure 5.1. The statistical correlations generated a family of curves to describe the scatter in the data as shown by Figure 5.2 and Figure 5.3. The collection of curves on each

figure represents the scatter in the data corresponding to the indicated standard deviations or percentiles relative to the best fit curve.

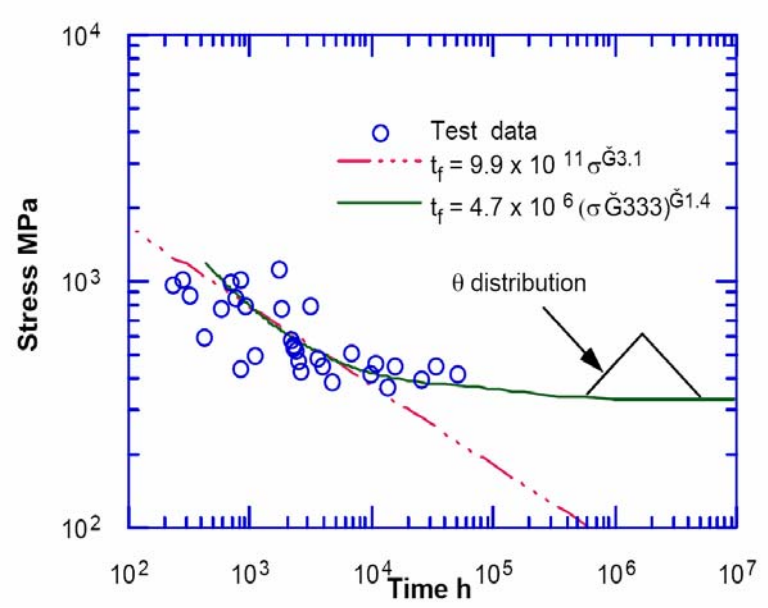

Figure 5.1. Power Law and Scott-Type Fits of Amzallag Data as Presented in Draft Report on PRO-LOCA Report (Amzallag et al. 2002)

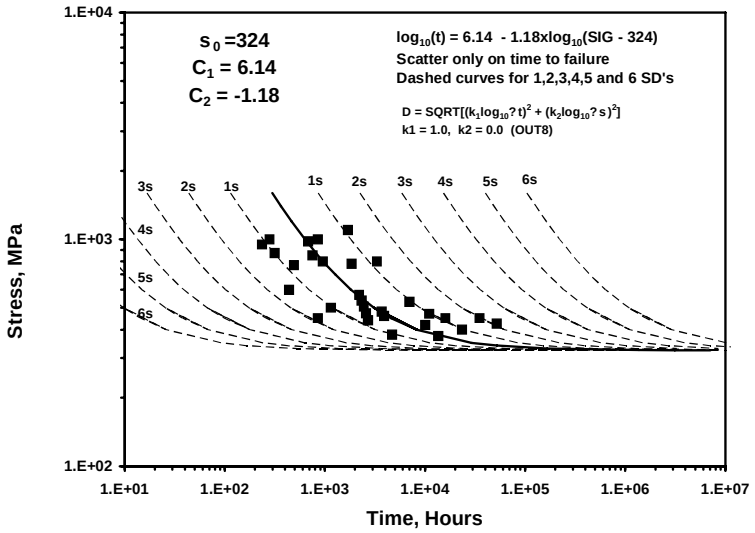

Figure 5.2. Probabilistic Treatment of Amzallag Data with Data Scatter Evaluated in Terms of Time to Failure

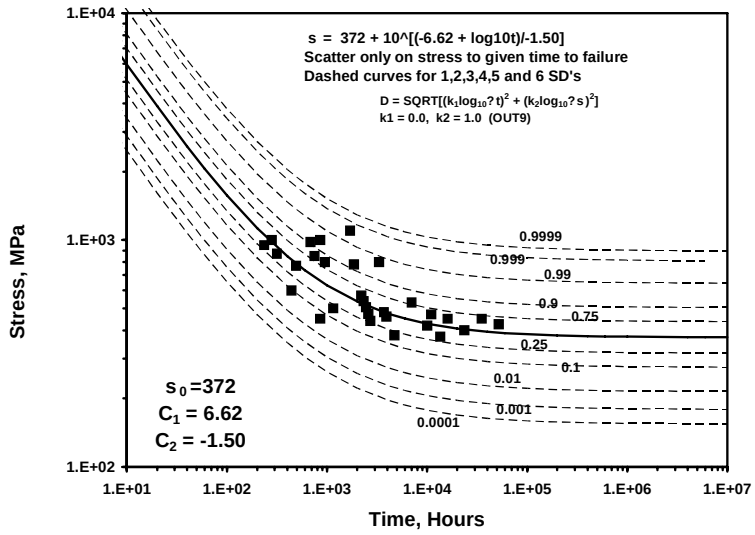

Figure 5.3. Probabilistic Treatment of Amzallag Data with Data Scatter Evaluated in Terms of Stress

A procedure much like that used by Argonne National Laboratory to represent fatigue crack initiation data (Keisler et al. 1995) was applied to derive equations to describe the PWSCC data. The scatter in the data were represented by differences in the data points relative to the best-fit curve as measured either in the vertical direction (stress scale) in Figure 5.2 or the horizontal direction (time scale) in Figure 5.3. Treatment of the variability relative to the stress scale (Figure 5.3) was selected as most suited for predictions of crack initiation at lower stress levels.

The equations used to generate the curves of Figure 5.3 can be applied to obtain various other presentations of the trends for crack initiation by PWSCC as indicated by Figure 5.4 and Figure 5.5. Effects of temperature on crack initiation times are addressed using an Arrhenius dependence taking the activation energy as 50 kcal/mole.

Because the predicted times to crack initiation were derived from laboratory specimen tests, these times were used to predict crack initiation for the subunits of the larger component. This approach is the same as that used in PRAISE for predicting crack initiation from fatigue and IGSCC. The size of the subunits was taken to be on the order of 50.8 mm (2 in.), which is consistent with assumptions in PRAISE for fatigue and IGSCC cracking and also consistent with PRO-LOCA calculations. The depth of the initiated crack at the start of the crack-growth simulation was 3 mm (0.12 in.), again consistent with prior PRAISE and PRO-LOCA models. In the calculations presented below, the initial crack length was taken to be 10 mm (0.4 in.), or the same as that used in Section 3.

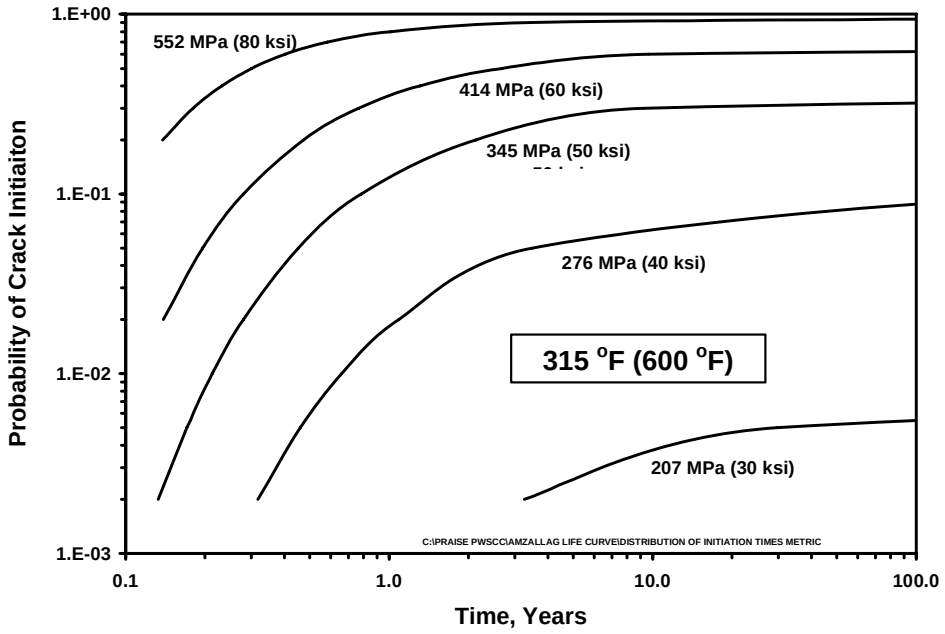

Figure 5.4. Probabilistic Representation of Amzallag Data for Temperature of 315°C (600°F)

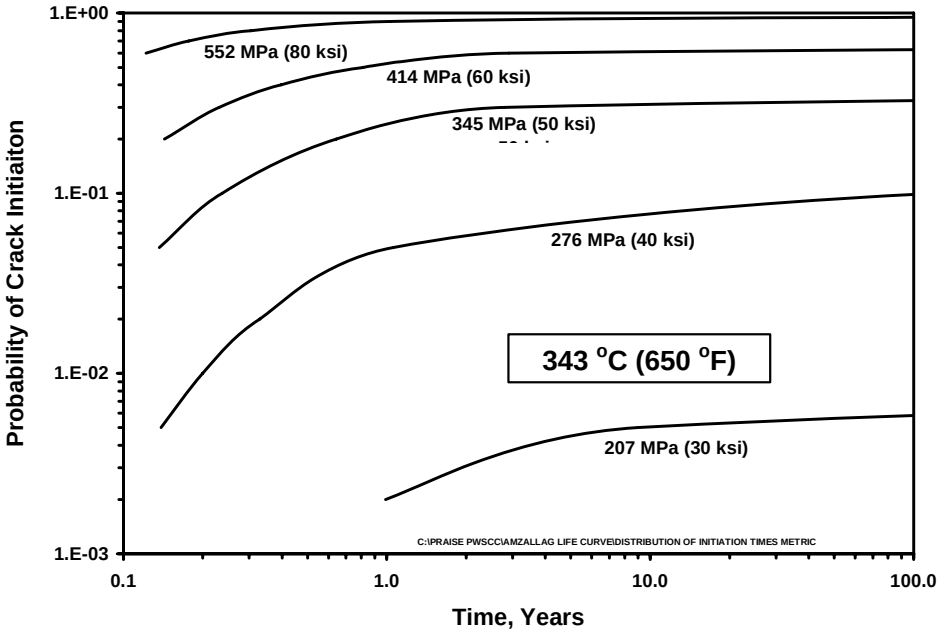

Figure 5.5. Probabilistic Representation of Amzallag Data for Temperature of 343°C (650°F)

5.2 Application to Hot-Leg Bi-metallic Weld

This section describes sensitivity calculations that apply the model for the initiation of PWSCC as presented in Section 5.1. These calculations also simulated the subsequent growth of the initiated cracks, using the same methods and crack-growth rate equations as used in Section 3. The hot-leg example of Section 3.1 was revisited for demonstrating an alternative crack-initiation model. In sensitivity calculations, results of calculations predict the reductions in probabilities of through-wall cracks that are associated with revised inputs for residual stresses, operational stress, and temperatures.

5.2.1 Baseline Case

Using the PRAISE code, probabilistic fracture mechanics calculations were performed for the PWR hot-leg example as described in Section 3.1. The times to initiate cracks by PWSCC were simulated using the same stress-time relationships that were used to generate the plots of Figure 5.3. Calculations were performed for both cases of residual stress (Figure 3.1and Figure 3.2) that were used for the benchmark calculation for the PWR hot leg.

Results for calculated probabilities of crack initiation and through-wall cracking (as a function of time) are shown in Figure 5.6 and Figure 5.7. Failure probabilities shown in Figure 5.7 are related to the very high surface stress caused by an inner surface grind out and subsequent repair welding. It is seen that PRAISE predicts very early times (one year or less) for crack initiation. The plots of Figure 5.6 and Figure 5.7 also show for comparison the crack-initiation times from the PRO-LOCA code, where these initiation times were derived from cracking experience of Alloy 600 CRDM nozzles. The calculated crack-initiation times from PRO-LOCA are somewhat longer (about 10 years for a 50% probability) compared to only a few years as predicted by PRAISE using the initiation model of Figure 5.3.

In summary, exploratory calculations with PRAISE were performed. The calculations demonstrated that laboratory data for crack initiation of PWSCC can be used as the basis for a PFM model. With this model it is possible to treat the effects of stress and temperature in an explicit manner using a common stress input for both crack initiation and crack growth. Results of the calculations appear to give results similar to those from the PRO-LOCA code. As with the PRO-LOCA model for crack initiation, the predicted failure probabilities for the baseline stress inputs are greater than indicated by plant-operating experience. However, as shown by the sensitivity calculations described in Section 5.2.2, considerations of a redistribution of stresses to reduce peak-surface stresses results in predicted failure probabilities in better agreement with operating experience. These calculations should, nevertheless, be considered exploratory in nature until future work can be based on application of additional data for crack initiation times and on improved correlations and statistical treatment of the crack initiation data.

5.2.2 Effects of Stress Redistributions

The very short predicted times to crack initiation from PRAISE, as shown in Figure 5.6 and Figure 5.7, are a direct result of the high stresses at the inner surface. These high stresses come largely from inputs for residual stresses based on finite element calculations. As noted above, there are uncertainties in the residual stresses, because there are no data on measured stresses in components such as the hot-leg weld as they would exist after extended periods of service and after repeated cycling of stress and temperature.

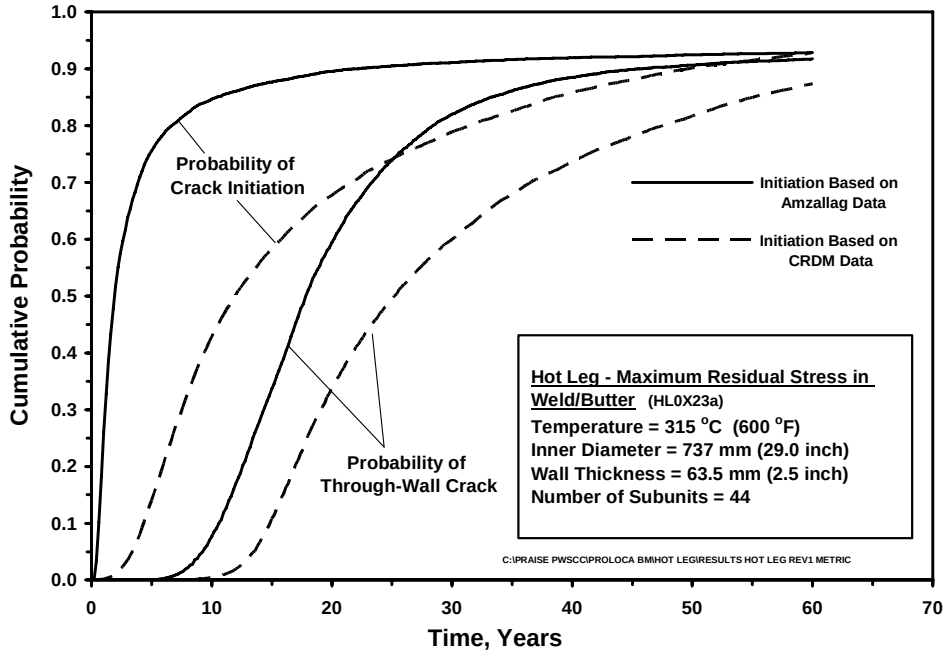

Figure 5.6. Calculated Failure Probabilities for Hot-Leg Weld – With Initiation Predicted Using Amzallag versus CRDM Data – Without 15% Grid Out and Repair

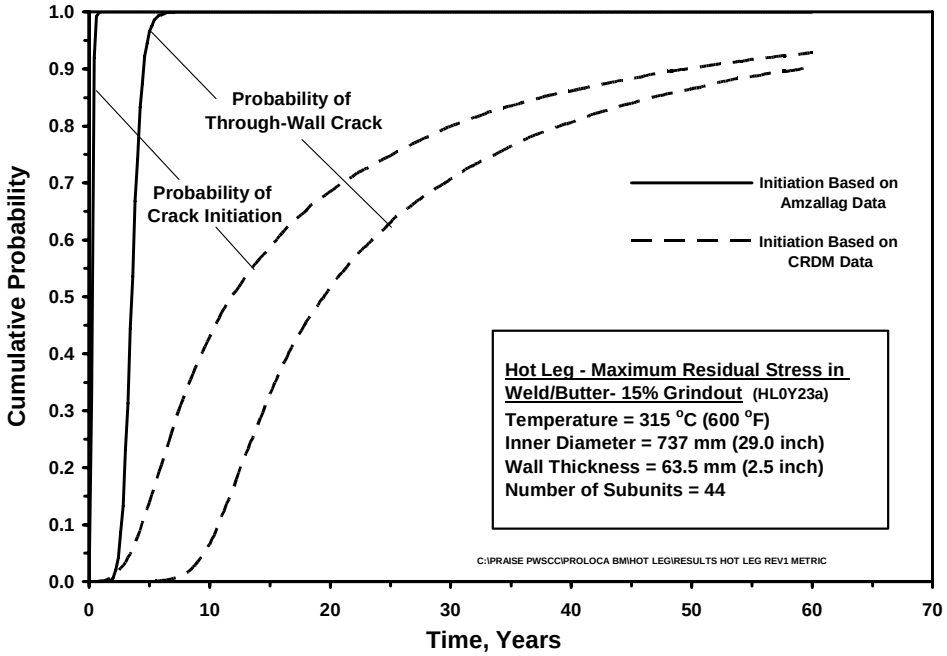

Figure 5.7. Calculated Failure Probabilities for Hot-Leg Weld – With Initiation Predicted Using Amzallag versus CRDM Data – With 15% Grid Out and Repair

In the calculations presented below, it was postulated that the peak surfaces are unrealistically high because of uncertainties in the finite-element calculations of residual stresses and/or stress relaxation after welding. Depending on the yield strength of the weld and surrounding base metal, the inside-surface stresses (residual stresses plus operational stresses) may exceed yield. Bi-metallic welds will also see excursions in temperature and associated cyclic stresses related to the thermal-expansion mismatch between the materials at the weld location. For the present calculations, the stress redistribution was treated as entirely the result of local yielding. These calculations assumed possible "yield strengths" of 207, 241, and 276 MPa (30, 35, and 40 ksi). These values are lower than believed representative for the Alloy 182 weld metal, but served as a convenient means to address the uncertainties in peak stresses that exist in a service-exposed weld.

The redistribution of stresses was evaluated with the resulting through-wall stress profiles shown in Figure 5.8 and Figure 5.9. In each case, if the stress exceeded the assumed yield stress at a given location, the stress at that location was reduced to the yield stress. The resulting axial load at that location was then calculated and compared with the axial load prior to the redistribution of stress. An increment of uniform axial stress was then added to restore the axial load to the original level. This process of adjustment was repeated until required incremental adjustments converged to zero.

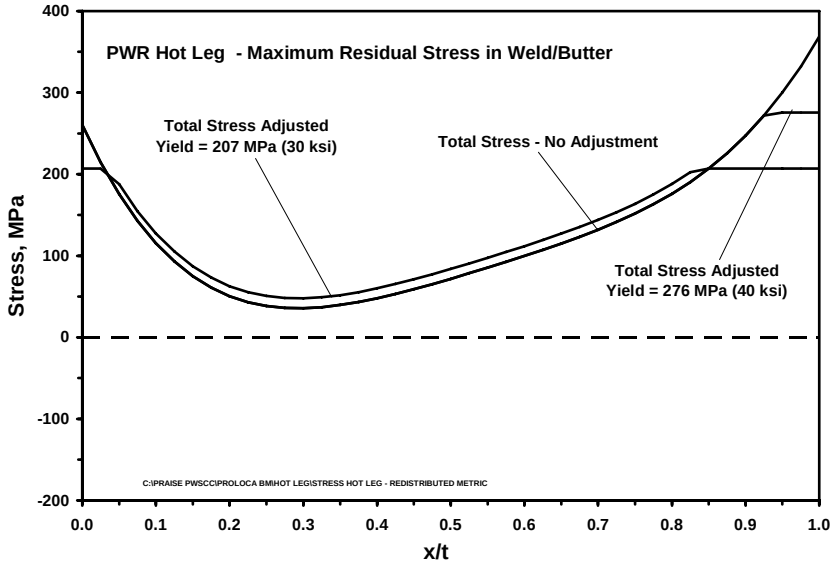

Figure 5.8. Stress Inputs Accounting for Yielding and Stress Redistribution – Hot-Leg Weld Without 15% Grid Out and Repair

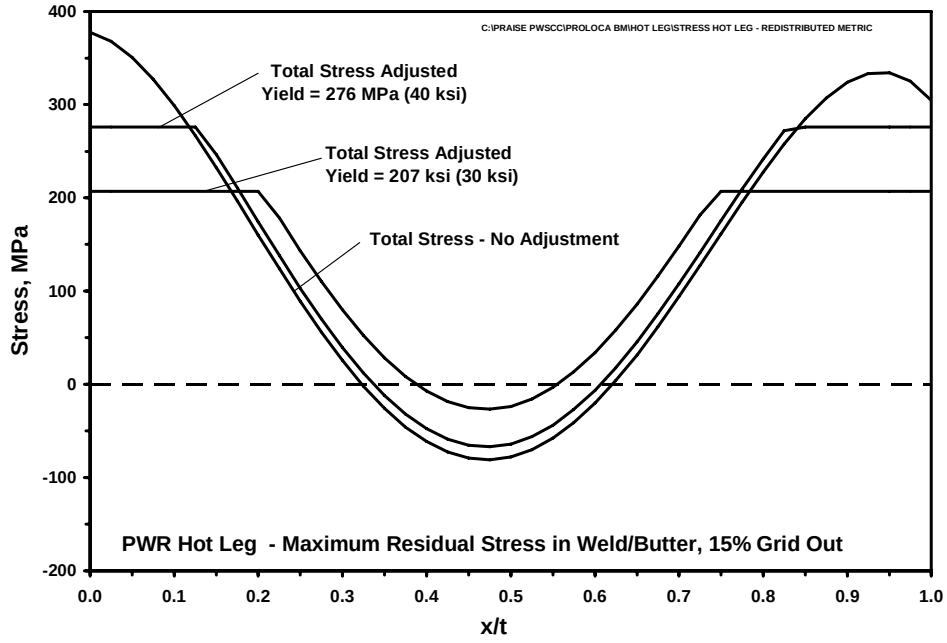

Figure 5.9. Stress Inputs Accounting for Yielding and Stress Redistribution – Hot-Leg Weld With 15% Grid Out and Repair

Figure 5.8 and Figure 5.9 show substantial reductions in peak stresses at the inner and outer surfaces, but relatively smaller reductions in stresses through the majority of the wall thickness. Therefore, the redistribution of stress should give a relatively large increase in the time required to initiate a crack, but a smaller effect on the time to grow the crack to a through-wall depth.

Figure 5.10 and Figure 5.11 show the results of PRAISE calculations that accounted for the reduced levels of peak stresses. The effect, as expected, was to significantly increase the predicted times to crack initiation and also to extend the time period needed to grow the cracks to through-wall depths. The results gave more predictions for probabilities of through-wall cracks, which were more consistent with plant-operating experience. Crack-initiation probabilities at 40 years were reduced from 90 to 100 percent to values as low as 20 percent (for yield strength of 207 MPa or 30 ksi). Calculated through-wall crack probabilities were also greatly reduced, particularly at times early in the plant life. For example, Figure 5.10 shows a through-wall crack probability of over 50 percent after 10 years; whereas, with stresses adjusted for a 207 MPa (30 ksi) yield strength, the probability is reduced to less than 1 percent.

In summary, reductions in peak stresses have a significant effect on calculated failure probabilities. With the selection of a suitable value for specified yield strength, it was possible with the PWSCC initiation model to use PRAISE to generate predicted failure probability curves that are similar to those based on the crack-initiation model of the PRO-LOCA code. Results of calculations appear to be reasonable and able to predict probabilities more consistent with plant-operating experience once the redistribution of stresses associated with a reduction in peak-surface stresses is addressed.

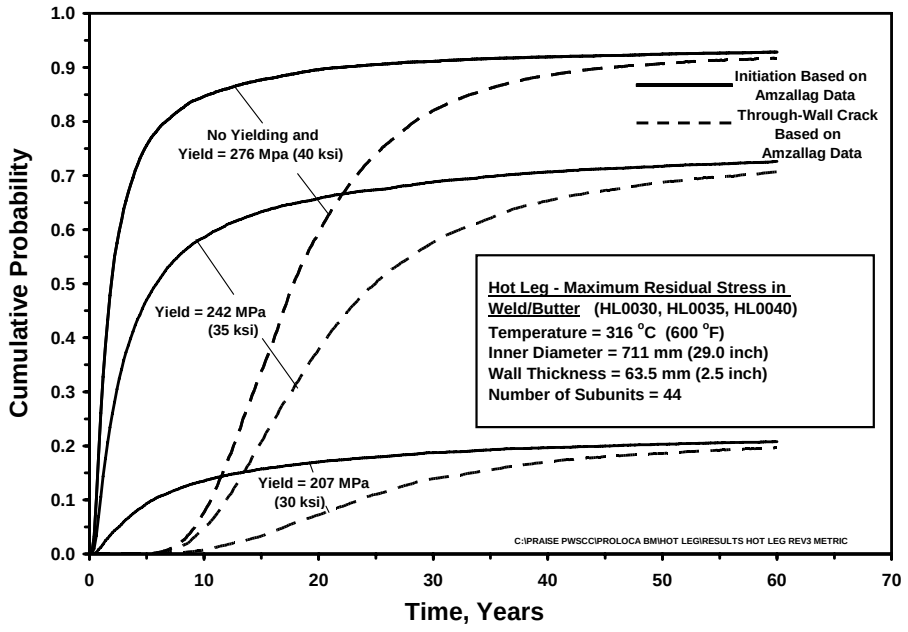

Figure 5.10. Calculated Failure Probabilities with Effect of Yielding and Stress Redistribution for Hot-Leg Weld – Initiation Predicted Using Amzallag CRDM Data – Without 15% Grid Out and Repair

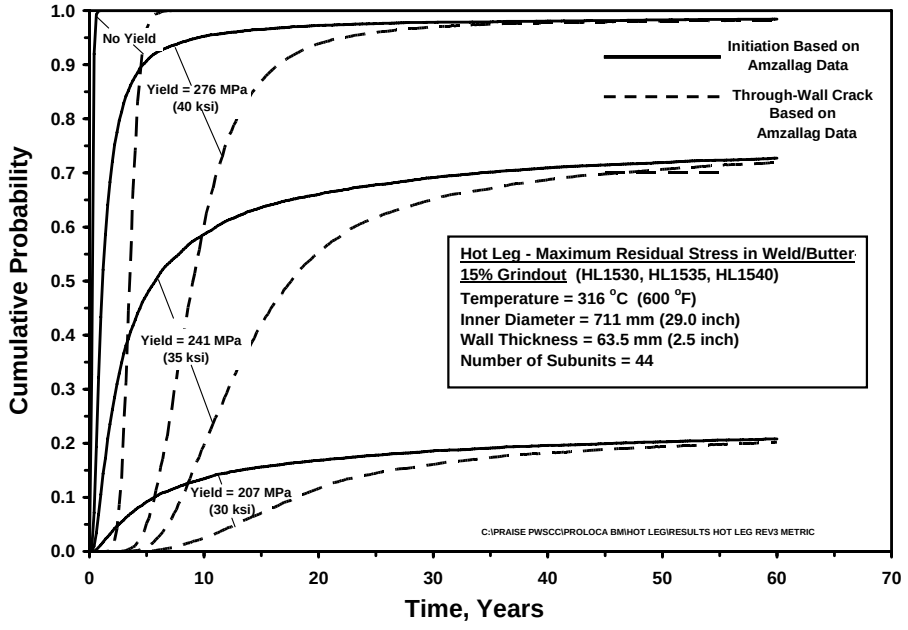

Figure 5.11. Calculated Failure Probabilities with Effect of Yielding and Stress Redistribution for Hot Leg Weld – Initiation Predicted Using Amzallag CRDM Data – With 15% Grid Out and Repair

5.2.3 Effects of Circumferential Stress Variation

The calculations just presented above considered the highest stressed location around the circumference of the pipe and assumed that all locations are stressed at this maximum level. In practice, some portion of the maximum stress is due to thermal expansion bending moments and dead-weight loadings. Both of these loadings will give stresses with circumferential variations, such that at 180° from the worst-case location the stresses will attain minimum levels. Although circumferential variations in welding residual stresses are neglected, it is possible that some variations in residual stresses can also occur and add to the variations from the other sources.

Sensitivity calculations were performed to quantify the potential effects of stress variations on calculated failure probabilities. These calculations applied an existing capability in the PRAISE code. Two cases were evaluated. One case assumed a 20 percent difference in stress at the minimum location relative to the maximum stress location. The other case was viewed as a bounding case for which the 20 percent value was increased to 50 percent.

Figure 5.12 and Figure 5.13 show the calculated probabilities of crack initiation and through-wall cracks, respectively. The baseline case assumed a redistribution of peak stresses to a limiting 241-MPa (35-ksi) level, but no circumferential variation. The calculations show a significant effect of circumferential-stress variations. Late in plant life (e.g., 40 years) the crack initiation and through-wall crack probabilities are reduced by a factor of about two. The differences in probabilities at times early in the plant life (10–20 years) are even greater with an order of magnitude difference being predicted.

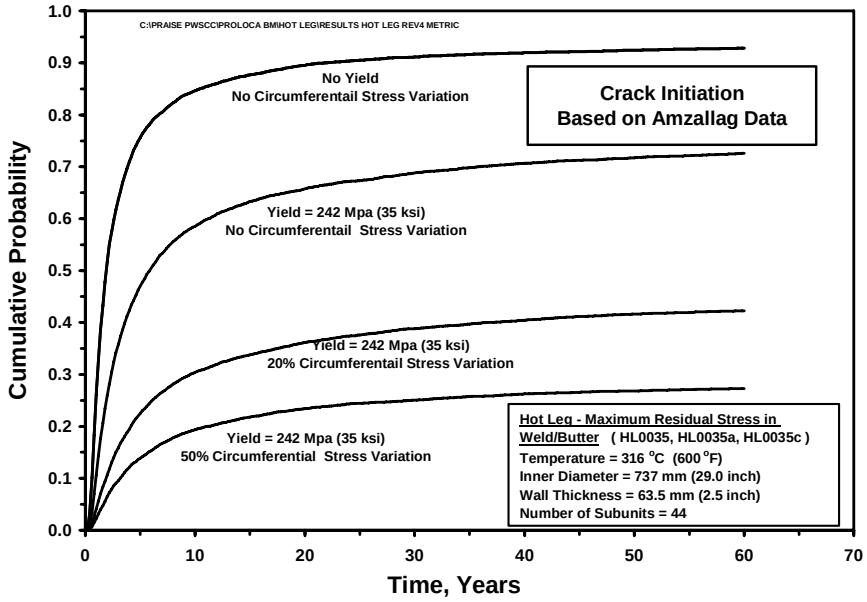

Figure 5.12. Calculated Probabilities of Crack Initiation with Effects of Circumferential Stress Variation and Stress Redistribution for Hot-Leg Weld – Initiation Predicted Using Amzallag CRDM Data – Without 15% Grid Out and Repair

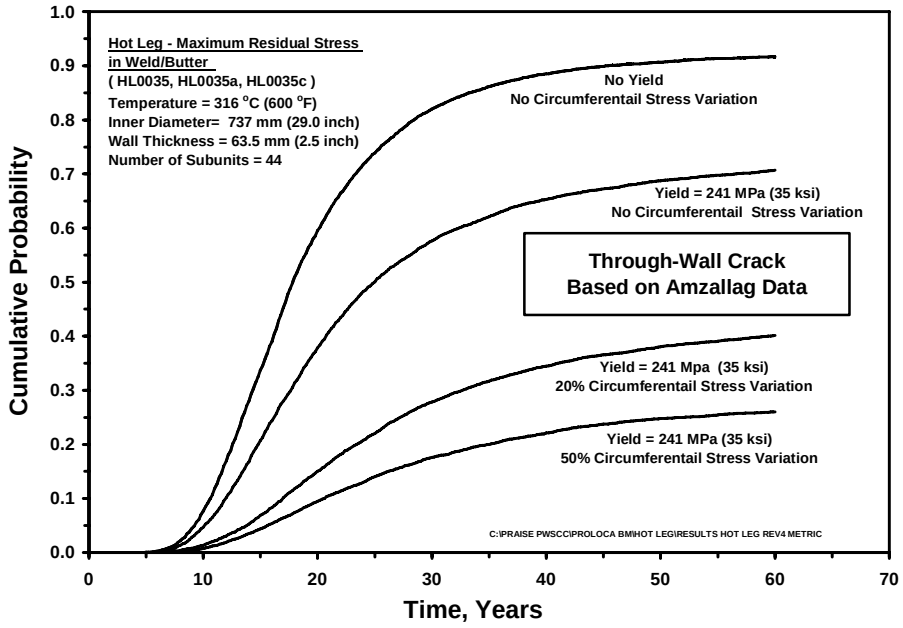

Figure 5.13. Calculated Probabilities of Through-Wall Crack with Effects of Circumferential Stress Variation and Stress Redistribution for Hot-Leg Weld – Initiation Predicted Using Amzallag CRDM Data – Without 15% Grid Out and Repair

5.2.4 Combined Effects Including Temperature Uncertainties

Figure 5.14 summarizes trends from the sensitivity calculations to address the effects of the stress inputs to the probabilistic model. The additional factor of temperature uncertainty was covered by calculations that reduced the operating temperature to 302°C (575°F) from 316°C (600°F). The lower temperature reduces calculated leak probabilities by a factor of about two.

The results of Figure 5.14 were compared with failure probabilities from plant-operating experience. In this case the operating data indicated a cumulative failure probability for the hot-leg weld after 20 years equal to 2.94×10^{-3} per weld. From the calculations for Figure 5.14, the cumulative through-wall crack probability for 20 years of operation was 2.7×10^{-3}. This probability corresponds to a value from the lowest of the curves shown in Figure 5.14 and accounts for the combined effects of (1) stress reductions for a yield strength of 35 ksi, (2) a 20 percent variation in stress about the circumference of the pipe, and (3) an actual operating temperature of 302°C (575°F) compared to the nominal temperature of 316°C (600°F).

In summary, several conservatisms in the original PFM calculation were addressed with plausible, reasonable modifications to input parameters. The results brought the difference between the calculated and observed failure probabilities from a factor of 100 to a difference of less than 10 percent.

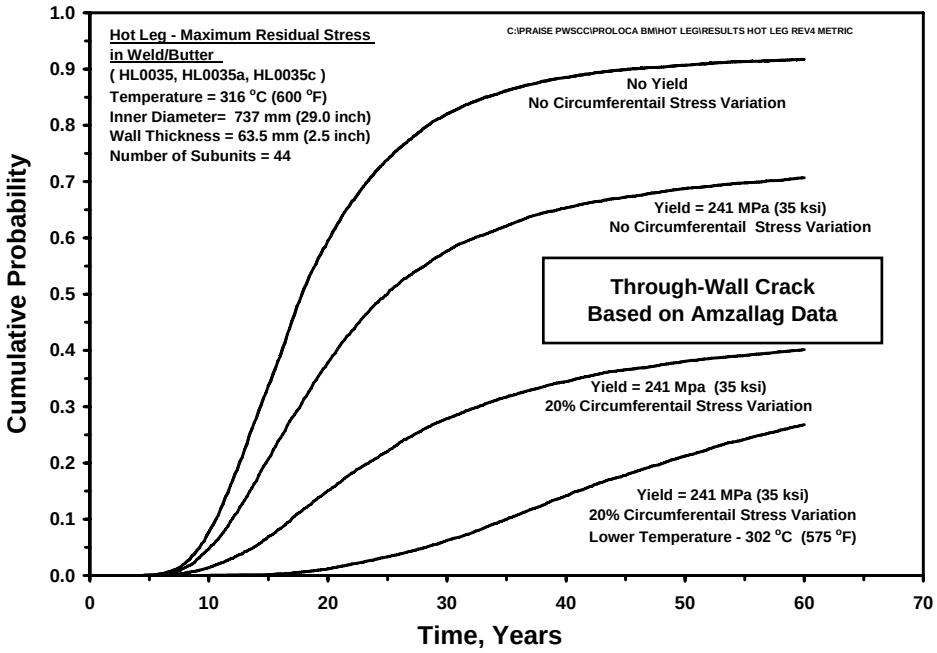

Figure 5.14. Calculated Probabilities of Through-Wall Crack with Effects of Circumferential Stress Variation, Temperature and Stress Redistribution for Hot-Leg Weld – Initiation Predicted Using Amzallag CRDM Data – Without 15% Grid Out and Repair

6.0 Summary and Conclusions

This report has addressed the possible application of probabilistic fracture mechanics computer codes to support the PMDA program as a method to predict component failure probabilities. The present report has described PFM calculations that were performed for selected components using the PRO-LOCA and PRAISE computer codes. The calculations have addressed the failure mechanisms of stress corrosion cracking, intergranular stress corrosion cracking, and fatigue for components and operating conditions that are known to have failed components in the field. The calculations allowed the two computer codes to be compared with each other and, more importantly, benchmarked both codes against the field experience.

The calculations have shown how uncertainties and modeling assumptions can impact calculated failure probabilities. Comparisons with field experience showed that both codes are capable of predicting high-failure probabilities for the components for which operating conditions are known to have produced field failures. It was found that uncertainties in the treatment of degradation mechanisms and in estimates of input parameters can give failure probabilities significantly higher than failure probabilities based on reported field failures. Sensitivity calculations were performed to address uncertainties associated with residual stresses, operating stresses, and temperatures. Results of these calculations showed that the identified uncertainties in the probabilistic calculations were sufficiently large to explain the differences between the predicted and observed failure probabilities. It was not possible, within the scope of the present work, to identify the specific elements of the PFM model and/or inputs that should be refined to achieve better agreement of the predictions with plant-operating experience.

7.0 References

Amzallag C, JM Boursier, C Pagès and C Gimond. 2002. "Stress Corrosion Life Assessment of 182 and 82 Welds Used in PWR Components." *Tenth International Conference on Environmental Degradation of Materials in Nuclear Power Systems— Water Reactor*. August 5-9, 2001. Lake Tahoe, Nevada. CDROM National Association of Corrosion Engineers.

Andresen PL. 1998. "Effects of Testing Characteristics on Observed SCC Behavior in BWRs." *Corrosion 98*. Paper 137. National Association of Corrosion Engineers, Houston, Texas.

Andresen PL. 2005. "Critical Processes to Model in Predicting SCC Response in Hot Water." *Corrosion/05*. Paper 05470. National Association of Corrosion Engineers, Houston, Texas.

Bell CD and OJV Chapman. 2003. *Description of PRODIGAL*. NURBIM Report D4/Appendix F. Rolls-Royce plc., Derby, United Kingdom.

Bishop BA. 1997. "An Updated Structural Reliability Model for Piping Risk Informed ISI." In *Fatigue and Fracture - 1997, Volume 2*, PVP Vol. 346, pp. 245-252. American Society of Mechanical Engineers, New York.

Boman BL, JM Davis, JR Smotrel and TD Brown. 2000. "Evaluation of Oconee-2 High Pressure Injection/Normal Makeup (HPI/NMU) Line Weld Failure." In *Assessment Methodologies for Preventing Failure: Service Experience and Environmental Considerations - Volume 2*, PVP-Vol. 410-2, pp. 111-117. American Society of Mechanical Engineers, New York.

Brickstad B, OJV Chapman, T Schimpfke, H Schulz and A Muhammed. 2004. *Review and Benchmarking of SRM and Associated Software*. NURBIM Final Report D4, Contract FIKS-CT-2001-00172. DNV, Stockholm, Sweden.

Brickstad B and W Zang. 2001. *NURBIT Nuclear RBI Analysis Tool, A Software for Risk Management of Nuclear Components*. Technical Report No 10334900-1. DNV, Stockholm, Sweden.

Dedhia DD, DO Harris and VE Denny. 1982. *TIFFANY: A Computer Code for Thermal Stress Intensity Factors for Surface Cracks in Clad Piping*. Report SAI-333-82-PA. Science Applications, Inc., Palo Alto, California. (LLNL Contract No. 8679501, Task 2)

Dickson TL. 1994. FAVOR: *A Fracture Mechanics Analysis Code for Nuclear Reactor Pressure Vessels, Release 9401*. ORNL/NRC/LTR/94/1. Martin Marietta Energy Systems, Inc., Oak Ridge National Laboratory, Oak Ridge, Tennessee.

Dickson TL, PT Williams and S Yin. 2004. *Fracture Analysis of Vessels – Oak Ridge, FAVOR, v04.1, Computer Code: User's Guide*. NUREG/CR-6855, ORNL/TM-2004/245. Oak Ridge National Laboratory, Oak Ridge, Tennessee.

Dillstrom P. 2003. *A Short Description of ProSACC*. NURBIM Report D4/Appendix G. DNV, Stockholm, Sweden.

Gosselin SR, FA Simonen, RG Carter, JM Davis and GL Stevens. 2005. "Enhanced ASME Section XI Appendix L Flaw Tolerance Procedure." In *Proceedings of the PVP2005, 2005 ASME Pressure Vessels and Piping Conference*, PVP2005-71100, July 17-21, 2005, Denver, Colorado. American Society of Mechanical Engineers, New York.

Harris DO and DD Dedhia. 1992. *Theoretical and User's Manual for pc-PRAISE, A Probabilistic Fracture Mechanics Computer Code for Piping Reliability Analysis*. NUREG/CR-5864. U.S. Nuclear Regulatory Commission, Washington, DC.

Harris DO and DD Dedhia. 1998. *WinPRAISE 98 PRAISE Code in Windows*. Engineering Mechanics Technology, Inc., San Jose, California.

Harris DO, DD Dedhia, ED Eason and SD Patterson. 1986. *Probability of Failure in BWR Reactor Coolant Piping: Probabilistic Treatment of Stress Corrosion Cracking in 304 and 316NG BWR Piping Weldments*. NUREG/CR-4792, Vol. 3. U.S. Nuclear Regulatory Commission, Washington, DC.

Harris DO, EY Lim and DD Dedhia. 1981. *Probability of Pipe Fracture in the Primary Coolant Loop of a PWR Plant Volume 5: Probabilistic Fracture Mechanics Analysis - Load Combination Program Project 1 Final Report*. NUREG/CR-2189, Vol. 5. U.S. Nuclear Regulatory Commission, Washington, DC. Publication information available at http://www.osti.gov/energycitations/product.biblio.jsp?osti_id=5341468

Hazelton W and WH Koo. 1988. *Technical Report on Material Selection and Processing Guidelines for BWR Coolant Pressure Boundary Piping*. NUREG-0313, Rev. 2. U.S. Nuclear Regulatory Commission, Washington, DC.

Keisler J, OK Chopra and WJ Shack. 1995. *Fatigue Strain–Life Behavior of Carbon and Low–Alloy Steels, Austenitic Stainless Steels, and Alloy 600 in LWR Environments*. NUREG/CR-6335. U.S. Nuclear Regulatory Commission, Washington, DC.

Khaleel MA and F Simonen. 1994a. "The Effects of Initial Flaw Sizes and Inservice Inspection on Piping Reliability." In *Service Experience and Reliability Improvement: Nuclear, Fossil, and Petrochemical Plants*, PVP-Vol. 288, pp. 95-07. American Society of Mechanical Engineers, New York.

Khaleel MA and FA Simonen. 1994b. "A Parametric Approach to Predicting the Effects of Fatigue on Piping Reliability." In *Service Experience and Reliability Improvement: Nuclear, Fossil, and Petrochemical Plants*, PVP-Vol. 288, pp. 117-125. American Society of Mechanical Engineers, New York.

Khaleel MA and FA Simonen. 2000. "Effects of Alternative Inspection Strategies on Piping Reliability." *Nuclear Engineering and Design* **197**:115-140.

Khaleel MA, FA Simonen, DO Harris and DD Dedhia. 1995. "The Impact of Inspection on Intergranular Stress Corrosion Cracking for Stainless Steel Piping." In *Risk and Safety Assessments: Where Is the Balance?*, PVP-Vol. 296, pp. 411-422. American Society of Mechanical Engineers, New York.

Khaleel MA, FA Simonen, HK Phan, DO Harris and D Dedhia. 2000. *Fatigue Analysis of Components for 60-Year Plant Life*. NUREG/CR-6674, PNNL-13227. U.S. Nuclear Regulatory Commission, Washington, DC.

Lydell BOY and A Olsson. 2006. *Reliability Data for Piping Components in Nordic Nuclear Power Plants*. 2005153-M-003 Rev. A1. Relcon AB, Malmö, Sweden.

Mills WL, CM Brown and M Burke. 2002. "Effect of Microstructure on Low Temperature Cracking Behavior of EN82H Welds." In *Proceedings of 10th Int. Conf on Environmental Degradation of Materials in Nuclear Power Systems-Water Reactors*. National Association of Corrosion Engineers.

Mohammed AA. 2003. *A Short Description of STRUEL*. NURBIM Report D4/Appendix H. The Welding Institute, Cambridge, United Kingdom.

Morin U, C Jannson and B Bengtson. 1993. "Crack Growth Rates for Ni-Base Alloys with the Application to an Operating BWR." In *Proceedings of 6th Int. Conf on Environmental Degradation of Materials in Nuclear Power Systems-Water Reactors*, p. 373. The Minerals, Metals & Materials Society (TMS), Warrendale, Pennsylvania.

OECD. 2005. *OECD-NEA Piping Failure Data Exchange Project (OPDE), Workshop on Database Applications*. OPDE/SEC(2004)4. Nuclear Energy Agency, Issy-les-Moulineaux, France.

OECD. 2006. *OPDE 2006:1 Coding Guideline (OPDE-CG) & OPDE User Instruction*. PR01 Version 02, Restricted Distribution. Nuclear Energy Agency, Issy-les-Moulineaux, France.

Rudland DL, H Xu, G Wilkowski, P Scott, N Ghadiali and F Brust. 2006. "Development of a New Generation Computer Code (PRO-LOCA) for the Prediction of Break Probabilities for Commercial Nuclear Power Plants Loss-of-Coolant Accidents." In *2006 Proceedings of the ASME Pressure Vessels and Piping Conference*, July 23-27, 2006, Vancouver, British Columbia, Canada. American Society of Mechanical Engineers, New York.

Schimpfke T. 2003. *A Short Description of the Piping Reliability Code PROST*. NURBIM Report D4/Appendix C. Gesellschaft fur Anlagen-und Reaktorsicherheit (GRS), Berlin, Germany.

Scott PM. 1991. "An Analysis of Primary Water Stress Corrosion Cracking in PWR Steam Generators." *NEA/CSNI Specialist Meeting on Operating Experience with Steam Generators*. September 16-20, 1991. Brussels, Belgium.

Scott PM. 1996. "Prediction of Alloy 600 Component Failures in PWR Systems." In *Proceedings of the CORROSION/96 Research Topical Symposia 1996*. National Association of Corrosion Engineers, Houston, Texas.

Shack WJ. 2003. "Parametric Studies of the Probability of Failure of CRDM Nozzles." *Proceedings of the Vessel Penetration Inspection, Crack Growth, and Repair Conference*. Gaithersburg, Maryland.

Simonen FA, KI Johnson, AM Liebetrau, DW Engel and EP Simonen. 1986. *VISA-II - A Computer Code for Predicting the Probability of Reactor Pressure Vessel Failure*. NUREG/CR-4486. U.S. Nuclear Regulatory Commission, Washington, DC.

Simonen FA, DO Harris and DD Dedhia. 1998. "Effect of Leak Detection on Piping Failure Probabilities." In *Fatigue Fracture and Residual Stress*, PVP-Vol. 373, pp. 105-113. American Society of Mechanical Engineers, New York.

Simonen FA and MA Khaleel. 1998a. "A Probabilistic Fracture Mechanics Model for Fatigue Crack Initiation in Piping." In *Fatigue, Fracture and Residual Stress*, PVP-Vol. 373, pp. 27-34. American Society of Mechanical Engineers, New York.

Simonen FA and MA Khaleel. 1998b. "Effects of Flaw Sizing Errors on the Reliability of Vessels and Piping." *ASME Journal of Pressure Vessel Technology* **120**:365-373.

Tregoning R, L Abramson and P Scott. 2005. *Estimating Loss-of-Coolant Accident (LOCA) Frequencies Through the Elicitation Process (NUREG-1829) - Draft Report for Comment*. Draft NUREG-1829 (June 30, 2005). U.S. Nuclear Regulatory Commission, Washington, DC. Available at www.nrc.gov/reading-rm/doc-collections/nuregs/staff/sr1829/index.html

USNRC. 1997. *Event Description: Unisolable Reactor Coolant System Leak*. LER No. 270/97-001. U.S. Nuclear Regulatory Commission, Washington, DC.

Westinghouse Owners Group. 1997. *Application of Risk-Informed Methods to Piping Inservice Inspection Topical Report*. WCAP-14572, Rev. 1. Westinghouse Electric Co., Pittsburgh, Pennsylvania.

White GA, NS Nordmann, J Hickling and CD Harrington. 2005. "Development of Crack Growth Rate Disposition Curves for Primary Water Stress Corrosion Cracking (PWSCC) of Ally 82, 182, and 132 Weldments." In *Proceedings of 12th Int. Conf on Environmental Degradation of Materials in Nuclear Power Systems-Water Reactors*. The Minerals, Metals & Materials Society (TMS), Warrendale, Pennsylvania.

Williams PT, TL Dickson and S Yin. 2004. *Fracture Analysis of Vessels – Oak Ridge, FAVOR, v04.1, Computer Code: Theory and Implementation of Algorithms, Methods, and Correlations*. NUREG/CR-6854, ORNL/TM-2004/244. Oak Ridge National Laboratory, Oak Ridge, Tennessee.

Appendix A

Use of Service Experience Data to Assess the Failure Probability of Piping Components

Appendix A

Use of Service Experience Data to Assess the Failure Probability of Piping Components

A.1 Objective

This appendix documents results and insights of a recent demonstration of the use of pipe-failure data to calculate weld "failure" rates and "rupture" frequencies. The demonstration is concerned with five primary coolant system inservice inspection locations: (1) PWR reactor coolant hot leg bi-metallic weld between reactor pressure vessel nozzle and hot-leg pipe, (2) PWR pressurizer spray line bi-metallic nozzle-to-safe-end weld (pressurizer side), (3) PWR pressurizer surge line bi-metallic nozzle-to-safe-end weld (hot-leg side), (4) BWR reactor recirculation 711-mm (28-in.) austenitic stainless steel weld, and (5) BWR reactor recirculation 305-mm (12-in.) austenitic stainless steel weld.

In this appendix, the term "failure" includes any degraded state (including part-through-wall flaw, through-wall flaw without active leakage, through-wall flaw with active leakage, and any significant structural failure) requiring repair or replacement with or without plant shutdown. The term "rupture" implies a significant structural failure; however, it does not convey information about the magnitude of a pressure boundary failure in terms of peak through-wall flow rate. For safety-related piping, a "rupture" normally implies a pressure boundary failure of sufficient magnitude to activate a standby safety system to compensate for any losses in primary water inventory. In this demonstration, all calculated weld failure frequencies are for through-wall flaws with or without active leakage.

A.2 Introduction

With the implementation of risk-informed in-service inspection (RI-ISI), methodology has followed requirements for more realistic pipe failure rates and rupture frequencies that relate to specific combinations of degradation mechanisms and inspection locations. There are basically five approaches for estimating piping reliability:

(1) Structural reliability modeling (SRM) based on probabilistic fracture mechanics
(2) Analytical modeling using Markov theory and statistical analysis of service data
(3) Direct statistical estimation using service data
(4) Expert judgment/expert elicitation
(5) Any combination of (1) through (4).

The Loss-of-Coolant-Accident (LOCA) Frequency Elicitation Project (Draft NUREG-1829) (Tregoning et al. 2005) includes applications of all five approaches. Associated with each of the listed approaches are strengths and weaknesses (or limitations). The strengths relate to issues such as model realism, maturity (as measured by number of applications, ease of application, and acceptance by peers),

extent of formal peer review, ability to treat uncertainties, and proven capability to solve different types of problems. The limitations (could) relate to issues concerned with difficulty of reproducing results (unknown verification), effort involved in preparing input data, compatibility with the requirements of risk-informed applications, or lack of demonstrated capability to solve the types of problems encountered in risk-informed applications for categorizing passive components. This appendix is concerned with the following questions about the validity of piping reliability estimates derived by SRM:

- Is it possible to validate SRM results by using service-experience data? According to some researchers the answer to this question ranges from an "almost no" to a "definite no" (Chapman and Fabbri 2000). An underlying argument rests on an assumed premise that there is not enough service data of ***sufficient*** quality to support meaningful quantitative assessments. Moreover, since the existing service data represents no more than a historical record of past piping performance, the use of service data in predictive piping reliability analysis is not possible.

- If the answer to the first question were to be "yes", despite warranted and un-warranted apprehensions, concerns or reservations, what are the requirements for formal validation and what constitutes a "valid result"? There are different views on the requirements for quantitative piping reliability analysis. There has been considerable progress in the development and application of pipe failure databases, however. Do the lessons learned in this work provide any relevant insights for the validation of SRM results?

A.3 Piping Component Reliability Analysis

Efforts to develop comprehensive, application-oriented databases on the service experience with piping components and systems have been underway for as long as there have been commercial nuclear power plants. These efforts and results have been recorded in a large number of articles in volumes of scientific journals, and in published technical reports. A current state-of-the-art perspective on the roles of service-data collections in the assessment of piping reliability is documented (Fleming 2004; Lydell and Olsson 2006; OECD 2005, 2006). For a database to be fit for risk-informed applications it has to meet stringent data quality requirements. Lydell and Olsson (2006) divide existing databases into three categories. These categories reflect levels of data quality and fitness-for-use:

- Category 0 database. This is a "hybrid" database, which includes some high-level features of a Category 1 and/or Category 2 database, but it is not a standalone, computerized database intended for use by multiple users. It has not undergone any independent peer review, and it is not subject to any maintenance. Usually a Category 0 database is developed for a single application.

- Category 1 database. This is a comprehensive collection of raw data (or field data) on specified types of piping components with or without a database quality assurance program in place, but usually with direct access to source data. Typically this type of database has a single user (can be a person or an organization), with sporadic or periodic database maintenance to support high-level evaluations of failure trends.

- Category 2 database. This type of database is expected to support Grade 3 or 4 probabilistic risk assessment (PRA) applications as defined in the Nuclear Energy Institute's "PRA Peer Review Process Guidance" (NEI-00-02; NEI 2000). In risk-informed applications, such as RI-ISI, data

quality is particularly important and necessitates consideration for traceability and reproducibility of derived reliability parameters (see Section A.8) including the source data producing database query results, and data processing and the statistical analysis of query results. From a user perspective, a Category 2 database should include detailed and correct information on failure events so that database queries generate relevant and complete results. That is, detailed information with respect to the unique reliability attributes and influences factors of piping and specific locations. OECD (2005) includes further details on the structure and quality requirements for a Category 2 database.[(a)]

A simple model of piping reliability makes direct use of information as recorded in a Category 2 database. Equation (A.1) is a representation of this model:

$$\rho_{ix} = \sum_{k=1}^{M_i} \rho_{ikx} = \sum_{k=1}^{M_i} \lambda_{ik} P_{ik}\{R_x | F\} I_{ik} \qquad \text{(A.1)}$$

where ρ_{ix} = Total frequency of major structural failure R for piping component i for rupture mode x. A "structural failure" assumes a significant peak through-wall flow rate well in excess of Technical Specification limits (see below for further details). The term "structural failure" is nebulous—apart from implying a structural failure, it does not convey information about its significance (for example, through-wall flow rate).

ρ_{ikx} = Frequency structural failure for piping component i due to damage or degradation mechanism k for failure mode x

λ_{ik} = Failure rate of piping component i due to damage mechanism k

$P_{ik}\{R_x|F\}$ = Conditional probability of "structural failure" in mode x for piping component i given presence of damage or degradation mechanism k

M_i = Number of different damage degradation mechanisms for component i

I_{ik} = Integrity management factor for component i and damage or degradation mechanism k; this factor accounts for variable integrity management strategies such as leak detection, volumetric NDE, etc., that might be different than the components in a pipe-failure database.

The term "failure" implies any degraded state requiring remedial action. Types of remedial actions include repair (temporary or permanent); induction heat stress improvement; in-kind replacement; or replacement using new, more resistant material. Depending on how this model of piping reliability is to be used, the precise definition of failure may be, and usually is, important. For example, it may be important to make a distinction between different through-wall flaw sizes and their localized or global effects on plant operation and safety. Localized effects include collateral damage (for example, damage to adjacent line or a jet stream causing damage to adjacent pipe insulation). Global effects include flooding of equipment areas or buildings. In recent risk-informed applications the following definitions of structural failure modes have been used (Table A.1):

(a) Copies of OECD (2005) may be obtained from the OPDE Project's U.S. National Coordinator at the Nuclear Regulatory Commission (Andrea Valentin, adw1@nrc.gov).

Table A.1. Example of Definition of Structural Failure

Mode of Structural Failure	Equivalent Pipe Break Diameter (EBD) [mm]	Peak Through-wall Flow Rate (FR) [kg/s]
Large Leak	$15 < \text{EBD} \leq 50$	$0.5 < \text{FR} \leq 5$
Small Breach	$50 < \text{EBD} \leq 100$	$5 < \text{FR} \leq 20$
Breach	$100 < \text{EBD} \leq 250$	$20 < \text{FR} \leq 100$
Large Breach	$250 < \text{EBD} \leq 500$	$100 < \text{FR} \leq 400$
Major Breach	$\text{EBD} > 500$	$\text{FR} > 400$ (6300 gpm)

Risk-informed applications often require assessments of specified failure modes corresponding to unique consequences as included in a PRA. For example, in internal flooding PRAs, it could be necessary to evaluate impacts of specific spray events on adjacent, safety-related equipment. Hence, initiating event frequency of a "large leak" could be required for any through-wall flaw of sufficient size to generate a spray effect. Another example could be the plant-specific assessment of a high-energy line break (HELB) initiating an event of sufficient magnitude to activate fire protection sprinklers in a specific area of a Turbine Building. In general, a point estimate of the frequency of pipe failure, λ_{ik}, is given by the following expression:

$$\lambda_{ik} = \frac{n_{ik}}{f_{ik} N_i T_i} \tag{A.2}$$

where n_{ik} = The number of failure (all modes including cracks, leaks, and ruptures are included) events for pipe component i due to damage mechanism k.

T_i = The total exposure time over which failure events were collected for pipe component i, normally expressed in terms of reactor years (or calendar years).

N_i = The number of components per reactor year that provided the observed pipe failures for component i.

f_{ik} = The fraction of number of components of type i that are susceptible to failure from degradation/damage mechanism (DM) *"k"* for conditional failure rates given susceptibility to DM *"k"*; this parameter is set to 1 for unconditional failure rates.

When the parameter f_{ik} is applied, the resulting failure rates and rupture frequencies are referred to as conditional failure rates as they are conditional on the susceptibility of the component to specific damage or degradation mechanisms. That is, for each component that these models are applied to, the damage mechanism susceptibility is known.

When the damage mechanism susceptibility is not known in advance, the above equations are combined under the condition $f_{ik} = 1$ to obtain the following expression for the point estimate of the rupture frequency:

$$\rho_{ix} = \sum_{k=1}^{M_i} \rho_{ikx} = \sum_{k=1}^{M_i} \lambda_{ik} P_{ik}\{R_x | F\} I_{ik} = \sum_{k=1}^{M_i} \frac{n_{ik}}{N_i T_i} P_{ik}\{R_x | F\} I_{ik} \quad \text{(A.3)}$$

Depending on the type of piping system under consideration, the conditional failure probability may be obtained by direct statistical estimation, or through probabilistic fracture mechanics, or expert judgment. Ultimately, an estimated conditional failure probability needs to reflect existing service experience as well as structural integrity characteristics.

A Bayesian approach can be used to develop uncertainty distributions for the parameters in Equations (A.1) through (A.3). Prior distributions are developed for the parameters λ_{ik} and $P_{ik}\{R_x / F\}$ and these prior distributions are updated using the evidence from the failure and exposure data as in standard Bayes' updating. The resulting posterior distributions for each parameter on the right side of Equation (A.1) are then combined using Monte Carlo sampling to obtain uncertainty distributions for the frequency of structural failure.

A critical step in applying Equations (A.1) through (A.3) is to correctly define the exposure term (number of exposed components and corresponding time period). This definition is rooted in detailed knowledge of relevant piping system design parameters (for example: material, flow conditions, type of welds) and in-service inspection practice. Not only does this knowledge have to account for a specific system, it has to account for a cross-section of different designs used for a particular type of system. For example, some reactor vendors use bi-metallic welds in primary coolant piping, while others do not. The degradation susceptibility differs significantly depending on material selections.

An integral aspect of Category 2 databases is the inclusion of detailed piping design information and piping component population data for a broad range of representative reactor vendor designs. Querying a database on failure event populations must go hand-in-hand with queries of corresponding component populations.

Rules for querying a database must be founded on an analyst's knowledge about piping design, structural integrity of piping, and degradation susceptibilities of different piping systems. Also a database must include sufficient technical detail so that queries account for unique service conditions, water chemistry parameters, and material properties. High-level database insights (Figures A.1 and A.2) provide a first level of defense against incorrect applications.

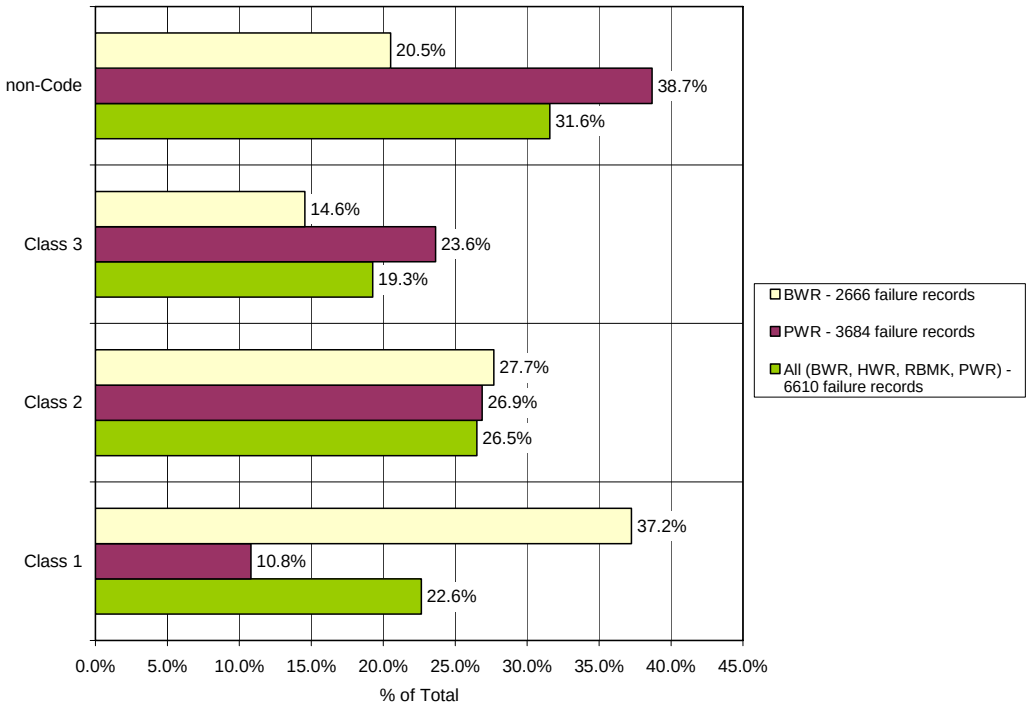

Figure A.1. Database Content[(a)] by ASME III Code Case

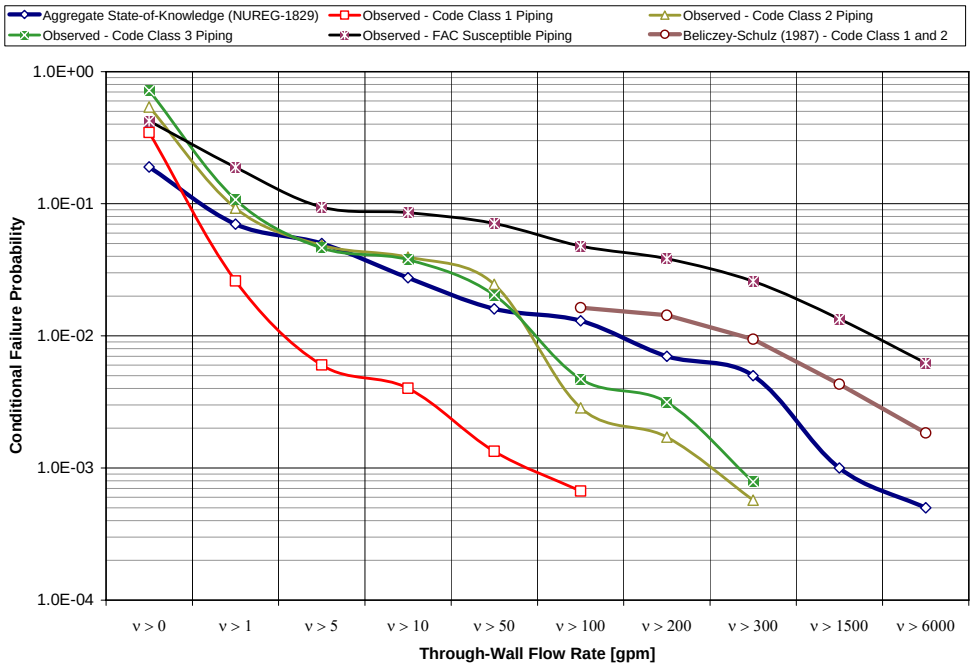

Figure A.2. Conditional Pipe Failure Probability According to Service Data

(a) PIPExp database as of 03/15/2006.

According to Figure A.1, the database insights change quite dramatically depending on how a query is formulated and what data filters are applied. From the perspective of statistical reliability parameter estimation, indiscriminate pooling of failure data could lead to incorrect results. Some high-level database insights include:

- ASME III Class 1 piping. The BWR-specific experience mainly consists of IGSCC in medium- to large-diameter piping. There have been no significant pipe failures due to IGSCC. Post-1987 (approximately), different types of IGSCC mitigation strategies have been implemented by all BWR plant operators. The PWR-specific experience consists almost exclusively of small-diameter socket weld failures and small-diameter, bi-metallic welds on cold-leg, hot-leg piping and pressurizer instrument line connection. There have been no significant pipe failures due to PWSCC, and the flaws that have been detected by visual inspection or nondestructive examination are almost exclusively short and axially oriented.

- Non-Code piping (extraction steam, feedwater heater drain and vent, and condensate piping). In general, compared with the PWR-specific experience, BWR plants experience fewer instances of pipe degradation and failure due to flow-accelerated corrosion (FAC) in carbon steel piping. This difference is attributed to different water chemistries and secondary-side water chemistry treatment programs.

Using the same service data as displayed in Figure A.1, four sets of data consisting of the fraction of the total event population for respective safety class are plotted in Figure A.2. These plots represent the conditional pipe failure probability as a function of peak through-wall flow rate. For comparison, included in Figure A.2 are two theoretical correlations for conditional pipe failure probability:

- Aggregate State-of-Knowledge (Draft NUREG-1829, Tregoning et al. 2005). This plot is for BWR primary piping and is the result of an expert elicitation process, but unlike the result presentation in Draft NUREG-1829, which includes plots of ρ_{ix}, Figure A.2 shows $R_x|F$ and the overall pipe failure rate is estimated directly from the available service data. It is to be noted that the Draft NUREG-1829 does not account for small-diameter piping failure.

- Beliczey-Schulz correlation (Beliczey and Schulz 1987). The four data points representing this correlation in Figure A.2 correspond to failed 19-mm, 51-mm, 76-mm, and 102-mm (¾-in., 2-in., 3-in., and 4-in.) Class 1 and 2 piping in a PWR, respectively. This correlation represents a mid-1980s German "aggregate state-of-knowledge" about the likelihood of structural failure. It is based on analysis of German service data, PFM, and experimental fracture mechanics studies. According to this German research, the probability of structural failure can be estimated from:

$$P_{ik}\{R_x|F\} = (9.6 \times DN/2.5 + 0.4 \times DN^2/25)^{-1} \quad \text{(A.4)}$$

  where DN = nominal pipe size in [mm]; according to Beliczey and Schulz (1987), the correlation applies for piping of nominal size 254 mm (10 in.) or less.

- Except for the "Aggregate State-of-Knowledge (Draft NUREG-1829)" and "Beliczey-Schulz (1987)", the remaining data plots in Figure A.2 represent observed pipe failure events. For Class 1

piping, all significant structural failures have involved small-diameter piping (instrument lines ≤ 25.4-mm [1-in.] diameter).

In totality, Figure A.2 is a snapshot of where we stand today. Obviously, the shape of an experience-based line in the chart would change should significant pipe failures occur in the future.

The uncertainty in the conditional pipe failure probability in Equation (A.4) is treated using the Beta Distribution. This distribution takes on values between 0 and 1 and is defined by two parameters A and B (or α and β in some textbooks). In reliability analysis the distribution is often used to express the uncertainty in failure rates per demand. The mean of the Beta Distribution is given by:

$$Mean = A/(A + B) \tag{A.5}$$

If A = B = 1, the Beta Distribution takes on a flat distribution between 0 and 1. If A = B = ½, the distribution is referred to as Jeffrey's non-informative prior and is a U-shaped distribution with peaks at 0 and 1. Expert opinion can be incorporated by selecting A and B to match up an expert estimate of the mean probability. For example, to represent an expert estimate of 1×10^{-2}, A = 1 and B = 99 can be selected. These abstract parameters can be associated with the number of failures and the number of successes in examining service data to estimate a conditional pipe failure probability in Equation (A.4).

Selecting appropriate A and B parameters is not a trivial task. Many different combinations of A and B will produce the same mean value. Insights from probabilistic fracture mechanics could be utilized in defining application- and location-specific A and B parameters.

A.4 Influence of Inspection and Leak Detection

Embedded in service data are underlying details of contributing causes of a degraded or failed state (high weld-residual stresses, sensitization of weld-heat-affected zone, lack of weld fusion, localized unfavorable flow conditions, failed inspections, design and construction defects, etc.). Obviously, an expression such as Equation (A.1) does not account for the physics of degradation or failure in any explicit way. On the other hand, if a database is of sufficient technical depth and the queries are appropriately defined, then the resulting parameter estimates would portray the effect of operating conditions, material characteristics, and loading conditions.

Markov modeling (Fleming 2004; Modarres 1993) is an established technique for analyzing interactions between degradation/damage mechanisms that cause degradation or failure, and inspection, detection and repair strategies that can reduce the probability that failure occurs, or that surface-breaking cracks and through-wall flaws will progress to major structural failure before being detected and repaired. This technique starts with a representation of a "system" in a set of discrete and mutually states. Figure A.3 is a representation of a general four-state Markov model of piping component reliability.

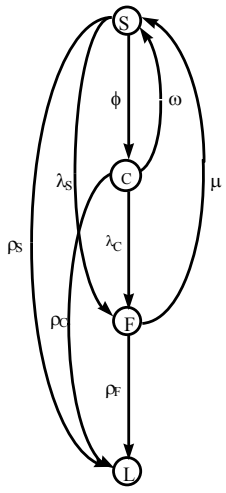

Piping Reliability States:
S = Success (or undamaged state),
C = Crack (non-through wall flaw),
F = Leaking through-wall flaw (leak rate is within Technical Specification limit),
L = Large leak (leak rate in excess, or well in excess of Technical Specification limit – a "structural failure").

State Transitions:	
ϕ	Occurrence of non-through wall flaw
λ_S	Occurrence of small leak given an undamaged state ('S')
λ_C	Occurrence of small leak given a flaw ('C')
ρ_S	Occurrence of large leak given no flaw
ρ_C	Occurrence of large leak given a non-through wall flaw
ρ_F	Occurrence of large leak given a small leak
μ	Detect and repair a through-wall flaw
ω	Inspect and repair a non-through wall flaw

Figure A.3. Four-State Markov Model of Piping Component Reliability

The "states" in Figure A.3 refer to various degrees of piping system degradation. That is, the existence of flaw(s), through-wall leak, or major structural failure. The flaws can be wall thinning, pitting, or cracking. In Markov model theory the processes shown in Figure A.3 can be specified by a set of differential equations (or Markov state equations) and their associated initial conditions. All Markov model parameters shown in Figure A.3 (and as listed in Section A.8) are estimated using service data. The failure frequencies obtained from Markov models are time-dependent. The reliability function for the Markov model, *r(t)*, is given by:

$$r(t) = 1 - L(t) = S(t) + C(t) + F(t) \tag{A.6}$$

where

$$S(t) + C(t) + F(t) + L(t) = 1 \tag{A.7}$$

and hazard rate *h(t)*

$$h(t) = -\,(r(t)^{-1}\, \mathrm{d}r(t)/\mathrm{d}t = (1 - L(t))^{-1}\, \mathrm{d}L(t)/\mathrm{d}t. \tag{A.8}$$

The hazard rate, *h(t)*, is the time-dependent frequency of structural failure ("L"). It starts at t = 0 (beginning of plant life) and gradually increases towards an asymptotic hazard rate. The hazard rate is not to be confused with the cumulative or annual average lifetime frequency of structural failure, quantities often generated by probabilistic fracture mechanics methods.

A.5 Data Specializations

Pipe failure is a function of sometimes complex interrelationships between pipe size (diameter and wall thickness), material, flow conditions, pressure and temperature, method of fabrication, loading conditions, weld residual stresses, etc. These relationships should always be embedded in a Category 2 reliability database and accessible for parametric evaluations. For circumferential welds their location within a piping system and residual stresses represent strong reliability influence factors. It is sometimes desirable to develop specialized weld failure rates to reflect these influences. For a weld of type "*i*" (defined by its location in a pipe line) and size "*j*" (defined by the nominal pipe diameter), the failure rate can be expressed as follows:

$$\lambda_{ij} = F_{ij}/(W_{ij} \times T) \tag{A.9}$$

and with

$$S_{ij} = F_{ij} / F_j \tag{A.10}$$

$$A_{ij} = W_j/W_{ij} \tag{A.11}$$

the failure rate of weld of type "*i*" and size "*j*" is expressed as

$$\lambda_{ij} = (F_j \times S_{ij})/(W_{ij} \times T) \tag{A.12}$$

$$\lambda_{ij} = S_{ij} \times A_{ij} \times \lambda_j \tag{A.13}$$

where λ_{ij} = Failure rate of a susceptible weld of type "i", size "j"

λ_j = Failure rate of a susceptible weld of size "j"

F_j = Number of size "j" weld failures

F_{ij} = Number of type "i" and size "j" weld failures

W_j = Size "j" weld count

W_{ij} = Type "i" and size "j" weld count

Susceptibility (S_{ij}) = The service experience shows the failure susceptibility to be correlated with the location of a weld relative to pipe fittings and other in-line components (flanges, pump casings, valve bodies). For a given pipe size and system, the susceptibility is expressed as the fraction of welds of type "*ij*" that failed due to a certain degradation mechanism. This fraction is established by querying the database.

Attribute (A_{ij}) = In the above expressions the attribute (A) is defined as the ratio of the total number of welds of size "*j*" to the number of welds of type "i". A_{ij} is a correction factor and accounts for the fact that piping system design and layout constraints impose limits on the number of welds of a certain type. For example, in a given system there tends to be more elbow-to-pipe welds than, for example, pipe-to-tee welds.

Combining a global (or averaged) failure rate with the weld configuration dependency provides failure rates that account for known or assumed residual stresses. Typically, a final weldment attaching a spool piece to, say, a heat exchanger nozzle or vessel nozzle tends to be the most vulnerable weld assembly in a piping system.

A.6 Case Studies

The results of five case studies are presented in this section. The case studies are applications of the PIPExp database and the concepts discussed in Sections A.3 through A.5 to derive current estimates of failure rates for selected BWR- and PWR-specific inservice inspection areas.

Defining an appropriate exposure term (the denominator in Equation A.2 or A.3) is not trivial. It requires detailed knowledge of piping system design features and degradation susceptibilities. As an example, PWR primary system design information such as that found in IAEA-TECDOC-1361 (IAEA 2003) was used for the PWR inspection areas considered in this study.

For the BWR inspection areas, the calculations have been set up to produce unconditional weld failure rates as represented by Equation (A.3). For the PWR inspection areas, the calculations have been set up to produce conditional weld failure rates as represented by Equation (A.2). These rates represent specific locations and degradation susceptibilities, whereas the BWR-specific rates are averaged across reactor recirculation system weld populations representative of General Electric BWR/3 and BWR/4 plant types.

- Case 1. Bi-metallic weld between reactor pressure vessel nozzle and PWR reactor coolant hot-leg pipe. This is the location where V.C. Summer and Ringhals Unit 4 (both 3-loop Westinghouse plants) have experienced cracking attributed to PWSCC; in the former case, a through-wall flaw was discovered, and in Ringhals Unit 4, the flaw was non-through-wall. The analysis is concerned with the calculation of the frequency of a through-wall flaw in this location using the available service experience. Input data for the calculation and the results are summarized in Figure A.4. Included for comparison are calculated weld failure frequencies for other reactor coolant inspection locations.

- Case 2. Bi-metallic weld in pressurizer spray line. To date non-through-wall cracks have been found at Millstone-3 (October 2005). This may not be a service-induced flaw, however. A pre-emptive weld overlay repair has been performed under the assumption of the presence of PWSCC. This calculation considers three different assumptions concerning the interpretation of the service data:

  Assumption 1: The service data consists of the weld-overlay repair performed at Millstone-3 in October 2005. Evidence is 0 (zero) through-wall flaws.

  Assumption 2: The calculation accounts for all relevant service data involving bi-metallic welds in the pressurizer spray line and pressurizer relief lines. Assume five susceptible welds per plant.

  Assumption 3: This calculation assumes that the weld flaw discovered at Millstone-3 was at or near through-wall.

- Case 3. Bi-metallic nozzle-to-safe-end weld (hot-leg side) of PWR pressurizer surge line. Three Mile Island Unit 1 and Tihange-2 (this plant is located in Belgium) have experienced non-through-wall cracking in this area that is attributed to PWSCC. There have been no reports of through-wall flaws for this inspection location. Input data for this calculation and the results are summarized in Figure A.6. This calculation considers three different assumptions concerning the interpretation of the service data:

  Assumption 1: The service data consists of the non-through-wall flaws in bi-metallic surge line welds at Three Mile Island-1 and Tihange-2. Evidence is 0 (zero) through-wall flaws.

  Assumption 2: This calculation assumes that the two bi-metallic surge line welds and the pressurizer spray line and relief line welds are equally susceptible to PWSCC.

  Assumption 3: This calculation assumes that one of the two weld flaws discovered at Three Mile Island-1 and Tihange-2 was at or near through-wall.

- Case 4. BWR reactor recirculation 28-in. austenitic stainless steel welds. This case pertains to the frequency of through-wall flaws given implementation of IGSCC-mitigation measures consisting of weld-overlay repair and hydrogen water chemistry. The calculation is limited to U.S. service experience involving IGSCC in BWR/3 and BWR plants. The effect of IGSCC mitigation on the failure frequency is at least a factor of 10 reduction factor. Additional details of the analysis are documented in Appendix D of Draft NUREG-1829. The results are summarized in Figure A.7.

- Case 5. Same as Case 4 but for 12-in. welds. The results are summarized in Figure A.7.

Unlike the experience with PWSCC in medium- and large-diameter primary coolant piping, the service experience with IGSCC in BWR primary coolant piping includes on the order of 1200 records for non-through-wall and through-wall cracks. With this volume of failure data, it is relatively straightforward to explicitly account for the effects of IGSCC mitigation.

Embedded in the service data are the effects of different inservice inspection programs, evolving NDE reliability, augmented inspections, etc. Markov modeling makes it possible to characterize these effects and to address the impact of different assumptions about the probability of detecting (POD) non-through-wall flaws. Figure A.8 shows the time-dependent failure frequency for a bi-metallic pressurizer spray line nozzle-to-safe-end weld. The calculation uses an assumption of annual ISI with POD = 50% and POD = 90%.

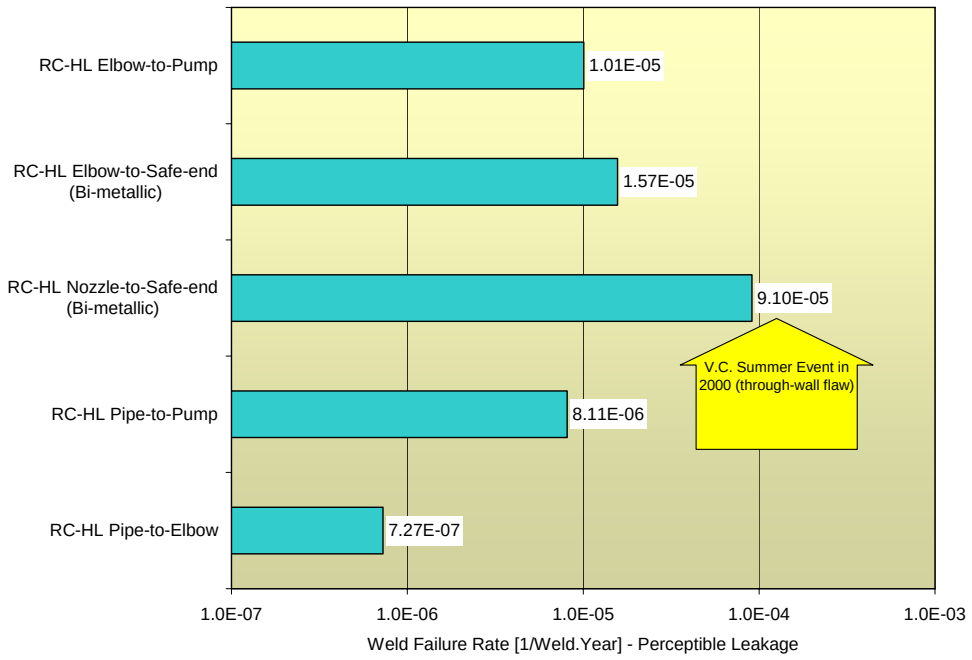

Service Experience (n_{ik}):	1 (1970–2005)		
Exposure Term ($f_{ik} \times N_i \times T_i$):	10,784 Weld Years (since 1/1/01)		
Comments: The results account for the accumulated (worldwide) service experience through the end of calendar year 2005. The exposure data accounts for 2-loop, 3-loop, and 4-loop PWR plants with bi-metallic welds in reactor coolant piping; it excludes consideration of French or German PWR plants. The PWR designs by Framatome and KWU/Siemens do not have any bi-metallic welds in the primary system piping. The calculation framework is described in Fleming and Lydell (2004).			
PWR System	**Number of Failure Records**		
	≤ NPS1	**1 < NPS ≤ 10**	**>NPS10**
Primary Piping	62	13	10

Figure A.4. Case 1: Calculated Failure Frequency for Bi-Metallic Weld in PWR Reactor Coolant Hot-Leg Piping – NPS is the nominal pipe diameter (inch)

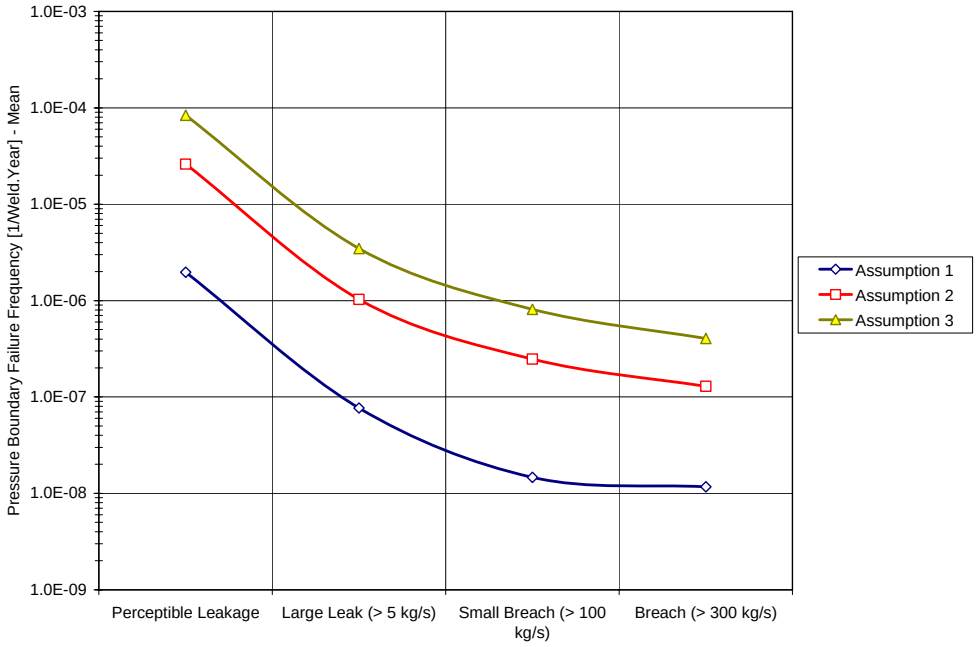

Service Experience (n_{ik}):	Assumption 1: 0 (since 1/1/70)
	Assumption 2: 1 (since 1/1/70)
	Assumption 3: as Case 1, but assume flaw at or near through-wall
Exposure Term ($f_{ik} \times N_i \times T_i$):	Assumption 1: 3621 Weld Years
	Assumption 2: 18,105 Weld Years
The chart includes extrapolated frequencies of structural failure of different magnitudes. This extrapolation uses Equation (A.1), and the uncertainty in the conditional failure probability is characterized with a Beta distribution with prior A- and B-parameters for "Breach" assumed to be 1 and 1999, respectively.	

Figure A.5. Case 2: Calculated Failure Frequency for Bi-Metallic Weld in PWR Pressurizer Spray Line

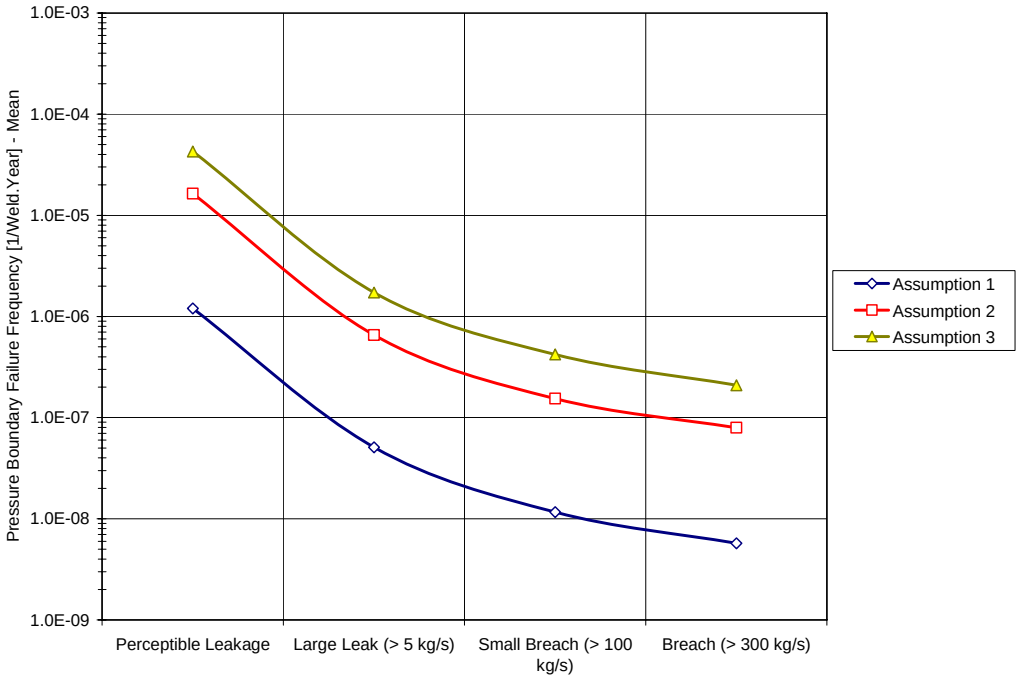

Service Experience (n_{ik}):	Assumption 1: 0 (since 1/1/70)
	Assumption 2: 1 (since 1/1/70)
	Assumption 3: as Case 1, but assume flaw at or near through-wall
Exposure Term ($f_{ik} \times N_i \times T_i$):	Assumption 1: 7242 Weld Years
	Assumption 2: 25,347 Weld Years
The chart includes extrapolated frequencies of structural failure of different magnitudes. This extrapolation uses Equation (A.1), and the uncertainty in the conditional failure probability is characterized with a Beta distribution with prior A- and B-parameters for "Breach" assumed to be 1 and 1999, respectively.	

Figure A.6. Case 3: Calculated Failure Frequency for Bi-Metallic Weld in PWR Pressurizer Surge Line

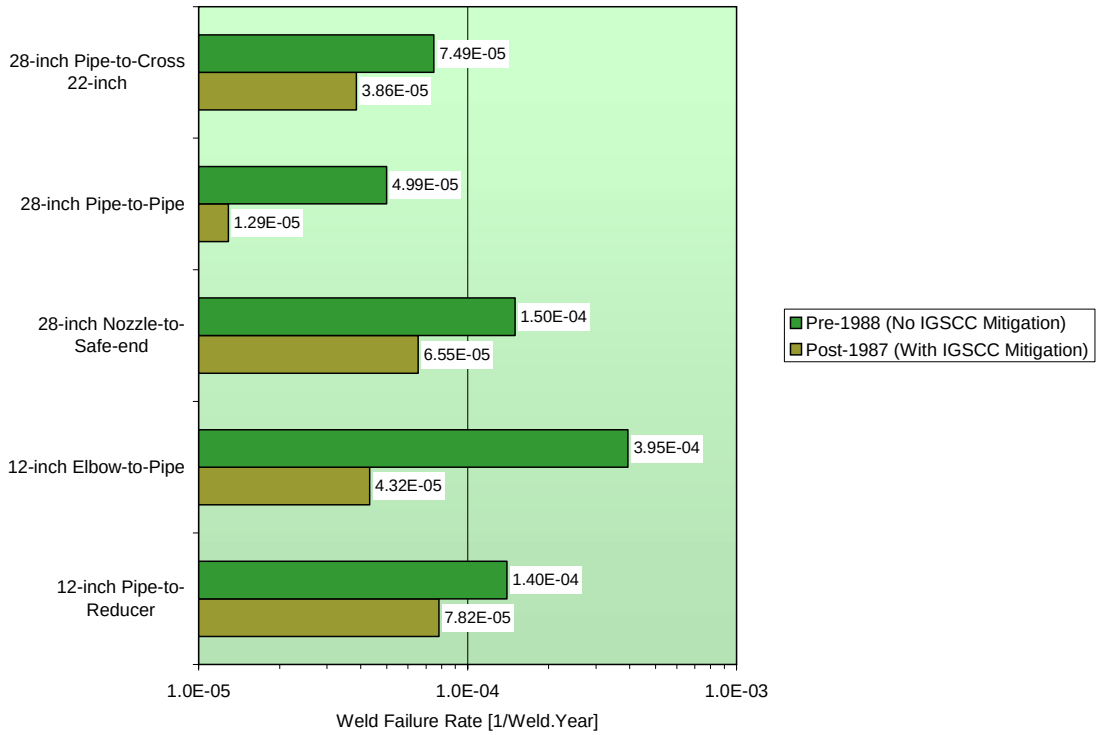

Figure A.7. Cases 4 and 5: Calculated Austenitic Stainless Steel Weld Failure Frequency for BWR/3 and BWR/4 Reactor Recirculation Piping With and Without IGSCC Mitigation

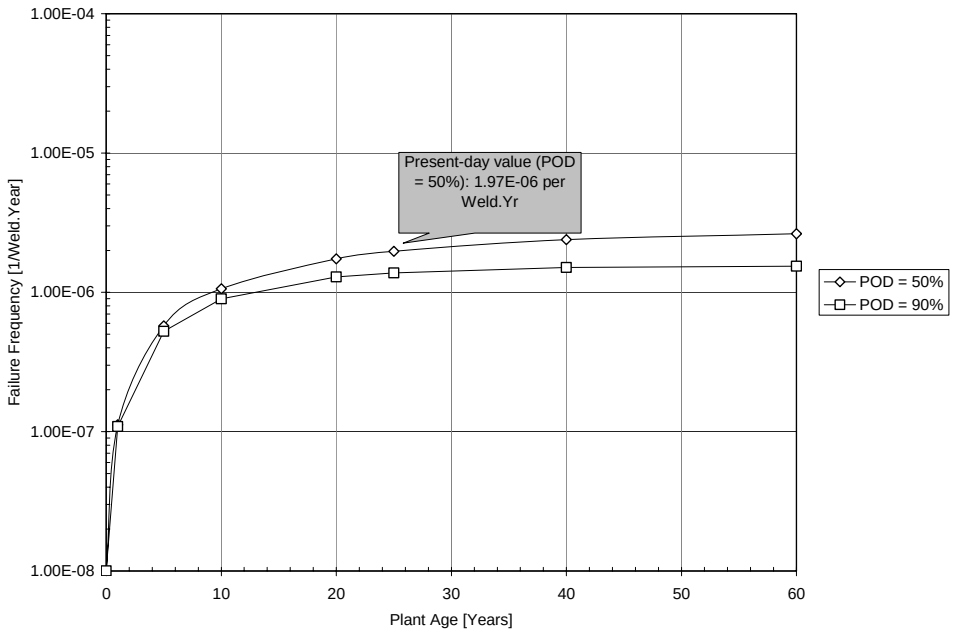

Figure A.8. Hazard Rate for Bi-metallic Pressurizer Spray Line Nozzle-to-Safe-End Weld

A.7 Statistical Estimation Approach vs. PFM

The derived weld failure rates represent bounding-type estimates for "perceptible leakage." That is, through-wall flaws that are discovered through bare-metal inspections rather than active leakage picked up by a leak detection system and/or monitoring system for radioactivity. Summarized in Figure A.9 are the results for the three PWR inspection locations. In comparing the results, the reader must bear in mind the different underlying assumptions. As demonstrated, the results are quite sensitive to the assumptions made about service data interpretation as well as to the formulation of the exposure terms.

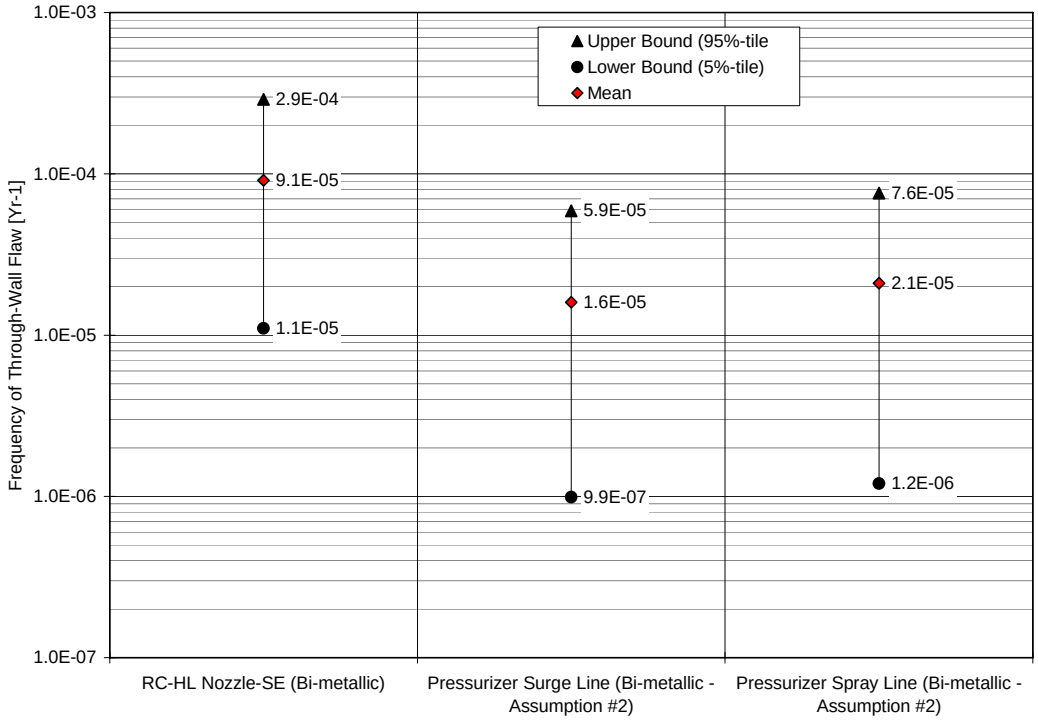

Figure A.9. Calculated Bi-metallic Weld Failure Rates for Three PWR Primary Piping Inspection Locations

Comparisons of results from applications of SRM and statistical estimation approaches to the same or similar problem are documented in Simola et al. (2004) and Tregoning et al. (2005). To perform meaningful comparisons it is very important to document the assumptions of each respective approach. Furthermore, whenever statistical analysis of service data is pursued, it becomes essential that the database supporting the analysis fulfills certain minimum data quality requirements.

For weld failure modes up to and including perceptible through-wall leakage, the difference between outputs from SRM models, and statistical estimation approaches should be well within an order of magnitude. Should the difference be larger, the assumptions behind respective calculation need revisiting.

A.8 List of Piping Reliability Parameters

Table A.1 provides a list of piping reliability parameters that define variables used in this appendix to develop failure probabilities for piping components.

Table A.1. Examples of Piping Reliability Parameters Derived from a Category 2 Database

Symbol	Description	Data Source and Strategy for Estimation	Intended Application and Extent of Demonstrated Database Application
λ_{ik}	Failure rate of pipe component "i" due to degradation or damage mechanism "k"	The failure rate is estimated directly using time-to-failure (TTF) data or indirectly via an operating piping failure data exchange (OPDE) database query to obtain a failure count over a certain observation period and for a certain piping component population.	Probabilistic safety assessment (PSA) (LOCA frequency, internal flooding, HELB frequency) and risk-informed applications (RI-ISI). Extensive insights available from past database (DB) applications.
TTF	Time to Failure	Obtained directly via OPDE database query.	Can be used in predictive reliability analysis to determine pipe replacement intervals. Hazard plotting techniques (or Weibull analysis) use TTF data directly to estimate reliability parameters. This analysis approach has been used extensively to analyze IGSCC data and raw water pipe failure data.
$P_{ik}\{R_x\|F\}$	Conditional pipe failure probability. Index "x" refers to mode (or magnitude) of failure as defined by through-wall peak flow rate threshold value.	Obtained directly via OPDE database query, Bayesian estimation strategy, PFM (SRM), or expert elicitation.	PSA (LOCA frequency, internal flooding, HELB frequency) and RI-ISI. Extensive insights available from past DB applications.
I_{ik}	Structural integrity management factor for component "i" and damage or degradation mechanism "k". This is an adjustment factor to account for variable integrity management strategies such as leak detection, volumetric NDE, etc., that might be different than the components included in a pipe failure database.	Obtained through application of the Markov model of piping reliability (iterative analysis).	Extensive insights from past application of the Markov model.

Symbol	Description	Data Source and Strategy for Estimation	Intended Application and Extent of Demonstrated Database Application
n_{ik}	Number of failures (all modes, including cracks, leaks, and significant structural failures)	Obtained directly via OPDE database query.	PSA (LOCA frequency, internal flooding, HELB frequency) and RI-ISI. Extensive insights available from past DB applications.
f_{ik}	The fraction of number of components or type "i" that are susceptible to failure from degradation or damage mechanism "k" for conditional failure rates given susceptibility to "k"; this parameter is set to 1 for unconditional failure rates.	Obtained directly via OPDE database query, from "Degradation Mechanism Analysis" tasks of RI-ISI program development projects, or via engineering judgment.	RI-ISI program development (e.g., Δ-risk evaluations).
N_i	The number of components per reactor year (or calendar year) that provided the observed pipe failures for component "i"	Input from piping system design reviews (size, weld counts, pipe lengths, and material data) specific to an application. Required for estimation of λ_{ik}.	Piping population databases have been developed as addressed in Task 1 report.
T_i	Total exposure time over which failures were collected for pipe component "i"; normally expressed in terms of reactor years (or calendar years)	Obtained directly via OPDE database query. Required for estimation of λ_{ik}.	
ϕ	Occurrence rate of a flaw (non-through-wall)	Obtained directly via OPDE database query, or can be estimated as a multiple of the rate of leaks based on ISI experience.	Input to Markov model of piping reliability.
λ_S	Occurrence rate of leak from a no-flaw state	Service data for leaks and reasoning that leaks without a pre-existing flaw are only possible for selected damage mechanism from severe loading.	Input to Markov model of piping reliability.
λ_C	Occurrence rate of a leak from a flaw state	Service data for leaks for selected conditions and degradation mechanisms.	Input to Markov model of piping reliability.
ρ_S	Occurrence rate of a "structural failure" from a no-flaw state	Service data for "structural failure" and reasoning that "structural flaws" without a pre-existing degradation are only possible for selected damage mechanisms and system-material combinations.	Input to Markov model of piping reliability.

Symbol	Description	Data Source and Strategy for Estimation	Intended Application and Extent of Demonstrated Database Application
ρ_C	Occurrence rate of a through-wall leak from a flaw (non-through-wall) state	Service data for leaks for selected conditions and degradation mechanisms.	Input to Markov model of piping reliability.
ρ_F	Occurrence rate of "structural failure" from a through-wall flaw state	Estimates of physical degradation rates and times to failure converted to equivalent failure rates, or estimates of water hammer challenges to the system in degraded state.	Input to Markov model of piping reliability.
μ	Repair rate via leak detection $\mu = \frac{P_{LD}}{(T_{LI} + T_R)}$	Model of equation for μ, and estimates of P_{LD}, T_{LI}, T_R.	Input to Markov model of piping reliability.
P_{LD}	Probability that a through-wall flaw is detected given leak detection or leak inspection	Estimate based on presence of leak detection system, technical specification requirements, and frequency of leak inspection. DB generates qualitative insights. Reliability of leak detection systems is high. Quantitative estimate based on expert judgment.	Input to Markov model of piping reliability; supports sensitivity analyses to address impact of different assumptions on piping reliability.
T_{LI}	Mean time between inspections for through-wall flaw	Estimate based on method of leak detection; ranges from immediate to frequency of routine inspections for leaks or ASME Section XI-required system leak tests.	Input to Markov model of piping reliability.
ω	Repair rate via NDE $\omega = \frac{P_I P_{FD}}{(T_{FI} + T_R)}$	Model of equation for ω, and estimates of P_I, P_{FD}, T_{FI}, T_R.	Input to Markov model of piping reliability.
P_I	Probability that a flaw will be inspected (index "I") per inspection interval	Estimate based on specific inspection strategy; usually done separate for ASME Section XI (or equivalent) and RI-ISI programs.	Input to Markov model of piping reliability.
P_{FD}	Probability that a flaw will be detected given that the weld or pipe section is subjected to NDE. Also referred to as POD.	Estimate based on NDE reliability performance data and difficulty of inspection for particular inspection site. OPDE provides qualitative insights about NDE reliability.	Input to Markov model of piping reliability.
T_{FI}	Mean time between inspections	Based on applicable inspection program; can be "never" or 10 years for ASME XI piping.	Input to Markov model of piping reliability.

Symbol	Description	Data Source and Strategy for Estimation	Intended Application and Extent of Demonstrated Database Application
T_R	Mean time to repair once detected	Obtained directly via OPDE query. The mean repair time includes time to tag out, isolate, prepare, repair, leak test, and tag-in.	Input to Markov model of piping reliability.

A.9 References

Beliczey S and H Schulz. 1987. "The Probability of Leakage in Piping Systems of Pressurized Water Reactors on the Basis of Fracture Mechanics and Operating Experience." *Nuclear Engineering and Design* **102**:431-438.

Chapman OJV and L Fabbri. 2000. "Problems Associated With the Use of Field Data to Assess the Probability of Failure of Passive Components for Use in Risk Analysis." *Discussion Document on Risk-Informed In-Service Inspection of Nuclear Power Plants in Europe*. Appendix 1, ENIQ Report No. 21. JRC Petten, Institute for Advanced Materials, Petten (The Netherlands).

Fleming KN. 2004. "Markov Models for Evaluating Risk-Informed In-service Inspection Strategies for Nuclear Power Plant Piping Systems." *Reliability Engineering and System Safety* **83**:27-45.

Fleming KN and BOY Lydell. 2004. "Database Development and Uncertainty Treatment for Estimating Pipe Failure Rates and Rupture Frequencies." *Reliability Engineering and System Safety* **86**:227-246.

IAEA. 2003. *Assessment and Management of Ageing of Major Nuclear Power Plant Components Important to Safety. Primary Piping in PWRs*. IAEA-TECDOC-1361. International Atomic Energy Agency, Vienna, Austria.

Lydell BOY and A Olsson. 2006. *Reliability Data for Piping Components in Nordic Nuclear Power Plants*. 2005153-M-003 Rev. A1. Relcon AB, Malmö, Sweden.

Modarres M. 1993. *What Every Engineer Should Know About Reliability and Risk Analysis*. Marcel Dekker, Inc., New York. ISBN 0-8247-8958-X, pp. 206-212.

NEI. 2000. *Probabilistic Risk Assessment (PRA) Peer Review Process Guidance*. NEI-00-02, Rev. A3, March 20, 2000. Nuclear Energy Institute.

OECD. 2005. *OECD-NEA Piping Failure Data Exchange Project (OPDE), Workshop on Database Applications*. OPDE/SEC(2004)4. Nuclear Energy Agency, Issy-les-Moulineaux, France.

OECD. 2006. *OPDE 2006:1 Coding Guideline (OPDE-CG) & OPDE User Instruction*. PR01 Version 02, Restricted Distribution. Nuclear Energy Agency, Issy-les-Moulineaux, France.

Simola K, U Pulkkinen, H Talja, P Karjalainen-Roikonen and A Saarenheimo. 2004. "Comparison of Approaches for Estimating Pipe Rupture Frequencies for Risk-Informed In-service Inspections." *Reliability Engineering and System Safety* **84**:65-74.

Tregoning R, L Abramson and P Scott. 2005. *Estimating Loss-of-Coolant Accident (LOCA) Frequencies Through the Elicitation Process (NUREG-1829) - Draft Report for Comment*. Draft NUREG-1829 (June 30, 2005). U.S. Nuclear Regulatory Commission, Washington, DC. Available at www.nrc.gov/reading-rm/doc-collections/nuregs/staff/sr1829/index.html